

Working together for a
cleaner energy future



Environmental Impact Assessment Report
Volume 3, Appendix 6.3: Marine Geology, Oceanography
and Physical Processes Baseline Report

MarramWind Offshore Wind Farm

December 2025

Document code:	MAR-GEN-ENV-REP-WSP-000154
Contractor document number:	852346-WEIS-IA-O1-RP-M6-107495
Version:	Final for Submission
Date:	08/12/2025
Prepared by:	ABPmer Limited
Checked by:	WSP UK Limited
Approved by:	MarramWind Limited

Contents

1. Introduction	6
1.1 Overview	6
1.2 Approach	6
1.3 Physical processes study area	7
2. Methodology	9
2.2 Desk study	9
2.3 Study area surveys	11
3. Metocean Regime	13
3.2 Water levels	13
3.3 Currents	14
3.4 Winds	17
3.5 Waves	21
3.6 Future change	32
4. Stratification and Frontal Systems	33
4.2 Overview	33
4.3 Water column stratification	33
4.4 Tidal mixing fronts	38
4.5 Future change	42
5. Surficial Sediments, Sediment Transport and Morphology	43
5.2 Seabed sediments	43
5.2.1 Overview	43
5.2.2 Option Agreement Area and offshore export cable corridor	43
5.3 Geology sub-strata	46
5.3.1 Overview	46
5.3.2 Option Agreement Area and offshore export cable corridor	46
5.4 Suspended sediments	51
5.5 Morphology	51
5.5.1 Overview	51
5.5.2 Option Agreement Area	53
5.5.3 Offshore export cable corridor	58
5.6 Sediment transport and seabed mobility	61
5.6.1 Overview	61
5.6.2 Sediment transport in the Option Agreement Area and offshore export cable corridor	61
5.6.3 Seabed mobility in the Option Agreement Area and offshore export cable corridor	63
5.6.4 Conceptual understanding of seabed change	66

6.	Coastal Geomorphology and Characteristics	69
6.2	Regional overview	69
6.3	Landfall	71
7.	Summary	75
7.2	Current baseline	75
7.2.1	Option Agreement Area	75
7.2.2	Offshore export cable corridor	76
7.2.3	Landfall zones	76
7.3	Future baseline	77
8.	References	79
9.	Glossary of Terms and Abbreviations	83
9.1	Abbreviations	83
9.2	Glossary	84

Table 2.1 Data sources used to inform the marine geology, oceanography and physical processes baseline	9
Table 2.2 Surveys undertaken to inform the marine geology, oceanography and physical processes baseline	11
Table 3.1 Summary tidal statistics for Peterhead (UKHO, 2025a)	13
Table 3.2 Frequency scatter tables of wind speed vs wind direction – landfall (ABPmer, 2025a)	20
Table 3.3 Frequency scatter tables of wind speed vs wind direction – offshore export cable corridor (ABPmer, 2025a)	20
Table 3.4 Frequency scatter tables of wind speed vs wind direction – OAA (ABPmer, 2025a)	21
Table 3.5 Frequency scatter table of significant wave height vs peak wave period – landfall (ABPmer, 2025a)	27
Table 3.6 Frequency scatter table of significant wave height vs peak wave direction – landfall (ABPmer, 2025a)	27
Table 3.7 Frequency scatter table of significant wave height vs peak wave period – offshore export cable corridor (ABPmer, 2025a)	28
Table 3.8 Frequency scatter table of significant wave height vs mean wave direction – offshore export cable corridor (ABPmer, 2025a)	29
Table 3.9 Frequency scatter table of significant wave height vs peak wave period – OAA (ABPmer, 2025a)	30
Table 3.10 Frequency scatter table of significant wave height vs mean wave direction – OAA (ABPmer, 2025a)	31
Table 3.11 Extreme value analysis of significant wave height and wave period based on wave data from ABPmer SEASTATES	31
Table 5.1 Summary of shallow geology within the OAA (adapted from Fugro, 2023a)	46
Table 5.2 Summary of shallow geology within the offshore export cable corridor	47
Table 5.3 Behaviour zones and associated characteristics identified in the OAA and along the offshore export cable corridor	67

Plate 3.1 Comparison of water level (top), depth-averaged current speed (middle), and depth-averaged current direction (bottom) between the metocean deployment (Fugro, 2023c) and ABPmer HD model (ABPmer, 2017)	14
Plate 3.2 Baseline tidal current speed and direction during a representative Spring tidal condition (ABPmer, 2017)	15
Plate 3.3 Baseline residual tidal current speed and direction calculated over a representative Spring-neap period (ABPmer, 2017)	16
Plate 3.4 Baseline peak Spring current speed and Spring tidal excursion ellipses (ABPmer, 2017)	17
Plate 3.5 Rose plot of wind speed and direction for the metocean deployment location, over the period 2022-2023 (directions indicate 'coming from') (ABPmer, 2025a)	18
Plate 3.6 Rose plot of wind speed and direction for the OAA, 1979-2022 (ABPmer, 2025a)	19
Plate 3.7 Comparison of measured and modelled wave parameters within the OAA (ABPmer, 2025a; Fugro, 2023c)	22
Plate 3.8 Rose plot of significant wave height and direction for the metocean deployment location, over the period 2022-2023 (directions indicate 'coming from') (ABPmer, 2025a)	23
Plate 3.9 Rose plot of significant wave height and direction near the landfall, over the period 1979-2023 (directions indicate 'coming from') (ABPmer, 2025a)	24
Plate 3.10 Rose plot of significant wave height and direction at a location representative of the offshore export cable corridor (middle), over the period 1979-2023 (directions indicate 'coming from') (ABPmer, 2025a)	25
Plate 3.11 Rose plot of significant wave height and direction at a location representative of the OAA, over the period 1979-2023 (directions indicate 'coming from') (ABPmer, 2025a)	26
Plate 4.1 Calculated PEA (ϕ), based on the Copernicus Reanalysis monthly temperature and salinity data for 2014, a stronger stratification year (Copernicus Marine Service, 2024a)	35
Plate 4.2 Calculated PEA (ϕ), based on the Copernicus Reanalysis monthly temperature and salinity data for 2010, an intermediate stratification year (Copernicus Marine Service, 2024a)	36
Plate 4.3 Calculated PEA (ϕ), based on the Copernicus Reanalysis monthly temperature and salinity data for 2015, a weaker stratification year (Copernicus Marine Service, 2024a)	37
Plate 4.4 Monthly PEA (ϕ) values, based on the Copernicus Reanalysis monthly temperature and salinity data, in the OAA from 2010-2023 (Copernicus Marine Service, 2024a)	38
Plate 4.5 Copernicus Reanalysis monthly maximum chlorophyll-a concentration throughout the water column for 2014 a stronger stratification year (Copernicus Marine Service, 2024b)	39
Plate 4.6 Copernicus Reanalysis monthly maximum chlorophyll-a concentration throughout the water column for 2010 an intermediate stratification year (Copernicus Marine Service, 2024b)	40
Plate 4.7 Copernicus Reanalysis monthly maximum chlorophyll-a concentration throughout the water column for 2015 a weaker stratification year (Copernicus Marine Service, 2024b)	41
Plate 5.1 Bedform morphology within the OAA	57
Plate 5.2 Baseline residual sediment transport rate and direction, for 250 μ m quartz sand, predicted over a representative Spring-neap tidal period (ABPmer, 2025b)	62
Plate 6.1 Aerial imagery of the landfall at Scotstown (Google, no date)	72
Plate 6.2 Aerial imagery of the landfall at Lunderton (North & South) (Google, no date)	73

Figure 1 Marine geology, oceanography and physical processes study area	8
Figure 2 Data locations	12
Figure 3 Seabed sediments within the OAA, offshore export cable corridor and across the wider study area	45
Figure 4 Surficial sediment thickness within the OAA and offshore export cable corridor	50
Figure 5 Morphological features within the study area	52
Figure 6 Bathymetry across the OAA	55
Figure 7 Bedforms mapped within the OAA	56
Figure 8 Bathymetry within the offshore export cable corridor	59
Figure 9 Bedforms mapped within the offshore export cable corridor	60
Figure 10 Bedform migration analysis within the offshore export cable corridor over the period 2009 (UKHO) to 2023 (Project)	64
Figure 11 Bathymetric change within the offshore export cable corridor over the -period 2009 (UKHO) to 2022-2023 (Project)	65
Figure 12 Conceptual understanding of physical processes within the study area	68
Figure 13 Coastal characteristics within the study area	70
Figure 14 Projected future MHWS change at the landfall	74

1. Introduction

1.1 Overview

1.1.1.1 This Appendix describes the baseline marine geology, oceanography and physical processes conditions within the physical processes study area in the absence of any of any offshore wind farm infrastructure. The baseline understanding is used to inform **Volume 1, Chapter 6: Marine Geology, Oceanography and Physical Processes** of the MarramWind Offshore Wind Farm (hereafter referred to as 'the Project') Environmental Impact Assessment (EIA) Report.

1.2 Approach

1.2.1.1 Physical processes within the physical processes study area have been considered under the following categories:

- metocean regimes;
 - ▶ water levels;
 - ▶ currents;
 - ▶ wind and waves; and
 - ▶ stratification and frontal systems;
- sediments, morphology, sediment transport and seabed mobility; and
- coastlines, beaches and nearshore processes.

1.2.1.2 The natural variability of the above is explored in the absence of any of the proposed structures for the development. Consequently, this provides the 'baseline' conditions within the physical processes study area upon which impacts from the Project can be assessed.

1.2.1.3 Baseline understanding has been developed in accordance with industry best practice, with attention given to:

- the identification of the processes maintaining the system, the reasons for any past changes, and sensitivity of the system to changes in the controlling processes;
- the identification and quantification of the relative importance of high-energy, low frequency ('episodic' events), versus low-energy, high frequency processes;
- the identification of the processes controlling temporal and spatial morphological change (for example, longevity and stability of bedforms; cliff recession; loss of beach volume; or bank and channel migration; intertidal accretion / erosion), which may require a review of bathymetric and topographic data;
- the identification of sediment sources, pathways and sinks, and quantification of transport fluxes;
- the identification of the inherited geological, geophysical and geotechnical properties of the sediments at the study area, and the depth of any sediment strata;
- the interaction of waves and tides and the subsequent quantification of the extent to which seabed sediment is mobilised; and
- the assessment of the scales and magnitudes of processes controlling sediment transport rates and pathways.

1.2.1.4 This report accompanies **Volume 1, Chapter 6: Marine Geology, Oceanography and Physical Processes** of the EIA Report to support the consent application for the Project.

1.3 Physical processes study area

1.3.1.1 The study area for the marine geology, oceanography, and physical processes assessment has previously been presented within the Project Scoping Report (MarramWind Limited, 2023) and is also shown in **Figure 1**. It includes the Option Agreement Area (OAA), the offshore export cable corridor, and the wider surrounding marine area across which potentially significant effects could occur.

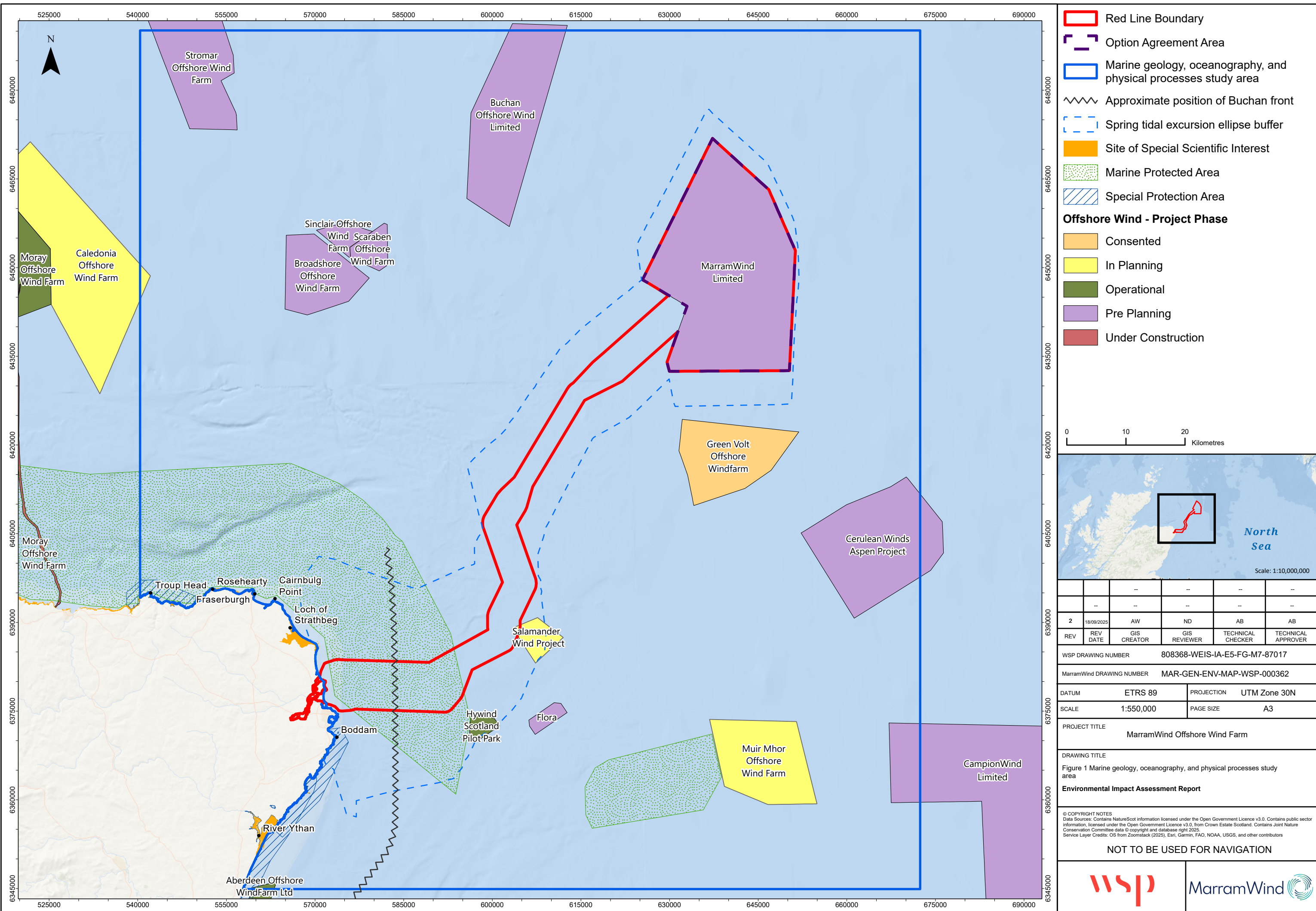
1.3.1.2 The study area has been informed by expert judgement, based on understanding of region-scale marine geology, oceanography, and physical processes, in particular that of the prevailing wave direction, tidal excursion distances and sediment transport pathways.

1.3.1.3 The physical processes study area is located off the north-east coast of Aberdeenshire (**Figure 1**). It has been defined on the basis of:

- The distance away from the Project which suspended sediment plumes may be advected (and interact with potentially sensitive receptors). This has been defined by a Spring tidal excursion ellipse buffer around the OAA and offshore export cable corridor.
- The distance up / down drift from the landfall, that littoral processes could theoretically be impacted by offshore infrastructure associated with the Project. This has been defined through consideration of coastal sub-cell information set out in Ramsay and Brampton (2000a; 2000b).
- The distance from the OAA that wave blockage impacts could theoretically be detected. This has been informed by expert judgement, drawing upon (amongst other things), the evidence base from other projects and consideration of the prevailing wave directions.

1.3.1.4 Direct changes to the seabed will be confined to the OAA and offshore export cable corridor, with indirect changes (for example, due to disruption of waves, tides or sediment pathways) experienced both inside and outside of the site boundary. These indirect changes are expected to diminish with distance from the OAA and offshore export cable corridor.

1.3.1.5 The study area overlaps with several nationally and internationally designated nature conservation sites, some of which are designated on the basis of the geological and geomorphological features contained within them. These include the Southern Trench Marine Protected Area (MPA) and Rosehearty to Fraserburgh Coast Site of Special Scientific Interest (SSSI), both designated in part for the geodiversity features they contain.



2. Methodology

2.1.1.1 This Appendix has used a combination of site specific surveys undertaken for the Project and publicly available data to inform the assessment. This Section outlines these various data sources and locations.

2.2 Desk study

2.2.1.1 Information on marine geology, oceanography, and physical processes within the study area was collected through a detailed desktop review of existing studies; datasets used to inform the analysis are summarised in **Table 2.1**, with locations provided in **Figure 2**.

Table 2.1 Data sources used to inform the marine geology, oceanography and physical processes baseline

Source	Date	Summary	Coverage of study area
Marine Directorate data portal	Data accessed: 2025.	Data layers of bathymetry, ocean climate, waves, sea level, seabed geology, surface and subtidal sediments. (Available at: www.marine.gov.scot).	Partial coverage of the study area.
Scottish Environment Protection Agency (SEPA)	Data accessed: 2025.	A range of datasets related to the environment including flood risk management. (Available at: https://www.sepa.org.uk/).	Partial coverage of the study area.
National Tide and Sea Level Facility	Data accessed: 2025.	Tidal water levels from point locations within the study area. (Available at: www.ntslf.org).	Partial coverage of the study area.
British Oceanographic Data Centre	Data accessed: 2025.	Hydrodynamic (HD) data (inc. current speed and direction) from point locations within the study area. (Available at: www.bodc.ac.uk/).	Partial coverage of the study area.
Centre for Environment, Fisheries and Aquaculture Science (Cefas) WaveNet data	Data accessed: 2025.	Wave records from point locations within the study area. (Available at: www.cefas.co.uk/cefas-data-hub/wavenet/).	Partial coverage of the study area.
ABP Marine Environmental Research Ltd (ABPmer) SEASTATES	1979 to 2022.	Modelled hindcast wave and HD data from across the study area. (Available at: www.seastates.net/).	Full coverage of the study area.
Marine Renewables Atlas	2008	Modelled hindcast wave and HD data from across the study area (Available at: https://www.renewables-atlas.info/).	Full coverage of the study area.

Source	Date	Summary	Coverage of study area
UK Climate Projections 2018 (UKCP18)	2018	Sea level rise predictions for coastal locations within the study area. (Palmer <i>et al.</i> , 2018).	Partial coverage of the study area.
Suspended Particulate Matter (SPM) mapping	2016	Monthly and seasonal SPM maps for the study area. (Cefas, 2016).	Full coverage of the study area.
Copernicus Marine Service	Data accessed: 2025.	Three-dimensional numerical model outputs of temperature, salinity and chlorophyll-a. (Available at: https://data.marine.copernicus.eu/products)	Full coverage of the study area.
British Geological Survey (BGS) offshore geoindex	Data accessed: 2025.	Seabed sediment maps (based on Folk classification) and borehole records from point locations within the study area. (Available at: www.bgs.ac.uk/GeoIndex/offshore.htm).	Partial coverage of the study area.
United Kingdom Hydrographic Office (UKHO) bathymetric data	2009	Bathymetric data for the study area in the form of multibeam and single beam data, as well as Admiralty Charts. (Available at: https://seabed.admiralty.co.uk/).	Full coverage of the study area.
European Marine Observation and Data Network data layers	Data accessed: 2025.	Bathymetric data for the study area and surrounding regions in the form of a continuous surface made of survey data from various European National Hydrographic Offices. (Available at: https://emodnet.ec.europa.eu/geoviewer/).	Full coverage of the study area.
MPA Geodiversity Mapping	2011	Mapping of geological and geomorphological features within Scottish MPAs, based on publicly available seabed surveys and research (Brooks <i>et al.</i> , 2011).	Partial coverage of the study area.
Dynamic Coast (Phase 1 & 2)	2017, 2021.	The Dynamic Coast project aims to provide the strategic evidence base on the extent of coastal erosion in Scotland. (Available at: www.dynamiccoast.com/).	Partial coverage of the study area.
Coastal Cells in Scotland: sub-cell 2d (Cairnbulg Point to Girdle Ness) and sub-cell 3a (Portknockie to Cairnbulg Point)	2000	Description of coastal characteristics (geology and geomorphology) and processes controlling change (Ramsay and Brampton, 2000a; 2000b).	Partial coverage of the study area.
Scottish Coastal Observatory (SCO)	Data accessed: 2025.	Monitoring data collected as part of the SCO, covering a range of marine environmental variables including temperature and salinity. (Available at: www.sco.ac.uk/).	Partial coverage of the study area.

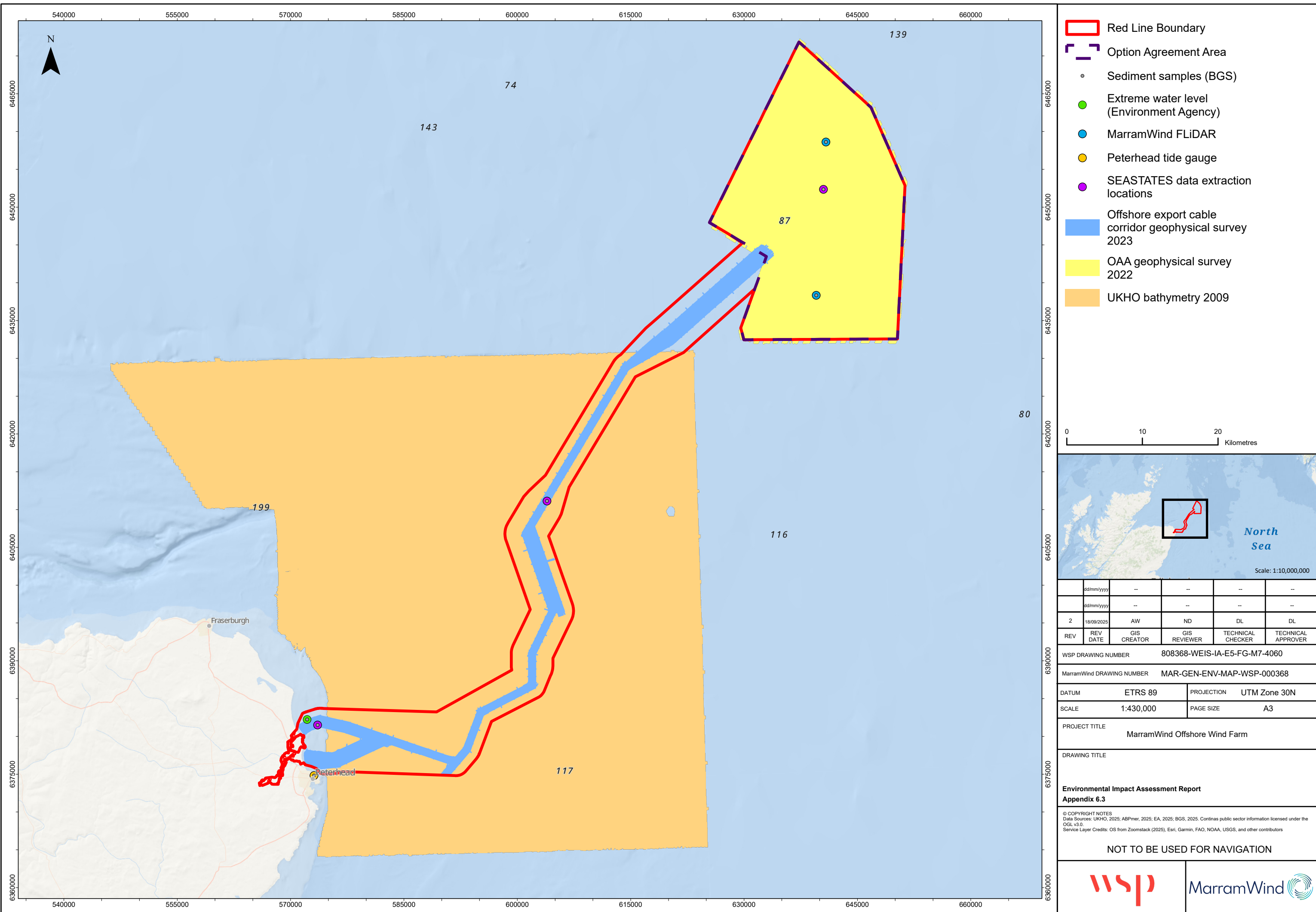
Source	Date	Summary	Coverage of study area
		https://marine.gov.scot/?q=data/scottish-coastal-observatory-data .	
Scottish Remote Sensing Portal	Data accessed: 2025.	LiDAR datasets to inform past coastal change. (Available at: https://remotesensingdata.gov.scot/).	Partial coverage of the study area.
(Key publications)	[various]	Public and grey literature considering coastal morphology and behaviour at sensitive coastal locations within the study area for example, Hansom <i>et al.</i> (2004) and Baxter <i>et al.</i> (2011).	Partial coverage of the study area.

2.3 Study area surveys

2.3.1.1 A summary of the surveys undertaken to inform the marine geology, oceanography, and physical processes baseline is outlined in **Table 2.2** below, with locations provided in **Figure 2**.

Table 2.2 Surveys undertaken to inform the marine geology, oceanography and physical processes baseline

Survey type	Scope of survey	Coverage of study area
OAA and offshore export cable corridor geophysical and environmental survey (Fugro, 2023a; 2023b). Year of survey: 2022-2023.	High resolution side scan sonar (SSS), multibeam bathymetry and sub-bottom profile data.	Full coverage of the OAA and partial coverage of the offshore export cable corridor.
Metocean survey (Fugro, 2023c). Year of survey: 2022-2023.	Wind speed, wave and current data from 20 September 2022 to 20 September 2023 FLiDAR buoys deployed within the OAA.	Partial coverage of the OAA.
Appendix 10.2: Environmental Intertidal Survey - Benthic Report 2023 Year of survey: 2023.	Mapping of inter-tidal biotopes. Sediment cores and contaminant sampling also undertaken.	Full coverage of the landfall (Scotstown Beach and Lunderton Beach).



3. Metocean Regime

3.1.1.1 This Section uses modelled and measured data to describe the baseline metocean conditions in the study area, including: water levels, currents, winds and waves and predicted future change.

3.2 Water levels

3.2.1.1 The physical processes study area is located within a semi-diurnal tidal environment with a tidal range increasing from north-east to south-west. Within the OAA, the Spring tidal range is typically between approximately 1.7 metres (m) to 1.9m, with a neap range of approximately 0.8m. Tidal range increases with proximity to the coast along the offshore export cable corridor, reaching approximately 3.1m at the landfall zones (ABPmer *et al.*, 2008).

3.2.1.2 Summary tidal statistics Peterhead (to the south-west of the OAA and to the south of the landfall) are shown in **Table 3.1**.

Table 3.1 Summary tidal statistics for Peterhead (UKHO, 2025a)

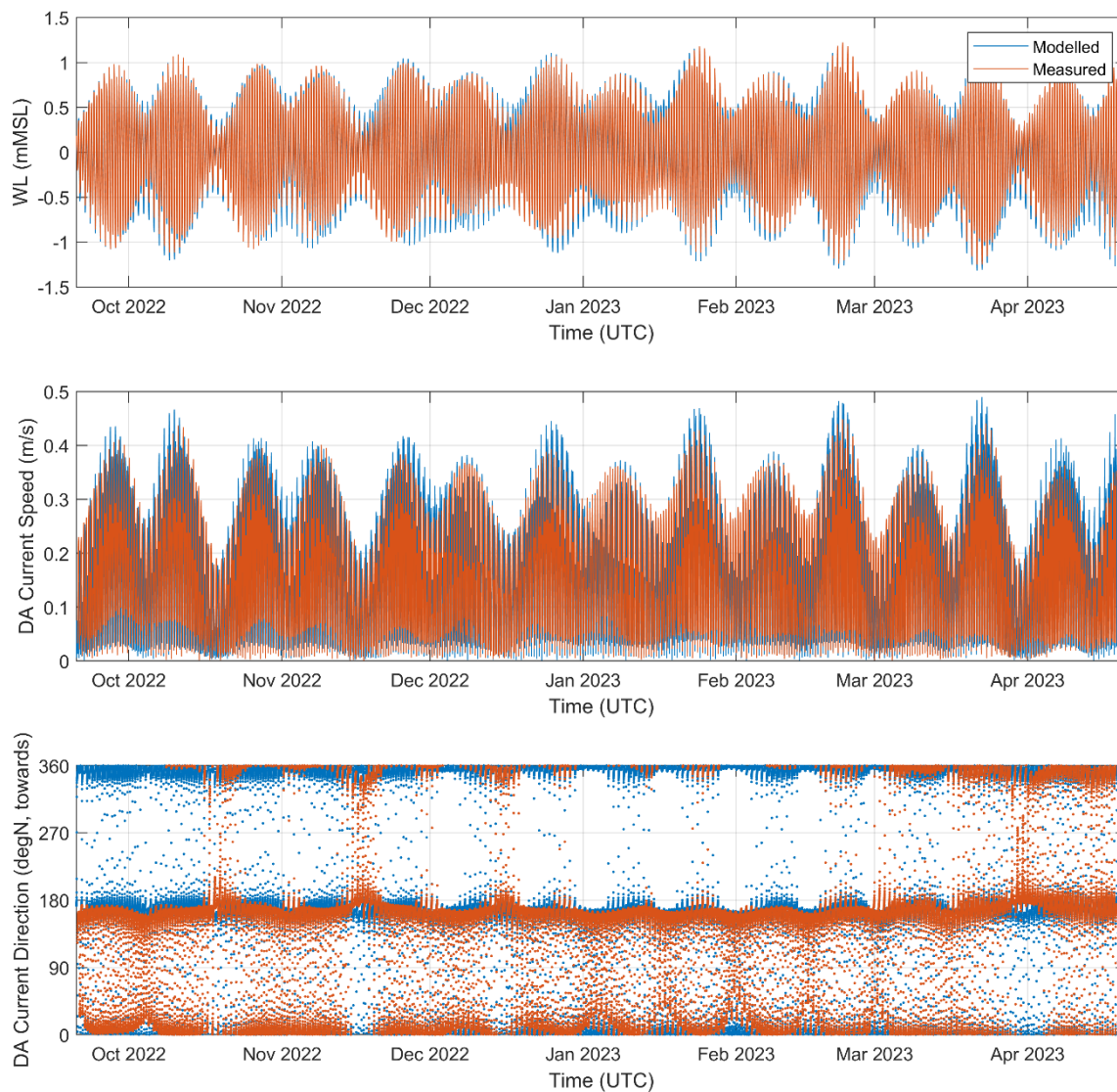
Water Level	Peterhead (m Chart Datum (CD))	Peterhead (m Ordnance Datum Newlyn (ODN))
Highest Astronomical Tide	4.4	2.23
Mean High Water Spring (MHWS) tide	4.0	1.83
Mean high water neap tide	3.2	1.03
Mean tide level	2.45	0.28
Mean low water neap tide	1.6	-0.57
Mean low water spring tide	0.7	-1.47
Lowest Astronomical Tide (LAT)	0.1	-2.07
Mean Spring range	3.3	
CD to ODN	-2.17	

3.2.1.3 Extreme water levels within the physical processes study area typically result from storm surge propagation in the North Sea are generally well understood, having been extensively studied. In brief, a storm surge is produced when high winds build up a wall of water, further exacerbated by the effects of atmospheric pressure (Prichard, 2013). The 50-year return period surge level (tide + surge) at the landfall is predicted to be 2.74mODN (Environment Agency, 2019). The impact of a surge will depend critically on the associated state of the tide with the biggest risk of flooding and erosion occurring if the surge peak coincides with high water on a Spring tide.

3.3 Currents

3.3.1.1 Modelled baseline tidal current speed and direction information is available for the study area from ABPmer's SEASTATES Northwest European Shelf Hindcast model (ABPmer, 2017). This HD model is in good agreement with the measured data collected from the OAA over the period September 2022 to May 2023 (Fugro, 2023c) – this is illustrated in **Plate 3.1** which shows timeseries comparison plots of the modelled and measured water levels, current speeds and directions. The visual comparison shows the general levels, shape and phasing of the tide is reproduced very well. Some minor differences are observed, where the model simply cannot be calibrated further to simultaneously reproduce all details of all tides at all locations. Some differences may also be the result of local effects of complex bathymetry that are either not represented in the available bathymetry data, or not fully resolved by the resolution of the model.

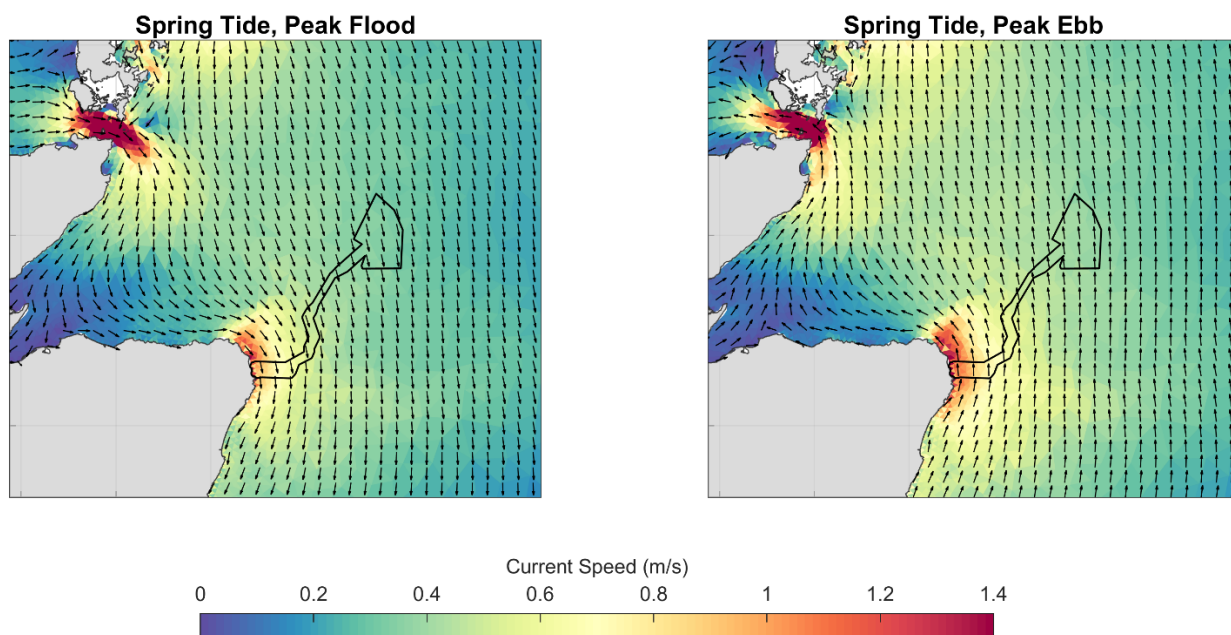
Plate 3.1 Comparison of water level (top), depth-averaged current speed (middle), and depth-averaged current direction (bottom) between the metocean deployment (Fugro, 2023c) and ABPmer HD model (ABPmer, 2017)



3.3.1.2 Maps of surface current speeds (and directions) during peak flood and peak ebb on a representative mean Spring tide are shown in **Plate 3.2**, based on modelled output from ABPmer's SEASTATES Northwest European Shelf Hindcast model (ABPmer, 2017).

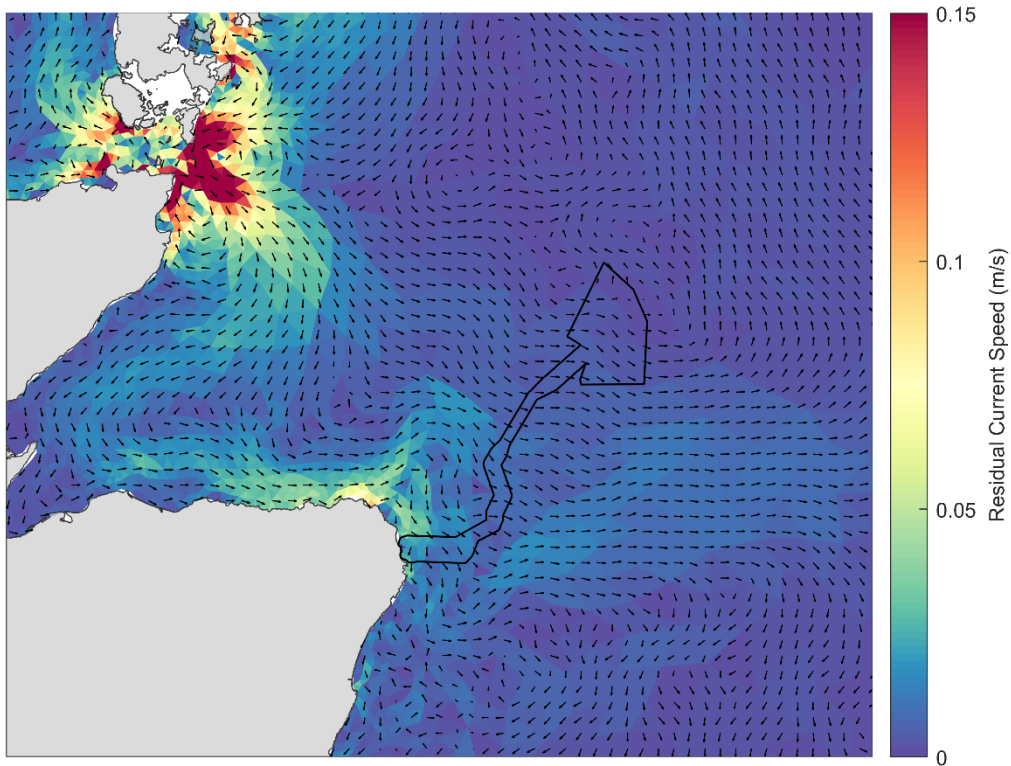
3.3.1.3 Within the physical processes study area, tidal currents are relatively weak, with mean Spring peak current speeds typically less than approximately 0.6 metres per second (m/s). Within the OAA, flow direction is approximately northwards during the ebb tide and south south-east during the flood tide. The strongest currents within the physical processes study area are found off Cairnbulg Point, immediately to the north of the landfall.

Plate 3.2 Baseline tidal current speed and direction during a representative Spring tidal condition (ABPmer, 2017)



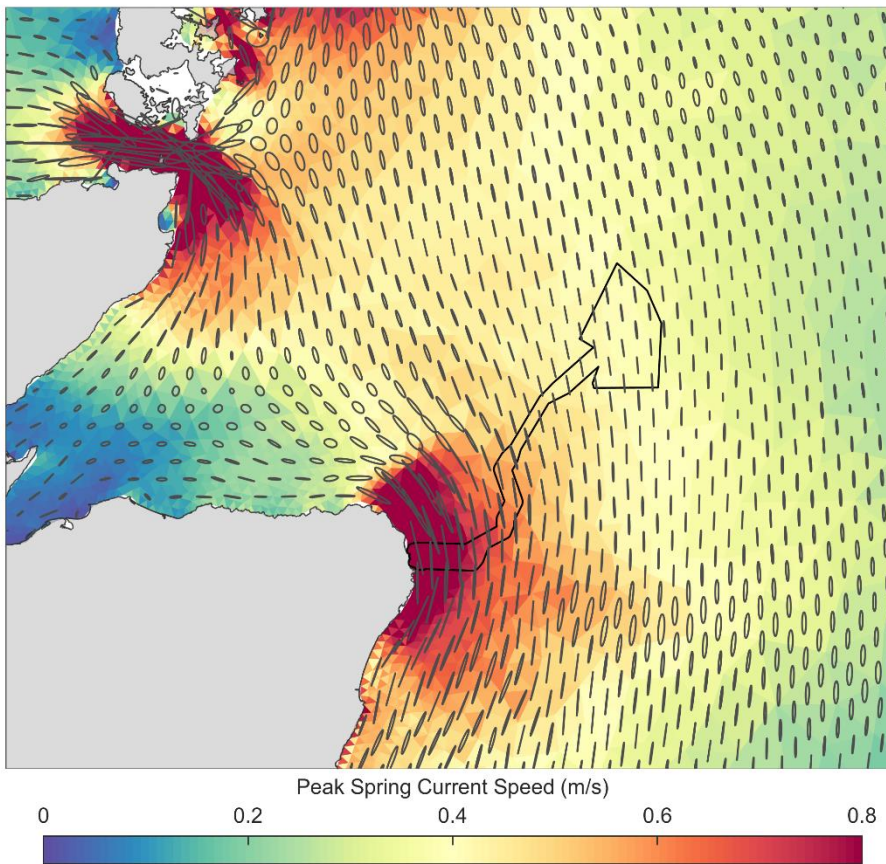
3.3.1.4 **Plate 3.3** shows modelled residual tidal flow across the physical processes study area. Finer sediment held in suspension will generally be transported in the direction of residual current flow and this is, therefore, an important consideration for the assessment of sediment plumes associated with construction-related activities. On the basis of **Plate 3.3**, residual flow fields are found to be relatively weak and variable across the physical processes study area. This is also the case within the OAA and along the offshore export cable corridor; the residual transport direction shows local variability, with the general trend being between southward and eastward.

Plate 3.3 Baseline residual tidal current speed and direction calculated over a representative Spring-neap period (ABPmer, 2017)



3.3.1.5 Spring tidal excursion ellipses are show in **Plate 3.4**. These ellipses show the approximate displacement path of water during a representative tidal cycle and so illustrate the spatial variation in the orientation of the tidal axis, the degree of directional rotation and the magnitude of tidal current speed. In general, tidal flow is rectilinear across the offshore export cable corridor and OAA, with Spring tidal excursion distances of approximately 10 kilometres (km) and with a north-northwest to south south-east axis.

Plate 3.4 Baseline peak Spring current speed and Spring tidal excursion ellipses (ABPmer, 2017)

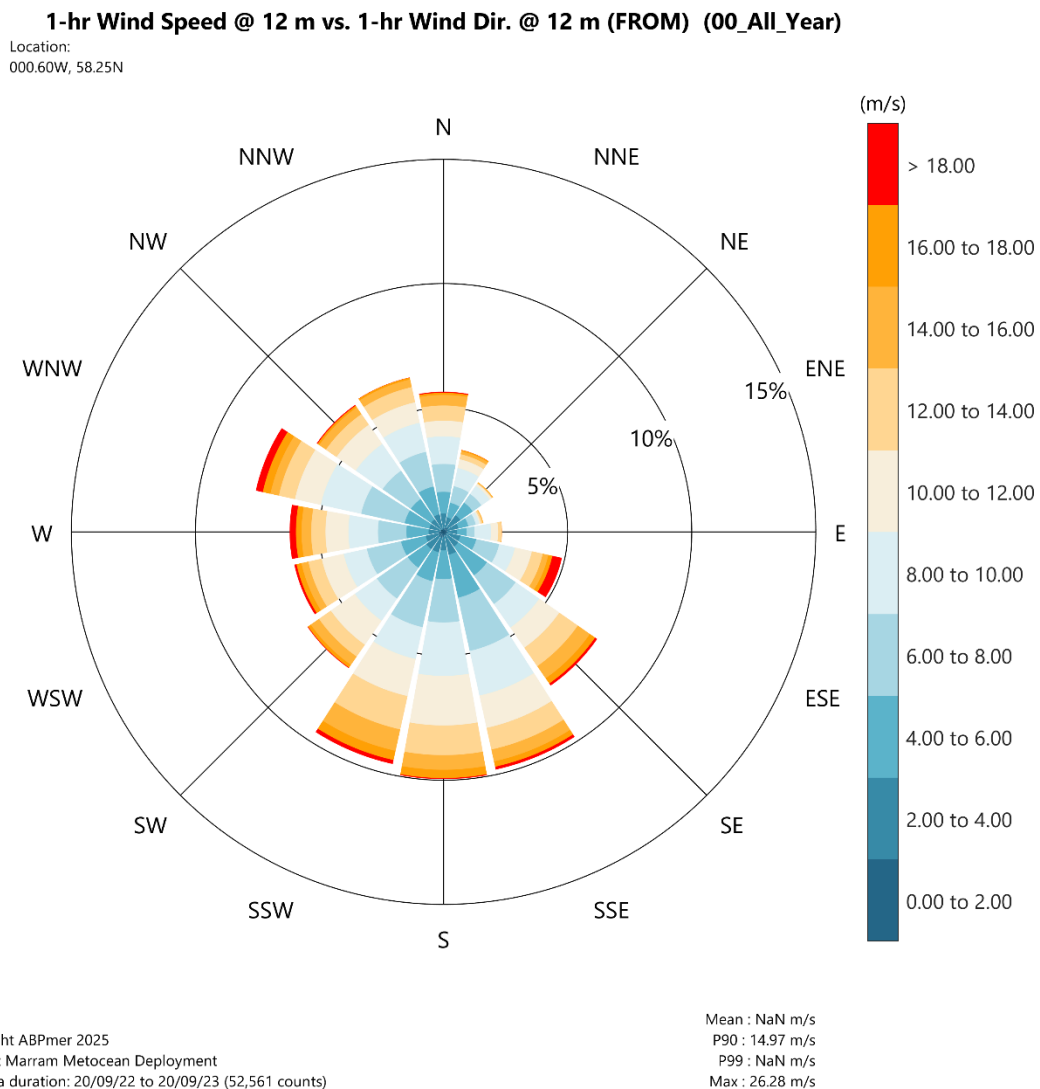


3.4 Winds

3.4.1.1 An understanding of the wind climate is relevant to physical processes in so far as it is a controlling parameter in the prevailing wave regime and non-tidal water levels and currents. The relationship between wave generation and meteorological forcing means that the wind and wave regimes are similarly episodic and exhibit both seasonal and inter-annual variation in proportion with the frequency and magnitude of changes in wind strength and direction.

3.4.1.2 A long-term hindcast record of wind data within the physical processes study area is available from ABPmer SEASTATES Northwest European Shelf Wave Hindcast Model (ABPmer, 2013; 2025a). This data has been compared with the 12 months of wind data collected from the study area between September 2022 to September 2023, which is summarised in **Plate 3.5**. This shows relatively close agreement to the wind rose produced from the modelled hindcast timeseries extracted for a location representative of the OAA, with dominant wind directions during the measured period from the south south-east to south south-west.

Plate 3.5 Rose plot of wind speed and direction for the metocean deployment location, over the period 2022-2023 (directions indicate 'coming from') (ABPmer, 2025a)



3.4.1.3 A frequency analysis of the ABPmer SEASTATES long-term hindcast data is presented as a wind rose in **Plate 3.6**, along with frequency scatter tables of wind speed against direction in **Table 3.2**, **Table 3.3** and **Table 3.4** (for the landfall, the offshore export cable corridor and the OAA, respectfully). These show that:

- the dominant wind directions are from the south and south south-west, with winds occurring from these directions for around 20% of the time;
- the strongest winds observed in the record most commonly occur from south-southwesterly directions; and
- the maximum observed wind speeds in the records are 31.22m/s in the OAA, 32.23m/s along the offshore export cable corridor and 26.28m/s at the landfall.

Plate 3.6 Rose plot of wind speed and direction for the OAA, 1979-2022 (ABPmer, 2025a)

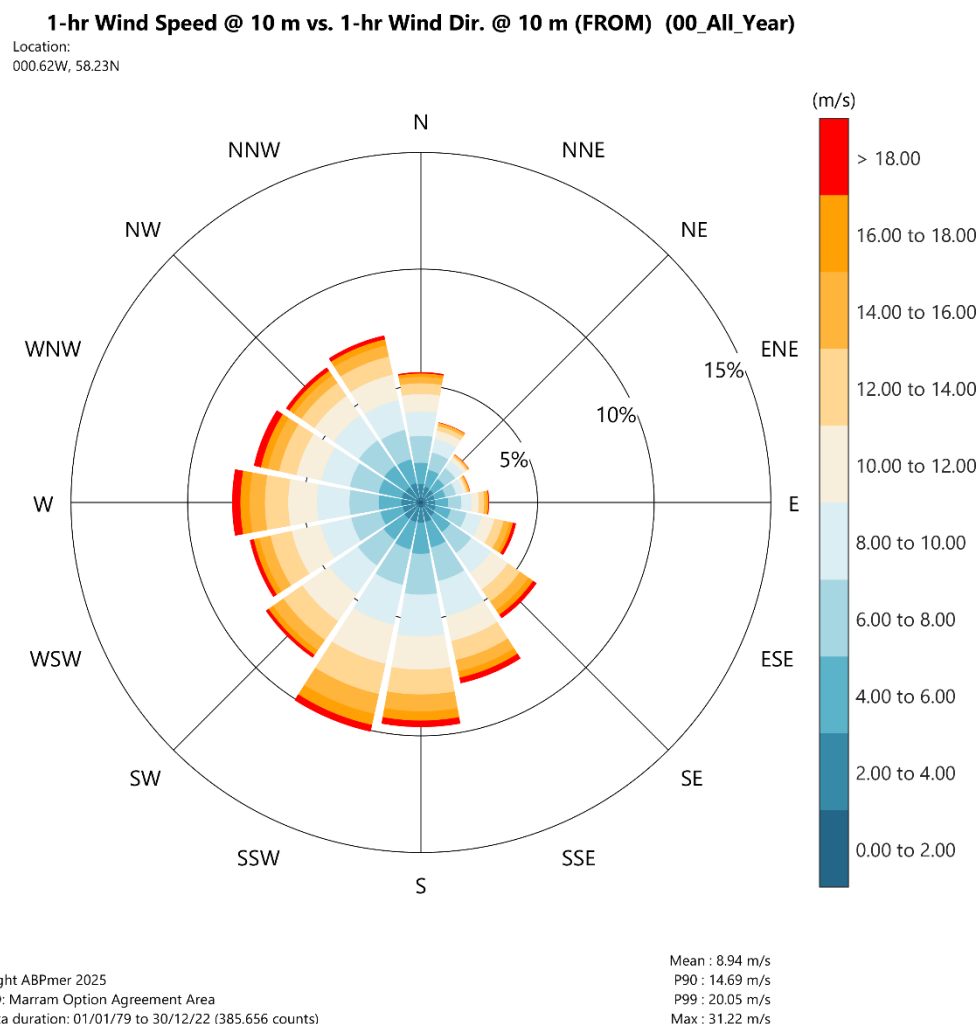


Table 3.2 Frequency scatter tables of wind speed vs wind direction – landfall (ABPmer, 2025a)

Marram Landfall - Wind Speed Wind Direction Scatter Table - All Data - Percentage (occurrences as proportion of all data)														
WindSpeed_10 (m/s)	WindDir_10 (degN, Coming)													
	Lower (>=)		337.5	22.5	67.5	112.5	157.5	202.5	247.5	292.5		Cum. Sum	Exced.	
	Upper (<)		22.5	67.5	112.5	157.5	202.5	247.5	292.5	337.5	Sum	Cum. Sum	Exced.	
	28	30										100.00	0.00	
	26	28								0.00	0.00	0.00	100.00	0.00
	24	26	0.00						0.00	0.00	0.00	0.00	100.00	0.00
	22	24	0.00						0.00	0.00	0.00	0.01	100.00	0.00
	20	22	0.00		0.00	0.00	0.01	0.00	0.02	0.01	0.04	99.99	0.01	
	18	20	0.01	0.00	0.00	0.01	0.03	0.01	0.04	0.04	0.16	99.94	0.06	
	16	18	0.04	0.01	0.02	0.07	0.12	0.03	0.10	0.12	0.50	99.79	0.21	
	14	16	0.13	0.03	0.07	0.19	0.37	0.13	0.30	0.34	1.56	99.28	0.72	
	12	14	0.33	0.07	0.16	0.49	0.92	0.36	0.60	0.74	3.67	97.72	2.28	
	10	12	0.60	0.12	0.34	0.95	1.97	1.00	1.31	1.45	7.74	94.05	5.95	
	8	10	1.23	0.27	0.59	1.67	3.28	2.29	2.51	2.54	14.39	86.31	13.69	
	6	8	1.82	0.66	0.91	2.60	5.14	3.91	3.58	3.49	22.10	71.92	28.08	
	4	6	2.36	1.17	1.37	3.24	5.38	4.45	3.61	3.36	24.94	49.81	50.19	
	2	4	2.13	1.40	1.55	2.51	3.32	3.02	2.52	2.30	18.77	24.87	75.13	
	0	2	0.71	0.71	0.73	0.82	0.84	0.81	0.76	0.73	6.11	6.11	93.89	
Sum		9.37	4.46	5.74	12.56	21.36	16.02	15.36	15.13	100.00				

Table 3.3 Frequency scatter tables of wind speed vs wind direction – offshore export cable corridor (ABPmer, 2025a)

Marram offshore export cable corridor - Wind Speed Wind Direction Scatter Table - All Data - Percentage (occurrences as proportion of all data)													
WindSpeed_10 (m/s)	WindDir_10 (degN, Coming)												
	Lower (>=)		337.5	22.5	67.5	112.5	157.5	202.5	247.5	292.5		Cum. Sum	Exced.
	Upper (<)		22.5	67.5	112.5	157.5	202.5	247.5	292.5	337.5	Sum	Cum. Sum	Exced.
	34	36										100.00	0.00
	32	34								0.00	0.00	100.00	0.00
	30	32	0.00						0.00		0.00	100.00	0.00
	28	30	0.00					0.00	0.00	0.00	0.01	100.00	0.00
	26	28	0.00					0.00	0.01	0.00	0.01	99.99	0.01
	24	26	0.00	0.00		0.00	0.01	0.00	0.03	0.02	0.06	99.98	0.02
	22	24	0.01	0.00	0.00	0.02	0.03	0.01	0.04	0.04	0.17	99.91	0.09
	20	22	0.03	0.01	0.02	0.06	0.11	0.04	0.13	0.09	0.49	99.75	0.25
	18	20	0.10	0.02	0.05	0.18	0.27	0.11	0.29	0.26	1.30	99.26	0.74
	16	18	0.25	0.06	0.12	0.33	0.67	0.30	0.51	0.48	2.73	97.96	2.04
	14	16	0.51	0.10	0.24	0.68	1.33	0.72	1.01	0.88	5.46	95.23	4.77
	12	14	0.85	0.15	0.43	1.10	2.11	1.59	1.70	1.44	9.36	89.77	10.23
	10	12	1.34	0.35	0.59	1.57	3.08	2.69	2.40	2.20	14.21	80.41	19.59
	8	10	1.72	0.69	0.83	2.14	3.99	3.35	2.77	2.60	18.09	66.20	33.80
	6	8	2.00	1.05	1.10	2.40	3.93	3.14	2.69	2.60	18.90	48.11	51.89
	4	6	1.87	1.09	1.11	2.00	3.01	2.45	2.06	2.20	15.80	29.21	70.79
	2	4	1.20	0.94	0.97	1.28	1.54	1.44	1.28	1.32	9.97	13.41	86.59
	0	2	0.40	0.42	0.41	0.45	0.46	0.44	0.44	0.41	3.43	3.43	96.57
Sum		10.30	4.89	5.89	12.22	20.53	16.29	15.36	14.53	14.53	100.00		

Table 3.4 Frequency scatter tables of wind speed vs wind direction – OAA (ABPmer, 2025a)

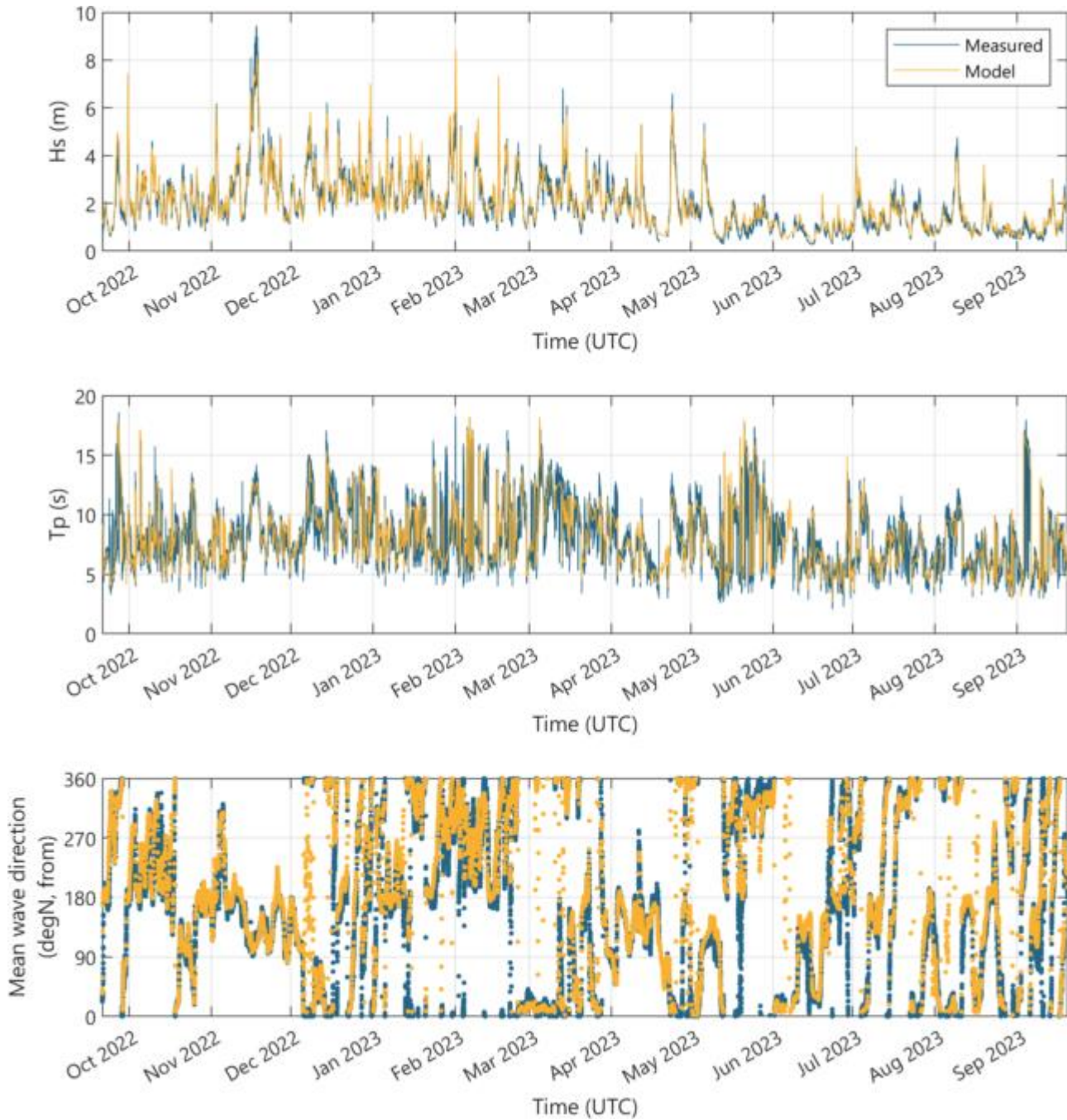
Marram Option Agreement Area - Wind Speed Wind Direction Scatter Table - All Data - Percentage (occurrences as proportion of all data)														
WindSpeed_10 (m/s)	WindDir_10 (degN, Coming)													
	Lower (>=)		337.5	22.5	67.5	112.5	157.5	202.5	247.5	292.5		Cum. Sum	Exced.	
	Upper (<)		22.5	67.5	112.5	157.5	202.5	247.5	292.5	337.5	Sum	Cum. Sum	Exced.	
	32	34										100.00	0.00	
	30	32							0.00	0.00	0.00	0.00	100.00	0.00
	28	30	0.00	0.00					0.00	0.00	0.00	0.01	100.00	0.00
	26	28	0.00					0.00	0.00	0.01	0.01	0.03	99.99	0.01
	24	26	0.00	0.00	0.00	0.01	0.02	0.01	0.03	0.02	0.09	99.96	0.04	
	22	24	0.01	0.00	0.01	0.03	0.05	0.02	0.07	0.04	0.23	99.88	0.12	
	20	22	0.04	0.01	0.02	0.10	0.16	0.08	0.17	0.10	0.67	99.64	0.36	
	18	20	0.10	0.02	0.06	0.25	0.37	0.24	0.34	0.25	1.63	98.97	1.03	
	16	18	0.28	0.05	0.15	0.42	0.81	0.56	0.70	0.50	3.47	97.35	2.65	
	14	16	0.57	0.11	0.26	0.85	1.42	1.19	1.24	0.86	6.50	93.88	6.12	
	12	14	0.98	0.18	0.44	1.27	2.14	2.14	1.87	1.44	10.45	87.38	12.62	
	10	12	1.56	0.38	0.65	1.74	2.82	2.92	2.48	2.09	14.65	76.93	23.07	
	8	10	2.02	0.79	0.89	2.12	3.50	3.02	2.69	2.58	17.60	62.28	37.72	
	6	8	2.19	1.14	1.11	2.15	3.33	2.74	2.52	2.62	17.80	44.68	55.32	
	4	6	1.83	1.15	1.11	1.70	2.53	2.21	1.93	2.16	14.63	26.88	73.12	
	2	4	1.17	0.92	0.86	1.07	1.36	1.31	1.26	1.27	9.22	12.25	87.75	
	0	2	0.38	0.38	0.34	0.39	0.38	0.38	0.39	0.39	3.03	3.03	96.97	
	Sum		11.14	5.12	5.89	12.09	18.88	16.82	15.71	14.34	100.00			

3.5 Waves

3.5.1.1 The wave climate is the result of the transfer of wind energy to the sea, creating seastates and the propagation of that energy across the water surface by wave motion. The amount of wind energy transfer and wind-wave development is a function of the available fetch distance across which the wind blows, wind speed, wind duration and the original state of the sea. The longer the fetch distance, the greater the potential there is for the wind to interact with the water surface and generate waves. In shallower water, water depth is an additional limiting factor on the size of waves.

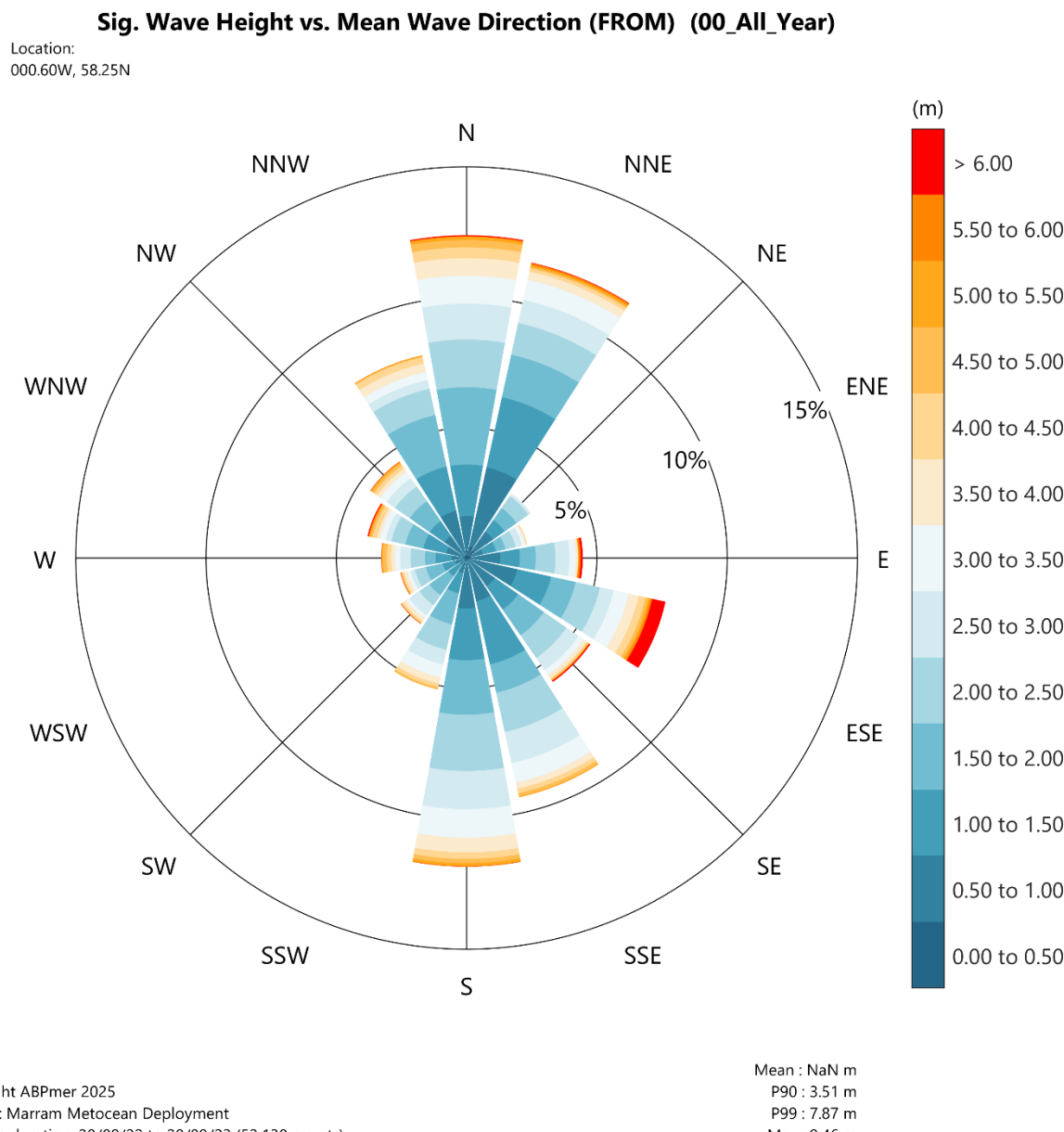
3.5.1.2 A long-term hindcast record of wave data is available for the physical processes study area from the ABPmer SEASTATES Northwest European Shelf Wave Hindcast Model (ABPmer, 2013), for the period 1979-2023. This hindcast data has been compared with the Project metocean data available for the OAA collected between September 2022 and September 2023 (Fugro, 2023c), with **Plate 3.7** showing timeseries comparison plots of the modelled and measured wave height, period and direction. The visual comparison shows the model performs well, satisfactorily capturing the magnitude and timing of a variety of wave event sizes. Some minor differences are observed, where the model simply cannot be calibrated further to simultaneously reproduce all details. Some differences may also be the result of local effects of complex bathymetry that are either not represented in the available bathymetry data, or not fully resolved by the resolution of the model.

Plate 3.7 Comparison of measured and modelled wave parameters within the OAA (ABPmer, 2025a; Fugro, 2023c)



3.5.1.3 **Plate 3.8** shows a wave rose summarising significant wave height and mean wave direction for the 12-month period of the metocean deployment (September 2022 to September 2023). This shows close agreement to the wave rose produced from the modelled hindcast timeseries extracted for a location representative of the OAA.

Plate 3.8 Rose plot of significant wave height and direction for the metocean deployment location, over the period 2022-2023 (directions indicate 'coming from') (ABPmer, 2025a)



3.5.1.4 The wave regime is dominated by locally generated wind waves across the wider North Sea region. The OAA is exposed to longer wave fetches (distances of open water over which waves can develop) from the north to north-east. Smaller, but more frequently occurring, wave conditions generated by local winds predominately come from southerly directions.

3.5.1.5 Across the wider physical processes study area, the local orientation of the coastline relative to the predominant wave direction will influence local conditions of sheltering, resulting sediment transport rates and directions.

3.5.1.6 The wave regime has been summarised in a series of wave roses **Plate 3.9 to Plate 3.11**, as well as frequency scatter tables of wave height, period and direction (**Table 3.5 to Table 3.10**).

3.5.1.7 This analysis shows that:

- The most frequent wave direction at the landfall is from the south-east which accounts for approximately 40% of the record. The largest significant wave height observed in the record was 7.42m.
- The most frequent wave direction along the offshore export cable corridor was from the north, accounting for 11% of the record. The largest significant wave height observed in the record at this location was 12.49m.
- The largest significant wave height observed in the record in the OAA was 12.99m. The most frequent wave direction at this location is also from the north (11% of the record). The next most frequent wave direction is from the south accounting for approximately 10.5% of the record.
- Longer period waves (peak wave period (T_p) \geq 8 seconds) are observed, accounting for approximately 38% of the record of peak wave periods at the landfall and increasing to around 45% in the OAA (Table 3.5 and Table 3.9).

Plate 3.9 Rose plot of significant wave height and direction near the landfall, over the period 1979-2023 (directions indicate 'coming from') (ABPmer, 2025a)

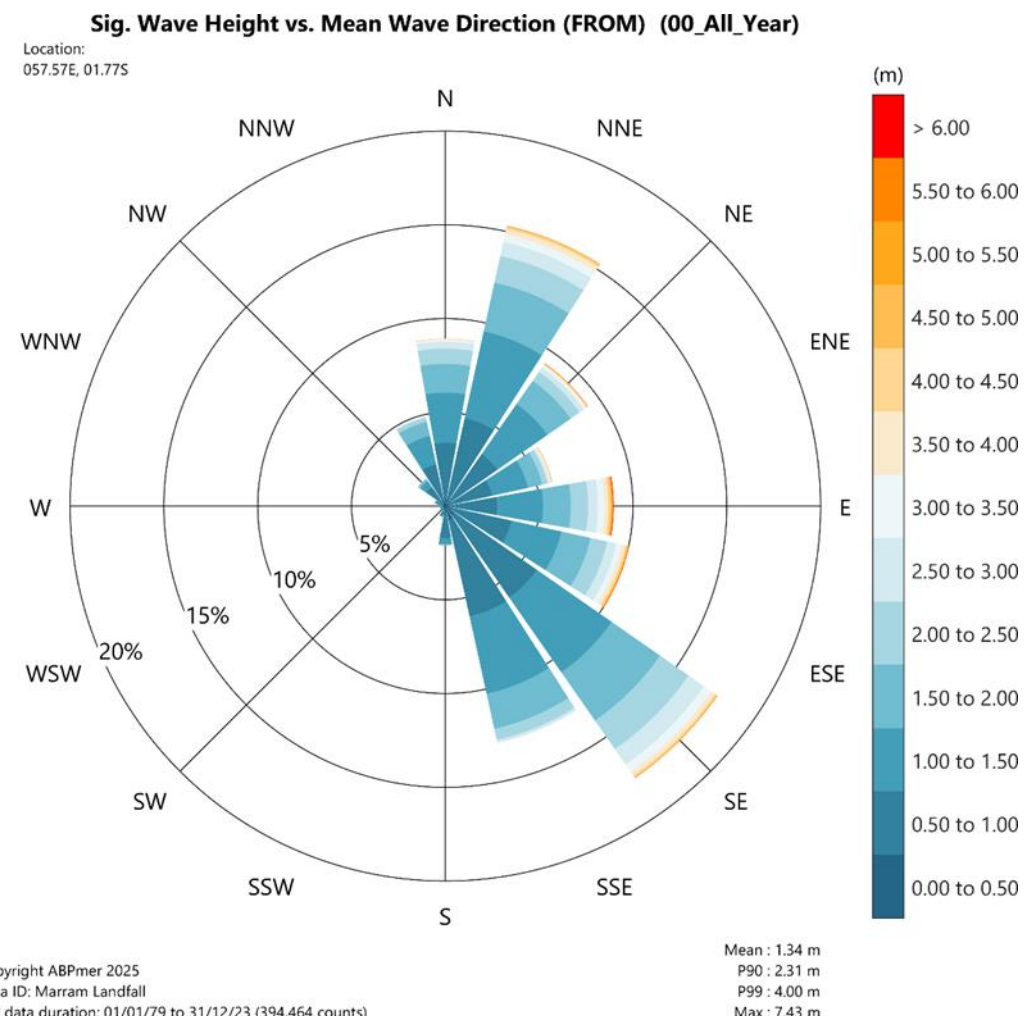


Plate 3.10 Rose plot of significant wave height and direction at a location representative of the offshore export cable corridor (middle), over the period 1979-2023 (directions indicate 'coming from') (ABPmer, 2025a)

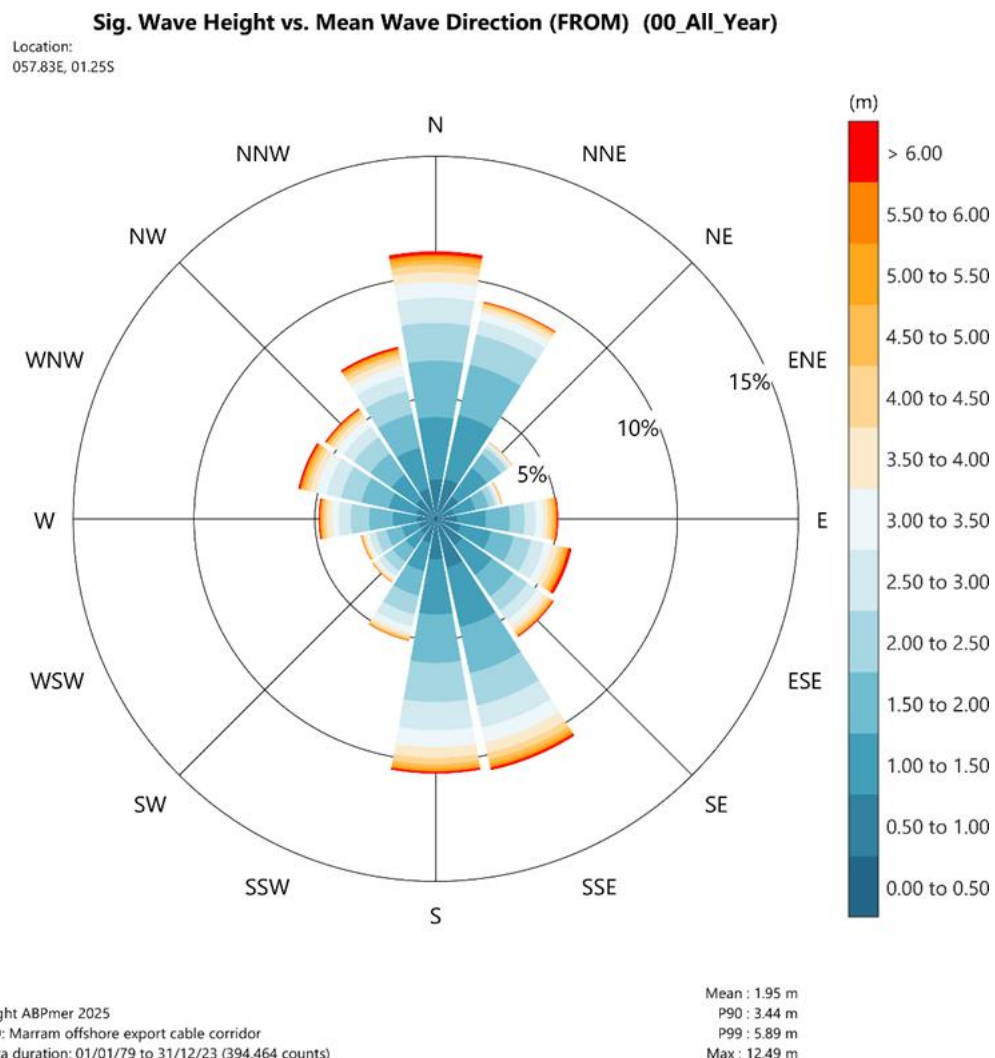


Plate 3.11 Rose plot of significant wave height and direction at a location representative of the OAA, over the period 1979-2023 (directions indicate 'coming from') (ABPmer, 2025a)

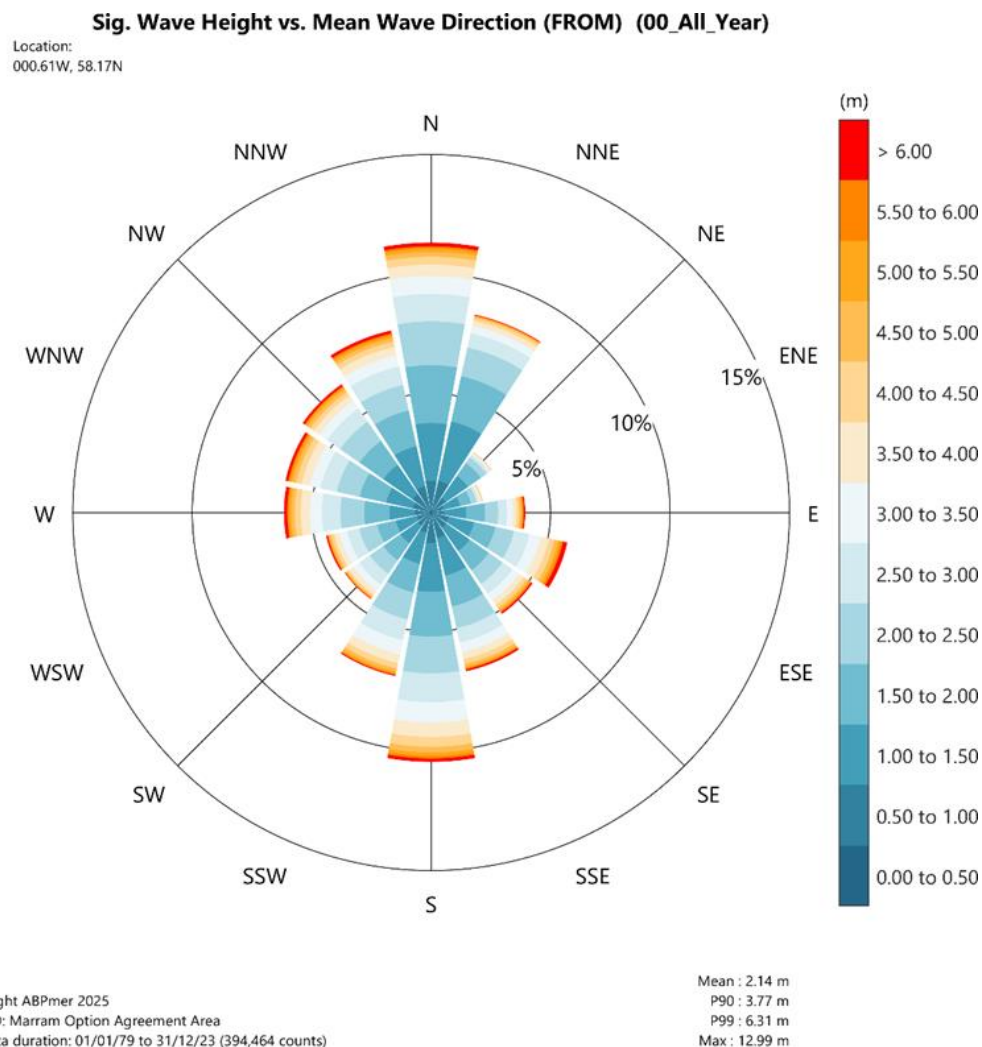


Table 3.5 Frequency scatter table of significant wave height vs peak wave period – landfall (ABPmer, 2025a)

Marram Landfall - Hs Tp Scatter Table - All Data - Percentage (occurrences as proportion of all data)																			
Significant Wave Height, Hs (m)	Peak Wave Period, Tp (s)														Sum	Cum. Sum	Exced.		
	0	2	4	6	8	10	12	14	16	18	20	22	24	26					
Lower (>=)	0	2	4	6	8	10	12	14	16	18	20	22	24	26					
Upper (<)	2	4	6	8	10	12	14	16	18	20	22	24	26	28	Sum	Cum. Sum	Exced.		
7.5	8.0															100.00	0.00		
7.0	7.5						0.01									0.01	100.00	0.00	
6.5	7.0					0.00	0.01	0.00								0.01	99.99	0.01	
6.0	6.5				0.00	0.02	0.01	0.00	0.00							0.04	99.98	0.02	
5.5	6.0			0.00	0.03	0.02	0.01	0.00								0.06	99.94	0.06	
5.0	5.5			0.00	0.09	0.02	0.01	0.00								0.13	99.88	0.12	
4.5	5.0				0.03	0.17	0.04	0.01	0.00	0.00						0.26	99.76	0.24	
4.0	4.5				0.00	0.14	0.29	0.06	0.01	0.01	0.00					0.51	99.50	0.50	
3.5	4.0				0.01	0.45	0.42	0.09	0.02	0.01	0.00					1.01	98.99	1.01	
3.0	3.5				0.10	1.16	0.55	0.12	0.03	0.02	0.00					1.99	97.98	2.02	
2.5	3.0			0.00	0.70	2.05	0.69	0.19	0.09	0.02	0.00	0.00				3.74	95.99	4.01	
2.0	2.5			0.06	2.68	3.32	0.98	0.40	0.19	0.04	0.01	0.01				7.68	92.25	7.75	
1.5	2.0		0.00	0.69	7.27	4.71	1.56	0.92	0.31	0.12	0.09	0.04	0.00			15.70	84.56	15.44	
1.0	1.5		0.01	4.86	14.35	5.02	2.73	1.29	0.49	0.39	0.24	0.07	0.01			29.47	68.86	31.14	
0.5	1.0		1.25	14.95	11.15	3.18	1.57	0.85	0.80	0.47	0.13	0.01	0.00	0.00		34.36	39.39	60.61	
0.0	0.5	0.00	1.20	2.68	0.50	0.26	0.14	0.13	0.07	0.03	0.01	0.00	0.00			5.03	5.03	94.97	
		Sum	0.00	2.47	23.24	36.78	20.33	9.25	4.15	2.04	1.10	0.48	0.14	0.02	0.00		100.00		
		Cumulative Sum	0.00	2.47	25.71	62.49	82.83	92.07	96.22	98.26	99.36	99.84	99.98	100.00	100.00		100.00		
		Exceedence	100.00	97.53	74.29	37.51	17.17	7.93	3.78	1.74	0.64	0.16	0.02	0.00	0.00				

Table 3.6 Frequency scatter table of significant wave height vs peak wave direction – landfall (ABPmer, 2025a)

Marram Landfall - Hs Mdir Scatter Table - All Data - Percentage (occurrences as proportion of all data)																		
Significant Wave Height, Hs (m)	Mean Wave Direction, Mdir (degN, Coming)														Sum	Cum. Sum	Exced.	
	337.5	22.5	67.5	112.5	157.5	202.5	247.5	292.5										
Lower (>=)																		
Upper (<)	22.5	67.5	112.5	157.5	202.5	247.5	292.5	337.5										
7.5	8.0															100.00	0.00	
7.0	7.5		0.00	0.00												0.01	100.00	0.00
6.5	7.0		0.00	0.01	0.00											0.01	99.99	0.01
6.0	6.5		0.00	0.03	0.01											0.04	99.98	0.02
5.5	6.0	0.00	0.01	0.03	0.01											0.06	99.94	0.06
5.0	5.5	0.00	0.02	0.08	0.02											0.13	99.88	0.12
4.5	5.0	0.02	0.06	0.11	0.06											0.26	99.76	0.24
4.0	4.5	0.06	0.11	0.20	0.14											0.51	99.50	0.50
3.5	4.0	0.15	0.23	0.34	0.29	0.00										1.01	98.99	1.01
3.0	3.5	0.33	0.42	0.58	0.66	0.00	0.00									1.99	97.98	2.02
2.5	3.0	0.75	0.74	0.85	1.38	0.00	0.00									3.74	95.99	4.01
2.0	2.5	1.68	1.44	1.52	2.92	0.04	0.01	0.01	0.08	0.08	7.68	92.25	7.75					
1.5	2.0	3.23	3.33	2.72	5.49	0.44	0.04	0.04	0.41	0.41	15.70	84.56	15.44					
1.0	1.5	5.61	7.01	4.68	9.11	1.79	0.10	0.10	1.07	1.07	29.47	68.86	31.14					
0.5	1.0	5.98	6.59	5.14	10.17	3.57	0.41	0.43	2.07	2.07	34.36	39.39	60.61					
0.0	0.5	0.88	0.65	0.53	1.26	0.88	0.17	0.17	0.49	0.49	5.03	5.03	94.97					
		Sum	18.68	20.61	16.82	31.52	6.72	0.74	0.76	4.14	4.14	100.00						

Table 3.7 Frequency scatter table of significant wave height vs peak wave period – offshore export cable corridor (ABPmer, 2025a)

Marram offshore export cable corridor - Hs Tp Scatter Table - All Data - Percentage (occurrences as proportion of all data)																			
		Peak Wave Period, Tp (s)																	
		Lower (>=)	0	2	4	6	8	10	12	14	16	18	20	22	24	Sum	Cum. Sum	Exced.	
		Upper (<)	2	4	6	8	10	12	14	16	18	20	22	24	26	Sum	Cum. Sum	Exced.	
Significant Wave Height, Hs (m)	12.5	13.0															100.00	0.00	
	12.0	12.5							0.00							0.00	100.00	0.00	
	11.5	12.0							0.00							0.00	100.00	0.00	
	11.0	11.5						0.00	0.00							0.00	100.00	0.00	
	10.5	11.0						0.00	0.00							0.00	100.00	0.00	
	10.0	10.5						0.00	0.00							0.00	99.99	0.01	
	9.5	10.0						0.00	0.00							0.01	99.99	0.01	
	9.0	9.5						0.01	0.01	0.00						0.02	99.99	0.01	
	8.5	9.0					0.00	0.02	0.01	0.00						0.03	99.96	0.04	
	8.0	8.5					0.00	0.04	0.02	0.00						0.06	99.93	0.07	
	7.5	8.0					0.00	0.05	0.02	0.00						0.08	99.87	0.13	
	7.0	7.5					0.01	0.10	0.02	0.00						0.13	99.79	0.21	
	6.5	7.0					0.03	0.17	0.02	0.00	0.00					0.23	99.66	0.34	
	6.0	6.5				0.00	0.08	0.23	0.03	0.00	0.00					0.33	99.43	0.57	
	5.5	6.0					0.19	0.33	0.04	0.00	0.00					0.56	99.10	0.90	
	5.0	5.5				0.00	0.47	0.38	0.05	0.01	0.00					0.91	98.55	1.45	
	4.5	5.0				0.01	0.90	0.41	0.06	0.01	0.00	0.00				1.40	97.64	2.36	
	4.0	4.5				0.00	0.06	1.59	0.48	0.08	0.03	0.01				2.24	96.24	3.76	
	3.5	4.0				0.00	0.49	2.27	0.53	0.13	0.05	0.00				3.47	94.01	5.99	
	3.0	3.5				0.01	2.01	2.53	0.66	0.28	0.09	0.01	0.00	0.00		5.60	90.53	9.47	
	2.5	3.0				0.05	4.37	2.74	0.99	0.49	0.12	0.02	0.01	0.01	0.00	8.81	84.93	15.07	
	2.0	2.5				0.00	0.52	7.18	3.22	1.70	0.78	0.14	0.03	0.02	0.00	0.00	13.59	76.12	23.88
	1.5	2.0				0.00	4.02	7.94	4.08	2.63	0.74	0.17	0.09	0.04	0.01		19.73	62.53	37.47
	1.0	1.5				0.09	8.88	7.76	4.50	2.02	0.50	0.29	0.14	0.03	0.01	0.00	24.21	42.80	57.20
	0.5	1.0	0.00	2.07	8.25	4.28	1.82	0.66	0.34	0.21	0.05	0.01	0.00	0.00		17.68	18.59	81.41	
	0.0	0.5	0.00	0.39	0.38	0.06	0.03	0.03	0.00	0.00	0.00	0.00	0.00	0.00		0.90	0.90	99.10	
		Sum	0.00	2.55	22.10	34.17	24.45	11.42	3.64	1.13	0.36	0.13	0.03	0.01		100.00			
		Cumulative Sum	0.00	2.55	24.66	58.83	83.28	94.70	98.34	99.48	99.84	99.97	99.99	100.00	100.00				
		Exceedence	100.00	97.45	75.34	41.17	16.72	5.30	1.66	0.52	0.16	0.03	0.01	0.00	0.00				

Table 3.8 Frequency scatter table of significant wave height vs mean wave direction – offshore export cable corridor (ABPmer, 2025a)

Marram offshore export cable corridor - Hs Mdir Scatter Table - All Data - Percentage (occurrences as proportion of all data)														
Significant Wave Height, Hs (m)	Mean Wave Direction, Mdir (degN, Coming)													
	Lower (>=)		337.5	22.5	67.5	112.5	157.5	202.5	247.5	292.5		Sum	Cum. Sum	Exced.
	Upper (<)		22.5	67.5	112.5	157.5	202.5	247.5	292.5	337.5				
12.5	13.0											100.00	0.00	
12.0	12.5	0.00									0.00	100.00	0.00	
11.5	12.0	0.00									0.00	100.00	0.00	
11.0	11.5	0.00							0.00	0.00	0.00	100.00	0.00	
10.5	11.0	0.00							0.00	0.00	0.00	100.00	0.00	
10.0	10.5	0.00					0.00	0.00	0.00	0.00	0.00	99.99	0.01	
9.5	10.0	0.00		0.00		0.00	0.00	0.00	0.00	0.00	0.01	99.99	0.01	
9.0	9.5	0.00		0.01	0.00	0.00	0.00	0.00	0.00	0.00	0.02	99.99	0.01	
8.5	9.0	0.01		0.01	0.00	0.00	0.00	0.00	0.00	0.01	0.03	99.96	0.04	
8.0	8.5	0.01		0.01	0.00	0.01	0.00	0.01	0.01	0.01	0.06	99.93	0.07	
7.5	8.0	0.02	0.00	0.02	0.01	0.01	0.00	0.01	0.01	0.01	0.08	99.87	0.13	
7.0	7.5	0.03	0.00	0.02	0.02	0.02	0.00	0.01	0.01	0.02	0.13	99.79	0.21	
6.5	7.0	0.06	0.00	0.03	0.04	0.04	0.00	0.02	0.03	0.23	99.66	0.34		
6.0	6.5	0.08	0.00	0.04	0.06	0.07	0.01	0.04	0.04	0.33	99.43	0.57		
5.5	6.0	0.14	0.01	0.06	0.09	0.11	0.01	0.07	0.07	0.56	99.10	0.90		
5.0	5.5	0.21	0.01	0.11	0.13	0.19	0.03	0.10	0.12	0.91	98.55	1.45		
4.5	5.0	0.30	0.03	0.17	0.19	0.29	0.06	0.16	0.19	1.40	97.64	2.36		
4.0	4.5	0.50	0.06	0.27	0.29	0.52	0.08	0.22	0.30	2.24	96.24	3.76		
3.5	4.0	0.73	0.11	0.34	0.46	0.85	0.15	0.39	0.44	3.47	94.01	5.99		
3.0	3.5	1.18	0.18	0.54	0.70	1.31	0.33	0.63	0.73	5.60	90.53	9.47		
2.5	3.0	1.81	0.35	0.85	1.05	2.07	0.59	0.97	1.11	8.81	84.93	15.07		
2.0	2.5	2.97	0.84	1.16	1.58	2.94	0.99	1.44	1.67	13.59	76.12	23.88		
1.5	2.0	4.42	1.80	1.76	2.39	3.73	1.43	1.94	2.28	19.73	62.53	37.47		
1.0	1.5	5.02	3.12	2.18	3.25	4.43	1.62	1.97	2.62	24.21	42.80	57.20		
0.5	1.0	3.05	2.16	1.69	2.72	3.19	1.49	1.45	1.93	17.68	18.59	81.41		
0.0	0.5	0.17	0.12	0.09	0.12	0.14	0.07	0.08	0.12	0.90	0.90	99.10		
	Sum	20.72	8.79	9.36	13.11	19.93	6.86	9.53	11.69	100.00				

Table 3.9 Frequency scatter table of significant wave height vs peak wave period – OAA (ABPmer, 2025a)

Marram Option Agreement Area - Hs Tp Scatter Table - All Data - Percentage (occurrences as proportion of all data)																		
Significant Wave Height, Hs (m)	Peak Wave Period, Tp (s)															Sum		
	0	2	4	6	8	10	12	14	16	18	20	22	24	26				
	Upper (<)	2	4	6	8	10	12	14	16	18	20	22	24	26				
13.0	13.5															100.00	0.00	
12.5	13.0							0.00								0.00	100.00	0.00
12.0	12.5							0.00								0.00	100.00	0.00
11.5	12.0							0.00								0.00	100.00	0.00
11.0	11.5							0.00								0.00	100.00	0.00
10.5	11.0						0.00	0.00	0.00						0.01	99.99	0.01	
10.0	10.5						0.00	0.01	0.00						0.01	99.99	0.01	
9.5	10.0						0.01	0.01	0.00						0.02	99.98	0.02	
9.0	9.5						0.01	0.02	0.00						0.03	99.95	0.05	
8.5	9.0						0.03	0.02	0.00						0.06	99.92	0.08	
8.0	8.5						0.04	0.02	0.01						0.07	99.86	0.14	
7.5	8.0					0.00	0.08	0.03	0.00						0.11	99.79	0.21	
7.0	7.5					0.01	0.15	0.04	0.00	0.00					0.20	99.67	0.33	
6.5	7.0					0.03	0.24	0.04	0.00	0.00					0.32	99.47	0.53	
6.0	6.5				0.00	0.12	0.30	0.05	0.00	0.00					0.47	99.15	0.85	
5.5	6.0					0.30	0.46	0.04	0.01	0.00					0.81	98.68	1.32	
5.0	5.5					0.00	0.64	0.50	0.06	0.01	0.01	0.00			1.22	97.87	2.13	
4.5	5.0					0.01	1.23	0.52	0.07	0.02	0.01	0.00			1.86	96.66	3.34	
4.0	4.5					0.10	2.15	0.56	0.12	0.04	0.01	0.00	0.00		2.98	94.80	5.20	
3.5	4.0				0.00	0.73	2.85	0.62	0.22	0.09	0.01	0.01	0.00		4.54	91.82	8.18	
3.0	3.5				0.00	2.65	2.81	0.72	0.41	0.12	0.03	0.02	0.01	0.00	6.76	87.28	12.72	
2.5	3.0				0.06	5.25	2.79	1.14	0.72	0.14	0.07	0.04	0.01	0.00	10.23	80.52	19.48	
2.0	2.5				0.64	7.61	3.27	2.04	0.79	0.23	0.12	0.05	0.01		14.75	70.29	29.71	
1.5	2.0			0.00	4.06	7.28	4.01	2.59	0.67	0.35	0.18	0.06	0.01	0.00	19.20	55.53	44.47	
1.0	1.5		0.08	7.94	6.89	4.35	1.63	0.69	0.47	0.14	0.03	0.00	0.00		22.21	36.33	63.67	
0.5	1.0	0.00	1.35	6.49	3.65	1.29	0.53	0.30	0.10	0.04	0.02	0.01	0.00		13.79	14.12	85.88	
0.0	0.5		0.08	0.18	0.02	0.02	0.02	0.00	0.00	0.00					0.33	0.33	99.67	
Sum		0.00	1.51	19.38	34.19	25.88	12.20	4.36	1.60	0.62	0.22	0.05	0.01	0.00		100.00		
Cumulative Sum		0.00	1.51	20.89	55.08	80.96	93.15	97.51	99.11	99.73	99.94	99.99	100.00	100.00		100.00		
Exceedence		100.00	98.49	79.11	44.92	19.04	6.85	2.49	0.89	0.27	0.06	0.01	0.00	0.00		0.00		

Table 3.10 Frequency scatter table of significant wave height vs mean wave direction – OAA (ABPmer, 2025a)

Marram Option Agreement Area - Hs Mdir Scatter Table - All Data - Percentage (occurrences as proportion of all data)													
Significant Wave Height Hs (m)	Mean Wave Direction, Mdir (degN, Coming)												
	Lower (>=)		337.5	22.5	67.5	112.5	157.5	202.5	247.5	292.5	Sum	Cum. Sum	Exced.
	Upper (<)		22.5	67.5	112.5	157.5	202.5	247.5	292.5	337.5			
13.0	13.5										100.00	0.00	
12.5	13.0								0.00	0.00	0.00	100.00	0.00
12.0	12.5								0.00	0.00	0.00	100.00	0.00
11.5	12.0	0.00						0.00	0.00	0.00	0.00	100.00	0.00
11.0	11.5	0.00						0.00		0.00	0.00	100.00	0.00
10.5	11.0	0.00	0.00	0.00				0.00	0.00	0.00	0.01	99.99	0.01
10.0	10.5	0.00		0.00			0.00	0.00	0.00	0.00	0.01	99.99	0.01
9.5	10.0	0.00	0.00	0.01	0.00	0.00			0.01	0.01	0.02	99.98	0.02
9.0	9.5	0.01		0.01	0.00	0.01	0.00	0.00	0.01	0.01	0.03	99.95	0.05
8.5	9.0	0.01		0.01	0.01	0.01	0.01	0.00	0.01	0.01	0.06	99.92	0.08
8.0	8.5	0.01	0.00	0.01	0.01	0.01	0.01	0.00	0.01	0.01	0.07	99.86	0.14
7.5	8.0	0.02	0.00	0.01	0.02	0.02	0.02	0.00	0.02	0.02	0.11	99.79	0.21
7.0	7.5	0.04	0.00	0.02	0.03	0.04	0.04	0.00	0.04	0.03	0.20	99.67	0.33
6.5	7.0	0.06	0.00	0.03	0.05	0.06	0.01	0.06	0.04	0.32		99.47	0.53
6.0	6.5	0.09	0.00	0.04	0.07	0.09	0.03	0.08	0.07	0.47		99.15	0.85
5.5	6.0	0.14	0.01	0.09	0.11	0.16	0.05	0.11	0.13	0.81		98.68	1.32
5.0	5.5	0.23	0.01	0.12	0.14	0.26	0.08	0.19	0.19	1.22		97.87	2.13
4.5	5.0	0.34	0.02	0.17	0.23	0.40	0.12	0.28	0.29	1.86		96.66	3.34
4.0	4.5	0.56	0.04	0.25	0.35	0.68	0.23	0.45	0.41	2.98		94.80	5.20
3.5	4.0	0.85	0.11	0.37	0.52	1.00	0.43	0.67	0.59	4.54		91.82	8.18
3.0	3.5	1.27	0.19	0.55	0.75	1.51	0.69	0.96	0.84	6.76		87.28	12.72
2.5	3.0	2.04	0.35	0.78	1.05	2.10	1.14	1.42	1.35	10.23		80.52	19.48
2.0	2.5	3.27	0.79	1.07	1.47	2.77	1.51	1.87	1.98	14.75		70.29	29.71
1.5	2.0	4.46	1.64	1.47	2.00	3.33	1.78	2.03	2.49	19.20		55.53	44.47
1.0	1.5	4.80	2.57	1.74	2.50	3.74	1.86	2.07	2.93	22.21		36.33	63.67
0.5	1.0	2.54	1.65	1.16	1.63	2.27	1.34	1.35	1.84	13.79		14.12	85.88
0.0	0.5	0.05	0.05	0.03	0.03	0.05	0.02	0.04	0.07	0.33		0.33	99.67
	Sum	20.82	7.45	7.94	10.97	18.50	9.33	11.68	13.31	100.00			

3.5.1.8 Extremes analysis of the long-term wave hindcast record available from ABPmer SEASTATES Northwest European Shelf Wave Hindcast Model (ABPmer, 2017) is shown in **Table 3.11**. Larger waves are typically observed in the OAA, with significant wave heights of approximately 9.2m for a 1:1 year event, increasing to 13.8m for a 1:50 year event. Equivalent extreme values for the landfall are 5.6m and 7.9m, respectively.

Table 3.11 Extreme value analysis of significant wave height and wave period based on wave data from ABPmer SEASTATES

Location	Return period (years)	Significant wave height Hs (m)	Mean wave period Tz (s)
Landfall	1	5.6	8.7
	5	6.7	9.5
	10	7.1	9.8

Location	Return period (years)	Significant wave height Hs (m)	Mean wave period Tz (s)
	25	7.6	10.1
	50	7.9	10.3
Offshore export cable corridor.	1	8.6	8.3
	5	10.5	9.2
	10	11.2	9.5
	25	12.0	9.8
	50	12.6	10.1
OAA	1	9.2	8.8
	5	11.2	9.7
	10	12.1	10.1
	25	13.1	10.5
	50	13.8	10.8

3.6 Future change

3.6.1.1 Information on the rate and magnitude of anticipated relative sea level change during the 21st century is available from UKCP18 (Palmer *et al.*, 2018). By 2060, relative sea level is predicted to have risen by approximately 0.3m above present day (2025) levels (Representative Concentration Pathway (RCP) 8.5, 95th percentile) at the landfall, with rates of change increasing over time. By 2080, relative sea level may have risen by approximately 0.55m above baseline (2025) levels (Representative Concentration Pathway 8.5)) (Palmer *et al.*, 2018).

3.6.1.2 Sea level rise may result in loss of intertidal habitat through the process of 'coastal squeeze', caused by the presence of coastal defences preventing natural roll back, and future equilibrium position of coastal features (Environment Agency, 2021). A rise in sea level may also allow larger waves and therefore more wave energy, to reach the coast in certain conditions and, consequently, result in an increase in local rates or patterns of erosion.

3.6.1.3 UKCP18 provides projections of changes to storm surge magnitude in the future as a result of climate change. These projections of change in extreme coastal water levels are dominated by the increase in mean sea level with only a minor (<10%) additional contribution due to atmospheric storminess changes over the 21st century (Palmer *et al.*, 2018).

4. Stratification and Frontal Systems

4.1.1.1 This Section uses modelled data to describe the baseline conditions of the vertical structure of the water column and productivity across the study area, covering: stratification timing, stratification strength, tidal mixing fronts, associated primary productivity and predicted future change.

4.2 Overview

4.2.1.1 Stratification is a naturally occurring seasonal HD process related to the vertical and horizontal distribution of seawater density, driven by temperature and / or salinity variations.

4.2.1.2 During Summer, surface waters warm, creating a vertical temperature gradient (thermocline). The development of stratification is counterbalanced by turbulent mixing, which is generated at the seabed by tidal currents and at the surface by wind and wave action. The interplay between these forces determines whether stratification will persist or break down.

4.2.1.3 Density gradients (pycnoclines) present in stratified water columns act as a physical barrier to vertical mixing (Simpson and Sharples, 2012). This reduces the upward transport of nutrients from deeper waters, which can limit primary production (PP) in surface waters as nutrients become depleted over time (Simpson and Sharples, 2012).

4.2.1.4 Tidal mixing fronts form at the boundaries between well-mixed and stratified waters, creating regions of enhanced biological activity. These fronts, common in shelf seas like the North Sea (Hill and Cota 2005; Hill *et al.*, 2008), facilitate nutrient exchange between surface and deeper layers, promoting PP through the stimulation of phytoplankton growth. Fronts act as biological hotspots, concentrating nutrients and attracting higher trophic levels. The strength and position of these fronts are influenced by factors such as tidal current speeds, freshwater inputs, and wind patterns, which can vary on timescales ranging from hours to years.

4.2.1.5 The North Sea is characterised by significant spatial and temporal variation in the vertical distribution of temperature and salinity. The OAA is located in an area described by van Leeuwen *et al.* (2015) as being “*seasonally stratified*”, defined as >120 days in the year where the water column is stratified and <90 in the year where the water column is fully mixed.

4.2.1.6 The baseline understanding of the existing temporal / spatial pattern of stratification and positioning of tidal mixing fronts has been developed using readily available three-dimensional numerical model outputs of temperature, salinity and chlorophyll-a from Copernicus Marine Service (Copernicus Marine Service, 2024a; 2024b). The data source, methodology and results of this baseline analysis are presented in more detail in **Appendix 6.1: Physical Processes Modelling**. The key findings are summarised in **Sections 4.3, 4.4 and 4.5**.

4.3 Water column stratification

4.3.1.1 The potential energy anomaly (PEA) provides a single, scalar value for the strength of stratification in a water body (Simpson and Bowers 1981; Gowen *et al.*, 1995; Yamaguchi *et al.*, 2019 and Dorell *et al.*, 2022). The threshold values of PEA can vary depending on the specific water body. Based on the density profiles and calculated PEA values for the physical processes study area and its surrounding regions, along with thresholds used in

the literature (Gowen *et al.*, 1995; Dorrell *et al.*, 2022), the following PEA classifications are applied in this study:

- mixed water column: $\phi < 25$ joules per cubic metre (J/m^3);
- weakly stratified water column: $25 \leq \phi < 50\text{J/m}^3$;
- moderately stratified water column: $50 \leq \phi < 100\text{J/m}^3$; and
- strongly stratified water column: $\phi > 100\text{J/m}^3$.

4.3.1.2 To assess seasonal and inter-annual variability in stratification strength, monthly mean PEA values were calculated across the physical processes study area, from January 2010 to December 2023. **Plate 4.1**, **Plate 4.2** and **Plate 4.3** illustrate the results for three specific years, 2014, 2010 and 2015, representing years with stronger stratification, intermediate stratification and weaker stratification, respectively. In the figure, seas are partitioned into those defined as mixed ($\phi < 25\text{J/m}^3$) and stratified ($\phi \geq 25\text{J/m}^3$).

4.3.1.3 During the Winter months (November to April), reduced solar heating and increased turbulent mixing from wind and waves result in very weakly stratified to mixed waters in the OAA, characterised by homogeneous temperature and density profiles, with PEA values around 30 J/m^3 . With the onset of Spring and Summer, calmer weather and longer, warmer days enhance stratification, overcoming the mixing effects of tide and winds. From May to October, this leads to a vertical temperature gradient and an increase in PEA values. Over the 14-year analysis period (2010-2023), PEA typically reaches around 140J/m^3 in mid-Summer, indicating a strongly stratified water column, consistent with the findings of van Leeuwen *et al.* (2015).

4.3.1.4 There is variability in the strength of summer stratification from year to year, with mid-Summer PEA values ranging from approximately 130J/m^3 in 2015 to approximately 170J/m^3 in 2014 (**Plate 4.4**).

4.3.1.5 To the east of the OAA, increasing depths and weaker tidal currents lead to stronger stratification with greater distance from the OAA. Conversely, closer to the coastline, shallower depths and stronger tidal currents result in reduced stratification. Approximately 60km south-west of the OAA towards the north-east Aberdeenshire coastline, the water column remains well-mixed throughout the year.

Plate 4.1 Calculated PEA (ϕ), based on the Copernicus Reanalysis monthly temperature and salinity data for 2014, a stronger stratification year (Copernicus Marine Service, 2024a)

2014 – Stronger Stratification

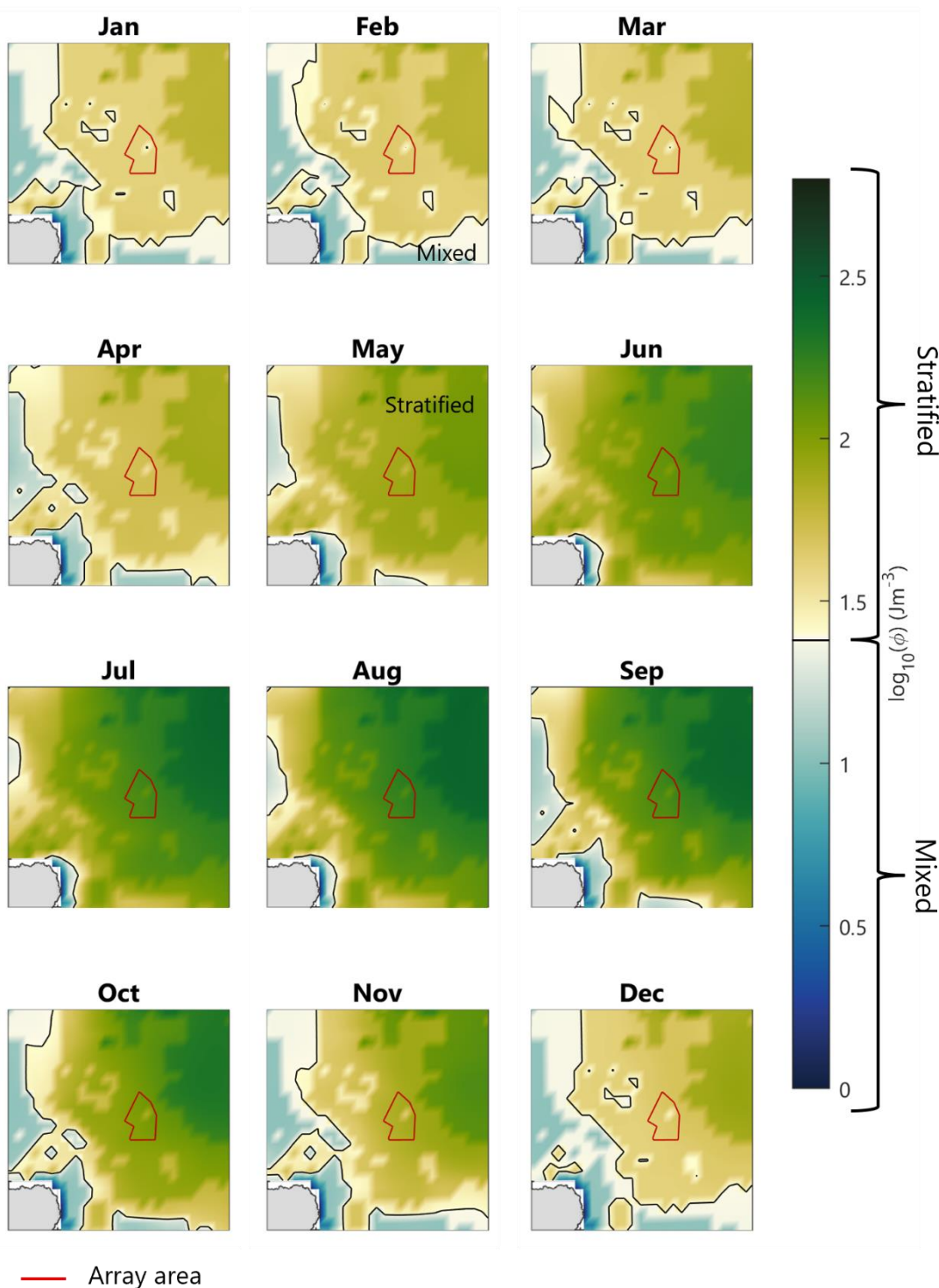


Plate 4.2 Calculated PEA (ϕ), based on the Copernicus Reanalysis monthly temperature and salinity data for 2010, an intermediate stratification year (Copernicus Marine Service, 2024a)

2010 – Intermediate Stratification

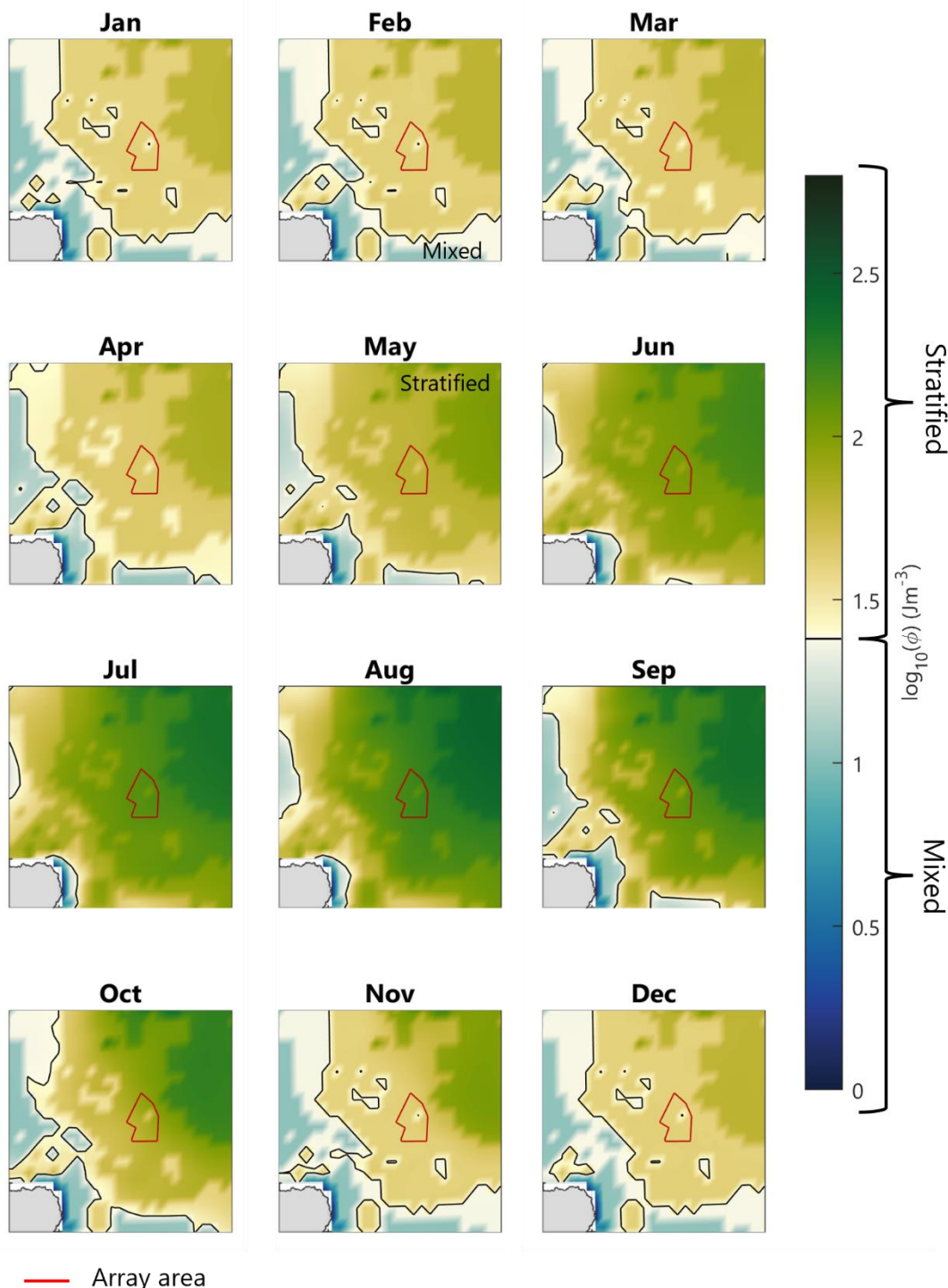


Plate 4.3 Calculated PEA (ϕ), based on the Copernicus Reanalysis monthly temperature and salinity data for 2015, a weaker stratification year (Copernicus Marine Service, 2024a)

2015 – Weaker Stratification

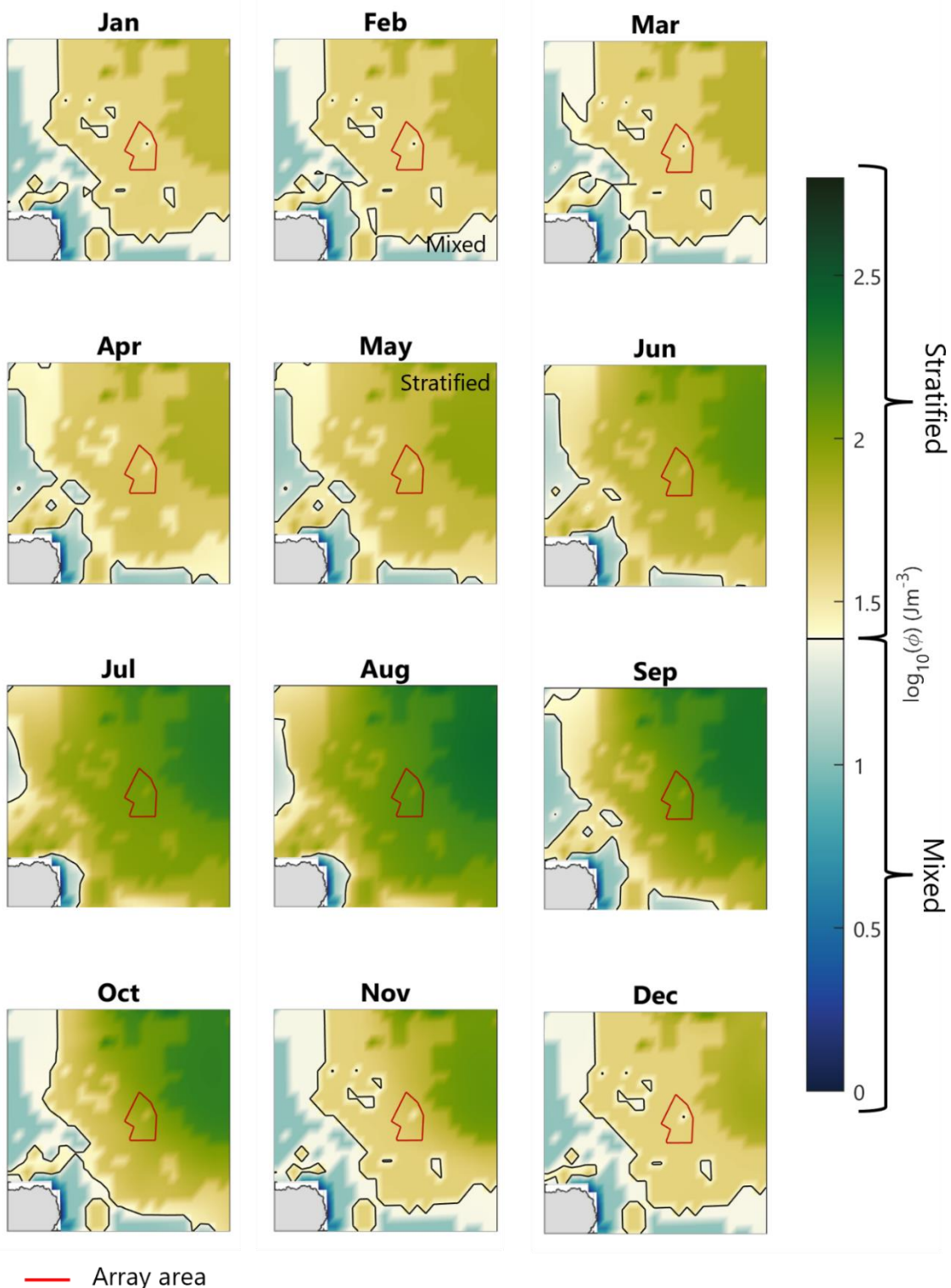
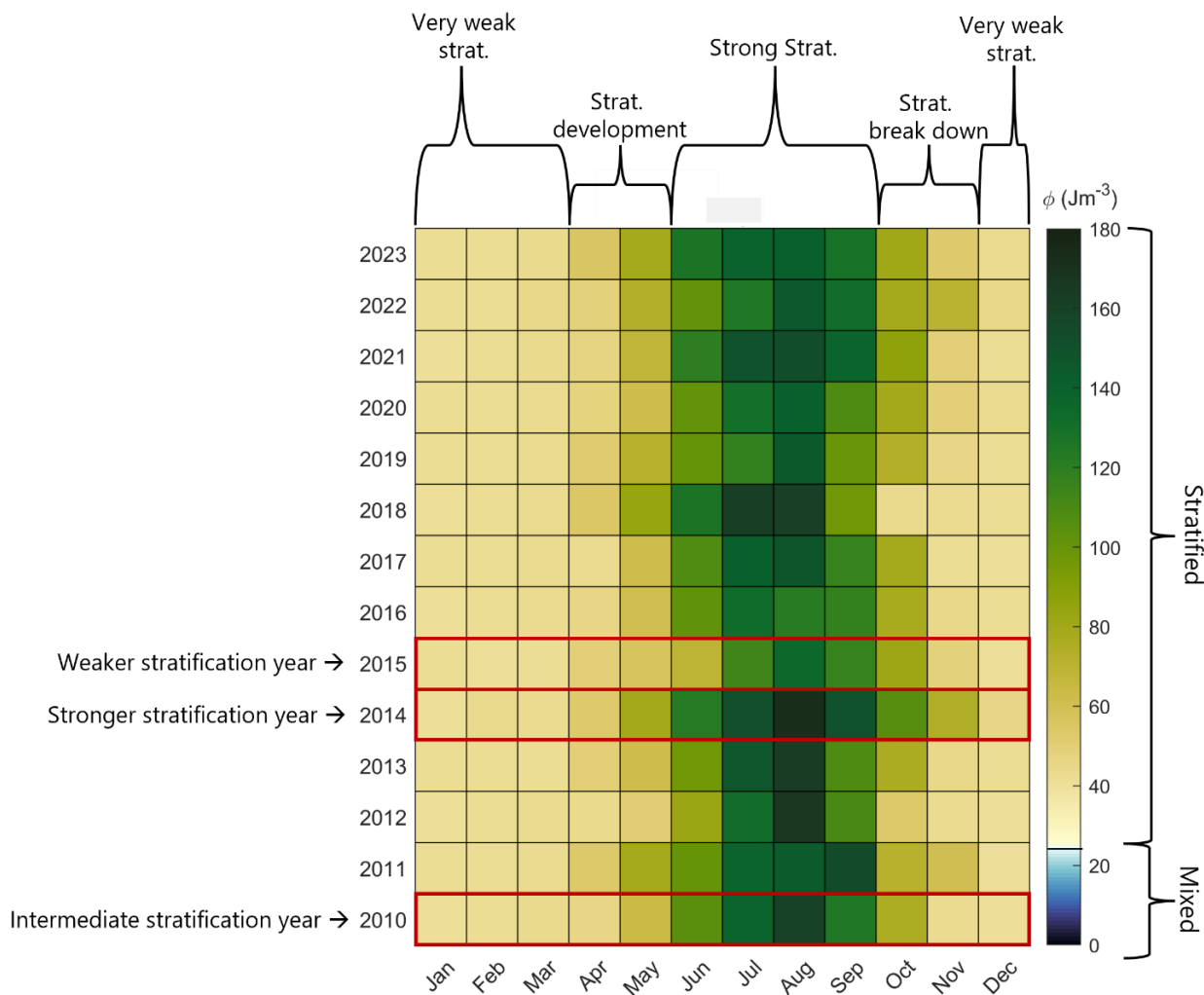


Plate 4.4 Monthly PEA (ϕ) values, based on the Copernicus Reanalysis monthly temperature and salinity data, in the OAA from 2010-2023 (Copernicus Marine Service, 2024a)



4.4 Tidal mixing fronts

4.4.1.1 The physical mixing at fronts locally supplies a relatively higher concentration of nutrients into the sunlit surface layer, therefore creating more favourable conditions for phytoplankton growth by preventing nutrient depletion in the surface layers. As a result, these areas often support higher levels of PP (and chlorophyll-a) compared to both the mixed and stratified waters on either side of the front (Garcia-Nieto *et al.*, 2024). **Plate 4.5, Plate 4.6** and **Plate 4.7** illustrate the maximum chlorophyll-a concentrations throughout the water column for the years 2014 (stronger stratification year), 2010 (intermediate stratification year) and 2015 (weaker stratification year), capturing both deep chlorophyll maxima and surface peaks.

4.4.1.2 During Summer, elevated chlorophyll-a concentrations - likely associated with a tidal mixing front - are commonly observed west of the OAA. However, their exact positioning varies significantly between years. In years with weaker stratification (for example, 2015), the tidal mixing front forms further offshore, resulting in elevated chlorophyll-a levels within the OAA. Conversely, during years of stronger stratification (for example, 2014), the front / elevated chlorophyll-a concentrations shift closer to the coast.

Plate 4.5 Copernicus Reanalysis monthly maximum chlorophyll-a concentration throughout the water column for 2014 a stronger stratification year (Copernicus Marine Service, 2024b)

2014 – Stronger Stratification

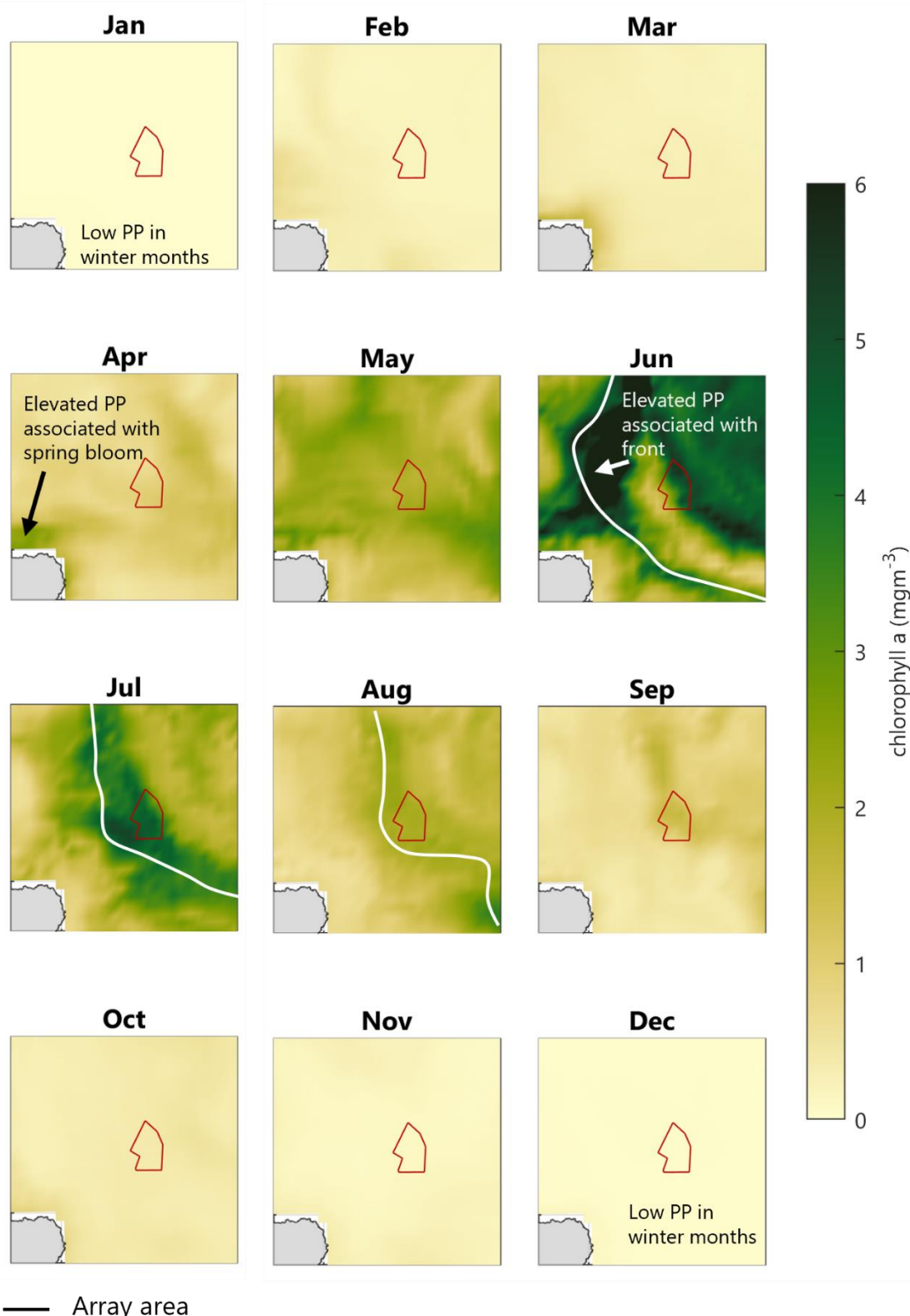


Plate 4.6 Copernicus Reanalysis monthly maximum chlorophyll-a concentration throughout the water column for 2010 an intermediate stratification year (Copernicus Marine Service, 2024b)

2010 – Intermediate Stratification

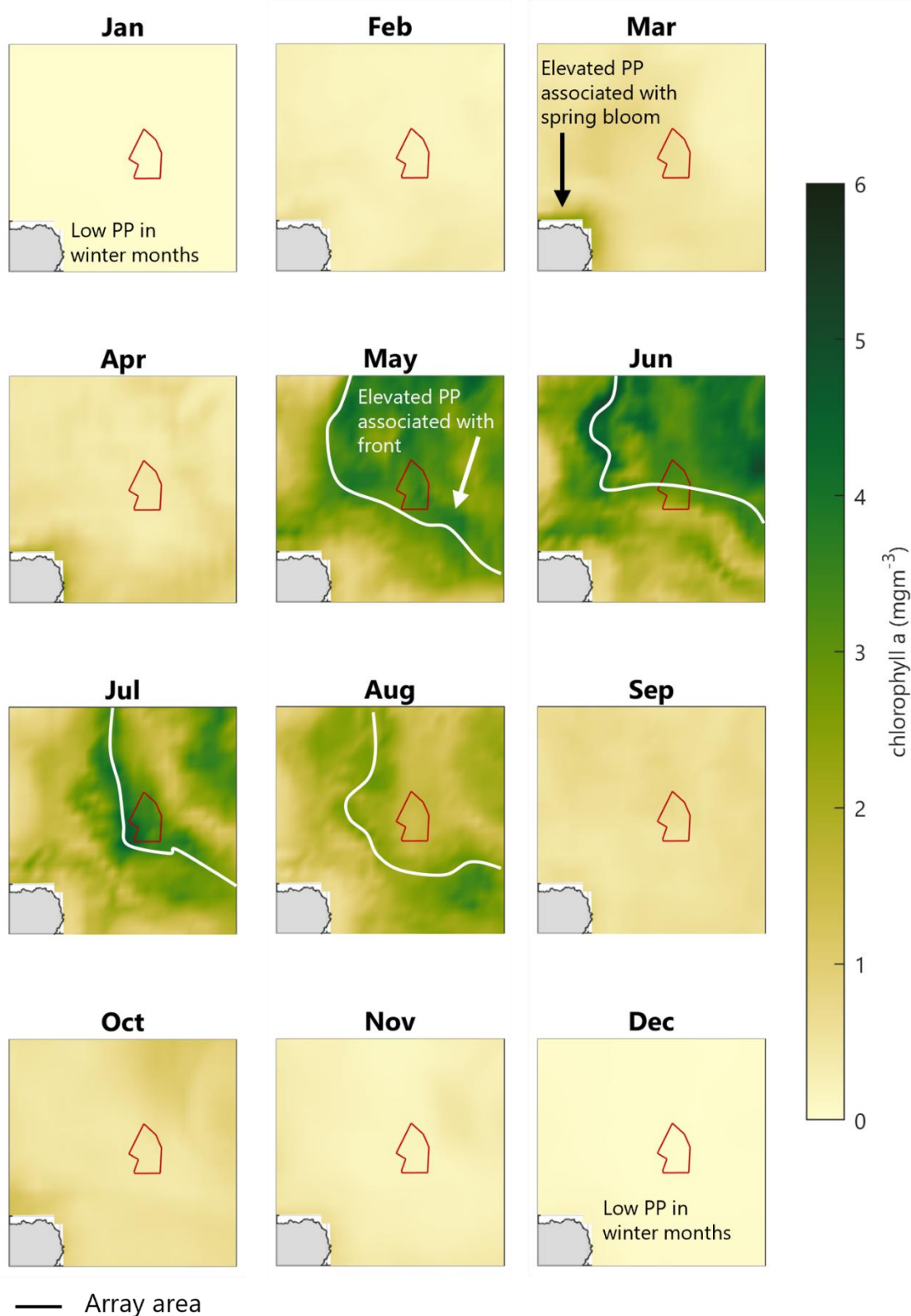
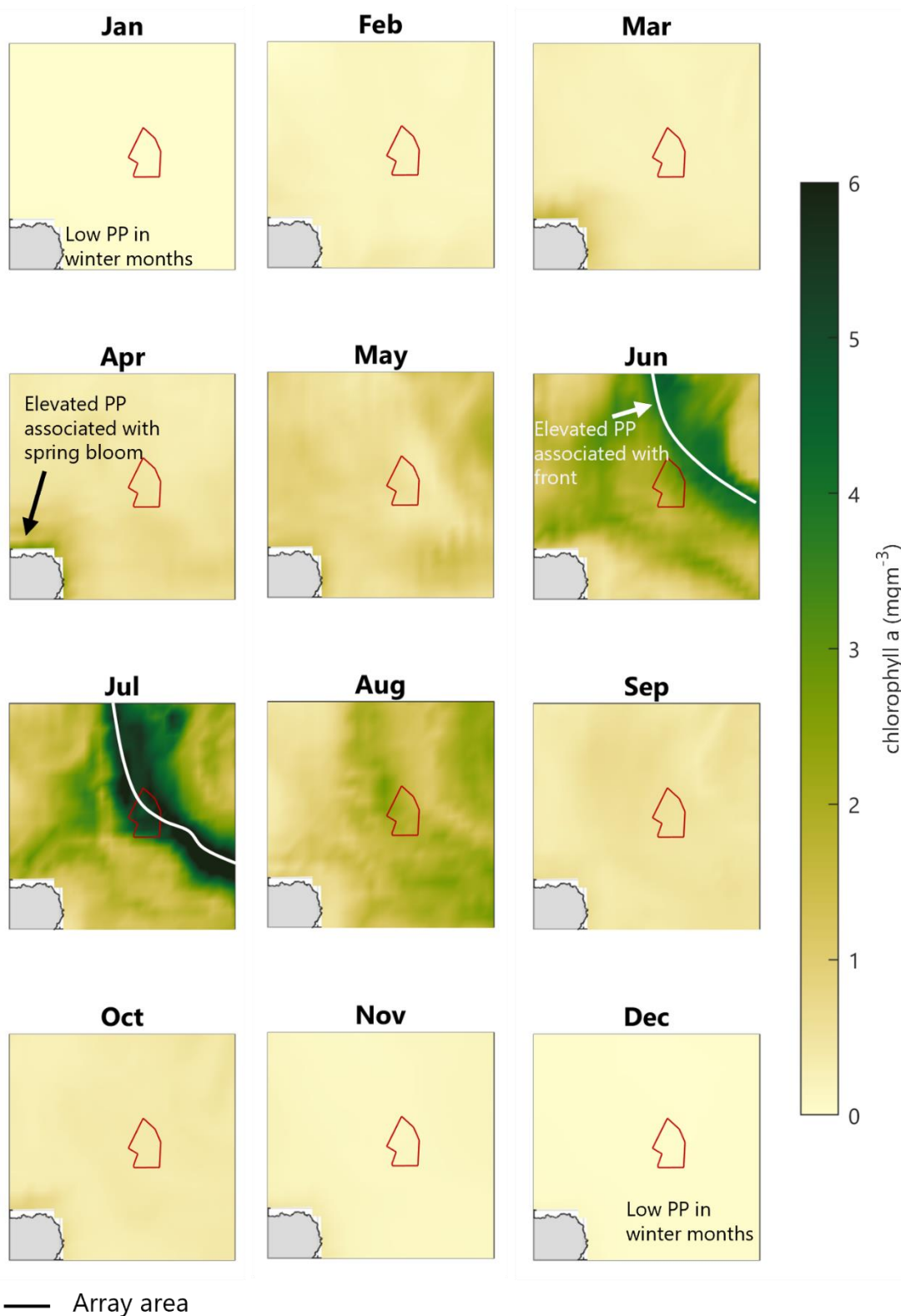


Plate 4.7 Copernicus Reanalysis monthly maximum chlorophyll-a concentration throughout the water column for 2015 a weaker stratification year (Copernicus Marine Service, 2024b)

2015 – Weaker Stratification



4.5 Future change

- 4.5.1.1 The stratification dynamics in the North Sea are expected to undergo significant changes due to the changing climate. With the Project becoming fully operational in three phases – by 2037, 2040 and 2043, and a project lifetime per phase of ~35 years, it is important to consider how the timing and strength of stratification will evolve during this time.
- 4.5.1.2 The timing of stratification is influenced by the interplay between solar heating and tidal mixing, with a smaller but notable contribution from wind-driven mixing. Global warming and changes to meteorological conditions is likely to alter the timing of Spring stratification, and subsequently the timing of the Spring phytoplankton bloom.
- 4.5.1.3 Model projections suggest that by 2100, the thermal stratification period in UK shelf seas will extend by approximately two weeks (Sharples *et al.*, 2025), with stratification occurring about one week earlier and breaking down 5 to 10 days later than present (Sharples *et al.*, 2022). The dominant driver behind this shift is the increase in air temperature, which accelerates solar heating of the surface waters and thus strengthens thermal gradients. Historically, stratification timing in the north-western North Sea has advanced by about half a day per year since the late 1980s, based on analyses from 1974 to 2003 (Sharples *et al.*, 2006; Holt *et al.*, 2012).
- 4.5.1.4 Model projections also suggest that seas across the north-west European shelf, including the northern North Sea, will experience greater surface-to-bottom temperature differences as the seasonal heating cycle intensifies (Tinker *et al.*, 2016), resulting in stronger stratification. Alongside the strengthening stratification there will be small shifts in the position of tidal mixing fronts as thermal stratification pushes into shower waters and / or stronger tidal regions.
- 4.5.1.5 Strengthening stratification reduces vertical mixing, limiting the upward transport of nutrients from the deep layers to the surface, where they fuel PP. This could lead to a decline in overall PP, as suggested by Chust *et al.* (2014).

5. Surficial Sediments, Sediment Transport and Morphology

5.1.1.1 This Section describes seabed sediments and seabed morphology both within the OAA and offshore export cable corridor, as well as across the wider study area. The process controls on sediment transport and associated seabed mobility are discussed, with a conceptual understanding of the wider system also set out.

5.2 Seabed sediments

5.2.1 Overview

5.2.1.1 Seabed sediments across the study area are highly variable, with coarse (sand and gravels) and fine (muddy) grained sediments present. The distribution broadly reflects spatial variation in current speeds, with coarser material encountered closer to the coast (where current speeds are high) and finer material found further offshore, including within the OAA (where current speeds are much lower). Close to the shore, the very high current speeds have scoured the seabed, leaving exposed areas of bedrock in places (Gafeira *et al.*, 2010).

5.2.1.2 A lack of major river sediment input and the resistance of most of the shorelines to erosion, has resulted in only minor amounts of clastic sediment (rock) input from the coastal areas to offshore waters off east and north-east Scotland over the last 10,000 years. This, coupled with strong tidal and non-tidal currents has provided favourable environments for the proliferation of calcareous seabed biota meaning in places the biogenic carbonate content of the sand fraction in seabed sediments may comprise up to 50% (Holmes *et al.*, 2004).

5.2.2 Option Agreement Area and offshore export cable corridor

5.2.2.1 Seabed sediments within the OAA and along the offshore export cable corridor have been described by Fugro (2023a; 2023b) and are summarised in **paragraph 5.2.2.2 et seq.** and in **Figure 3**.

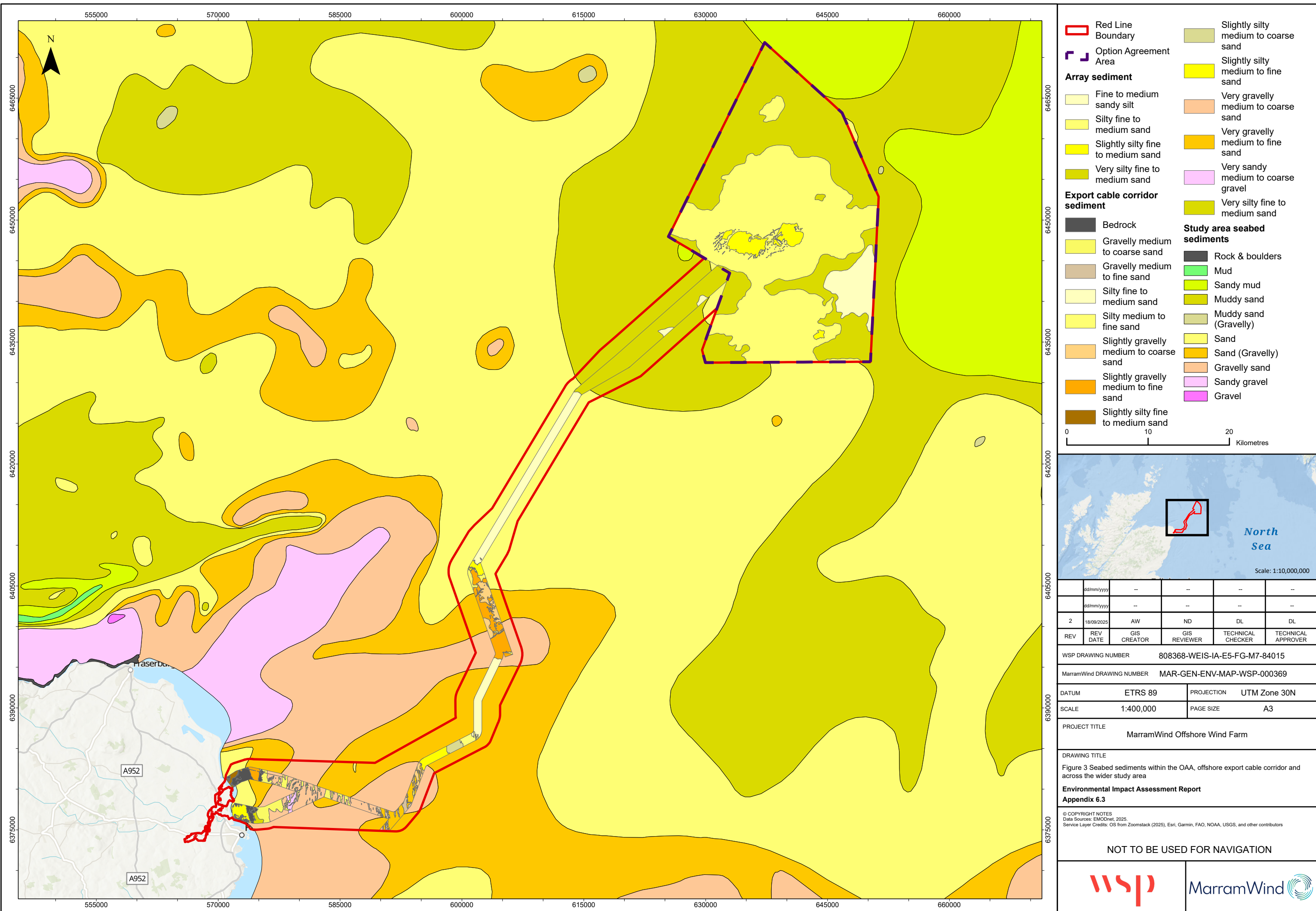
5.2.2.2 Within the OAA, seafloor sediments mainly comprise a combination of sand and silt, varying from slightly silty fine to medium sand to fine to medium sandy silt. Silty fine to medium sand is the predominant seafloor sediment.

5.2.2.3 The transitions between the different seafloor sediment types is a gradual lateral change in the percentage of silt present, as such the boundaries are not distinct. Where the sediment comprises slightly silty fine to medium sand, the sand is predominantly medium grained. In the areas of fine to medium sandy silt, the sand is mainly fine grained.

5.2.2.4 The areas of slightly silty fine to medium sand occur on the bathymetric high in the central region of the OAA and on a smaller area in the south-east. Areas of silty fine to medium sand extend across much of the central and southern regions of the OAA.

5.2.2.5 Very silty fine to medium sand occurs across large parts of the southern region and is the dominant sediment type in the north of the OAA too. The change from areas of silty fine to medium sand to areas of very silty fine to medium sand coincides with an increase in water depth. In the south-east of the OAA, where the water depths are greatest, there is an area of fine to medium sandy silt, largely coinciding with the extents of the sub-seafloor Witch Ground Formation within the survey area.

- 5.2.2.6 The only patches of gravels present are located within some of the seafloor depressions, where there are accumulations of gravel (shell and lithic fragments) and occasional cobbles / boulders.
- 5.2.2.7 Within the offshore export cable corridor, the seafloor sediments mainly comprise a combination of silt, sand, and gravel and are Holocene in age. Based on the results from the environmental grab samples, sand is the predominant main soil type with gradual changes in grain size across the route. Bedrock is observed outcropping at the seafloor in nearshore areas including at the landfall zones (Fugro, 2023b).



5.3 Geology sub-strata

5.3.1 Overview

5.3.1.1 The geological structure of the bedrock that underlies the seabed in this region is characterised by a complex pattern of down-faulted basins separated by platforms (relatively uplifted areas). The uplifted platforms formed approximately 420 million years ago and underlie the modern coastline and nearshore parts of the study area. The Mesozoic basins found further offshore formed more recently during faulting, approximately 142 to 250 million years ago (Holmes *et al.*, 2004). The modern-day seabed configuration reflects the combination of this large-scale geological structure and burial by younger sediments, in particular those deposited during the Quaternary period in response to the growth and decay of Pleistocene ice sheets and associated changes in relative sea level.

5.3.2 Option Agreement Area and offshore export cable corridor

5.3.2.1 The seabed within the OAA and offshore export cable corridor can be generally described as a widely distributed but thin veneer of relatively sandy sediment, laid down and reworked during the Holocene period (the last 11,700 years since the last major glacial period). These are the sediments that are or have been actively mobile in the recent geological past. The thickness of the Holocene veneer is typically thin (0.25m to 1m) and may be absent in some locations (exposed bedrock or other erosion resistant substrate). Any modern day bedforms that are present are formed of this relatively sandy Holocene sediment, and are limited in size and type by the relative thickness and abundance of such sediment present locally.

5.3.2.2 Underneath the Holocene sediments are various other geological formations, as named and described in **Table 5.1** and **Table 5.2**. The uppermost layer immediately below the Holocene veneer (or exposed where the Holocene veneer is locally absent) is variable around the OAA and along the offshore export cable corridor. The uppermost material below the Holocene veneer is the material type most likely to be also disturbed by construction activities. Geological formations other than the loose, sandy Holocene material are likely to be relatively erosion and transport resistant and will limit the depth of scour.

Table 5.1 Summary of shallow geology within the OAA (adapted from Fugro, 2023a)

Age	Formation	Basal horizon	Soil type
Holocene	Holocene	H02	Very loose, slightly silty, fine to medium sand with shell fragments and occasional gravel, cobbles and boulders.
Pleistocene	Witch Ground	H05	Extremely low to low strength slightly silty clay with beds of sand.
	Swatchway	H10	Extremely low to medium strength sandy clay with occasional gravel.

Age	Formation	Basal horizon	Soil type
	Coal Pit	H17*	Medium to high strength silty clay with dense to very dense sands and gravel, cobbles and boulders.
		H20	
	Fisher	H21	High strength sand, silt and clay.
	Ling Bank	H25	High to very high strength over-consolidated silty clay with layers of dense silty sand, with gravel, cobbles and boulders.
	Aberdeen Ground	n/a**	Very high to extremely high strength over-consolidated clay with sand and silt and occasional gravel.

Notes:

* Upper Coal Pit Unconformity – marks youngest phase of significant channelling with the Coal Pit.

** base of Aberdeen Ground not defined by 2DUUHR data as exceeds record length.

Table 5.2 Summary of shallow geology within the offshore export cable corridor

Age	Formation	Member / unit	Basal horizon	Soil type
Holocene		Mobile Sediments.	n/a	Loose to medium dense fine to coarse slightly gravelly sand with shells, pockets of organic material and rare mica.
		Esker	n/a	Sands and gravel*.
		Holocene internal.	H02a	Not sampled by geotech but could represent coarse deposits or small amounts of biogenic gas.
		Holocene (upper).	H02b	Very loose to medium dense slightly silty fine to coarse sand with shell fragments, gravel, cobbles and boulders.
		Holocene (lower).	H02c	Loose to very dense fine to coarse gravelly sand with shell fragments.
Early Holocene to Pleistocene	Forth (base H03).	St. Andrews Bay Mbr	H03a	Fine medium dense sand with shells and shell fragments, in places rare pockets of organic matter.

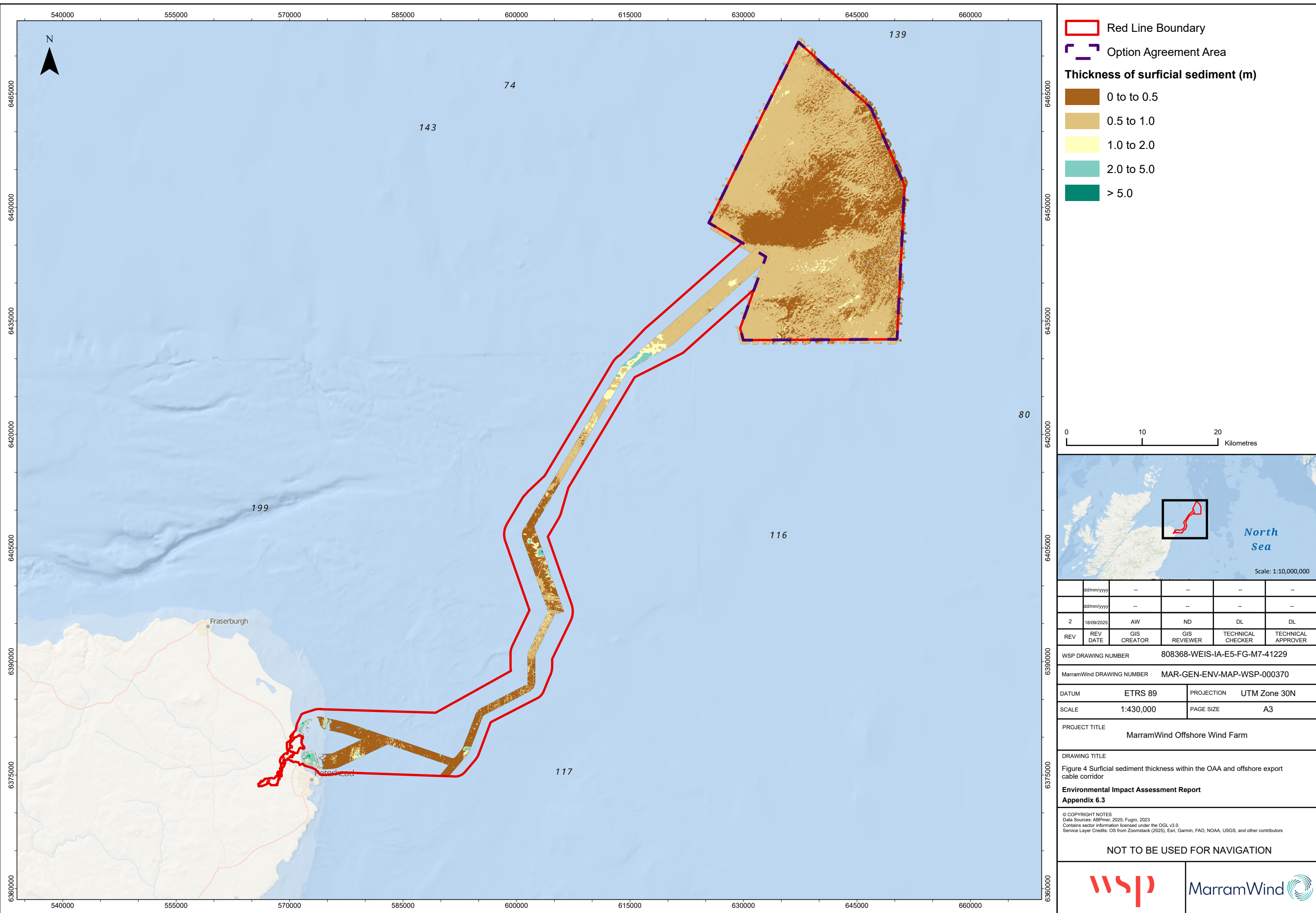
Age	Formation	Member / unit	Basal horizon	Soil type
		Largo Bay Mbr	H03	Extremely low to low strength clay interbedded with sandy silt, shells and shell fragments.
		Witch Ground (base H05).	Glenn Mbr	H05a / H05b palaeo pockmarks.
		Witch Mbr	H05c	Very low strength silt.
		Fladen Mbr	H05	Extremely low to low strength silt, sandy in places with rare pockets of organic matter.
Pleistocene	Swatchway	n/a	H10	Very low to high strength slightly sandy gravelly clay with rare shell fragments.
	Wee Bankie (Base H11).	Upper	H11a	Fine to coarse loose to very dense sand with high strength clay, gravel, cobbles, boulders and shells.
		Lower	H11b	
	Coal Pit.	H20 (base) Internals: H12, H13, H14, H17, H18.	H10	Low to very high strength clay with dense to very dense sands, gravel, cobbles and boulders. H12 to H14 defines top and base of low strength, well layered soft clays H18 division between low strength clays (above) and very high strength clays (beneath).
	Fisher**.			High strength sand, silt and clay.
	Ling Bank**.			High to very high strength over-consolidated silty clay with layers of dense silty sand, with gravel, cobbles and boulders.
	Aberdeen Ground.			Very high to extremely high strength over-consolidated clay with sand and silt and occasional gravel.
	Undifferentiated	n/a	n/a	Igneous – granite.
Cretaceous	Upper	n/a	n/a	Limestone and chalk with thin marls.
	Lower	n/a	n/a	Argillaceous shales, siltstone and calcareous mudstones with thin limestone beds.
Permian – Triassic	Undifferentiated	n/a	n/a	Sandstones, siltstones, marls and conglomerates.

Age	Formation	Member / unit	Basal horizon	Soil type
Devonian	Old Red Sandstone facies.	n/a	n/a	Sandstone, conglomerates, mudstones, siltstone and thin limestone beds.
Dalradian	Southern Highland Group (Upper Dalradian).	n/a	n/a	Metasedimentary
	Argyll Group (Lower Dalradian).	n/a	n/a	

Notes:

* Esker composition anticipated to be “**sand and gravel**”. MRW-ECC-VC-45 sampled “**fine to medium sand with rare shell fragments**”. Possible that VC only sampled Holocene ripples that have formed against the esker.

** Base far exceeds depth of interest and not relevant for proposed route description. Picked only for geological context.



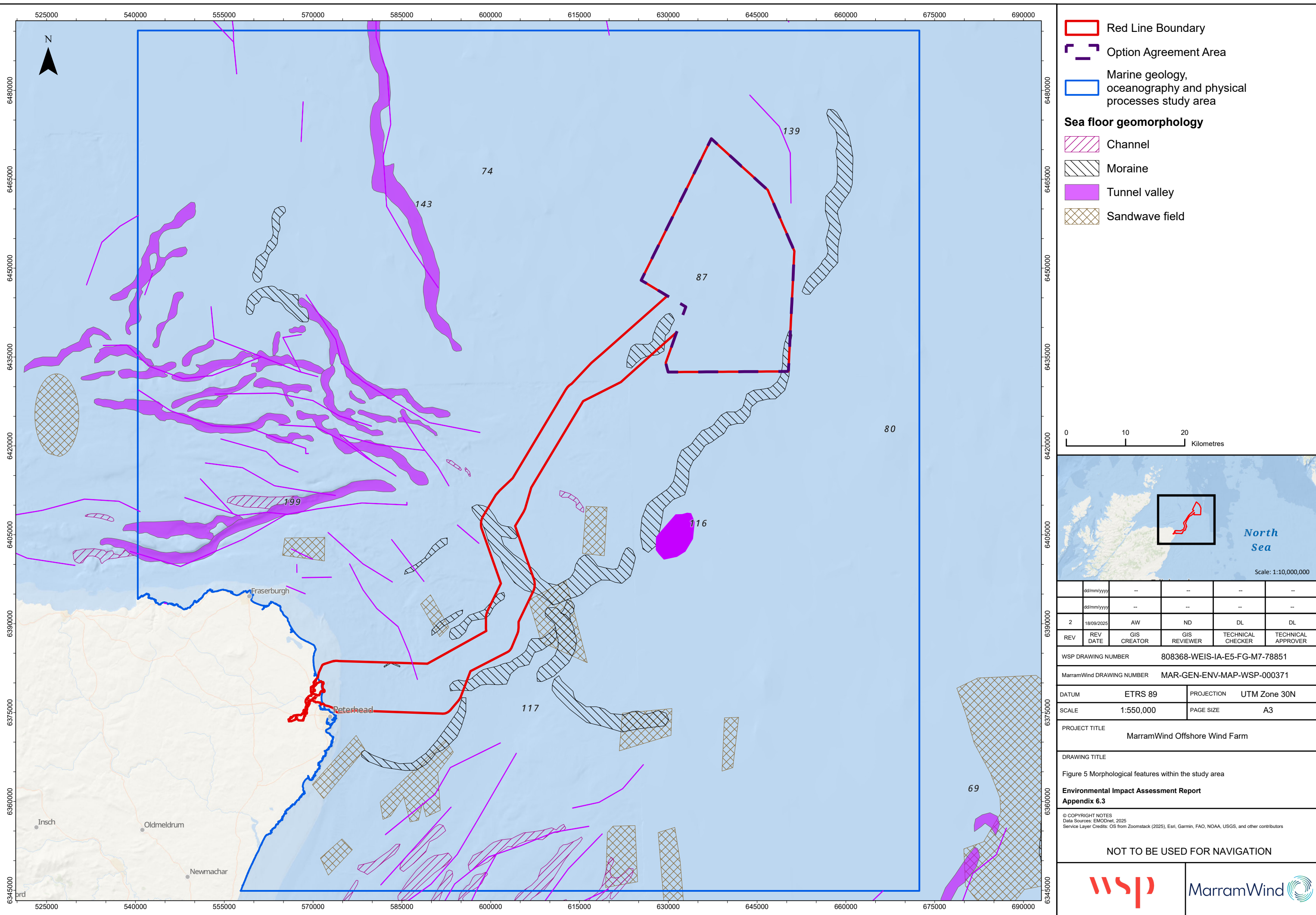
5.4 Suspended sediments

- 5.4.1.1 Monthly-averaged satellite imagery of SPM suggests that, within the OAA, average (surface) SPM is generally very low, between approximately 0.5 milligrams per litre (mg/l) to 2.0mg/l (Cefas, 2016). During the Summer months, values within the OAA are generally <1mg/l, increasing slightly in the Winter months to ~ 2-3mg/l. Still small, but relatively higher values, are anticipated during larger Spring tides and storm conditions. Higher suspended sediment concentrations are also likely to be observed at any given time closer to the seabed.
- 5.4.1.2 SPM values along the offshore export cable corridor are also generally very low but increase slightly from the OAA towards the landfall. In the Winter months, SPM values range from 1-5mg/l, decreasing to an average of <1mg/l in Summer months.

5.5 Morphology

5.5.1 Overview

- 5.5.1.1 A range of active and relict bedforms and geomorphological features are present within the study area, reflecting contemporary seabed processes and past glacial and geological activity (**Figure 5**). Sand wave fields are present in the south of the study area (BGS, 1984), along with moraines, tunnel valleys and pockmarks - shallow seabed hollows originating from the release of shallow gas or fluids at the sediment / water interface (Judd, 2001).
- 5.5.1.2 Arguably the most distinctive seabed feature within the study area is the Southern Trench – located in the Outer Moray Firth, running parallel to the Aberdeenshire Coast. The main trench and its sub-trenches are of glacial origin, formed from at least two erosion events in different directions. These events may have been driven by different processes of fluvial and / or ice-marginal erosion, for example, by movement of a fast stream of glacier ice, sub-ice water or possibly from the catastrophic release of meltwater (Holmes *et al.*, 2004; Brooks *et al.*, 2011).



5.5.2 Option Agreement Area

5.5.2.1 Seabed morphology within the OAA has previously been described by Fugro (2023a) and is summarised here and in **Figure 6**. The seafloor deepens very gently from a minimum water depth of -87.8m LAT in the central region of the OAA to a maximum water depth of -133.7m LAT, in the south-east. The minimum water depth is located on a bathymetric high (depth range of -88m to -97m LAT) in the centre of the OAA. The maximum water depth is located within a large depression interpreted to be a pockmark – a feature formed by gas escaping from the seabed.

5.5.2.2 The average gradient within the OAA is very gentle (<1°). Steep and very steep gradients are mainly associated with the flanks of large depressions (pockmarks) located in the south-east of the OAA.

5.5.2.3 The morphology within the survey area is varied. Bedforms are present on the bathymetric high, there are large depressions interpreted as pockmarks and areas characterised by an irregular seafloor where erosional features such as relict ploughmarks are observed (**Figure 7**).

5.5.2.4 No significant large flow-transverse bedforms such as small-scale ripples, ripples, megaripples, sand waves or sand dunes were observed within the OAA during the Project geophysical survey (Fugro, 2023a). However, numerous elongated crests with an average height of 0.2m and an average wavelength of 20m were observed on the main patches of slightly silty fine to medium sand, within the bathymetric high (**Figure 7**). The bedforms have a very low relief (~0.2m in height) and were designated by Fugro (2023a) as sediment ridges (**Plate 5.1**).

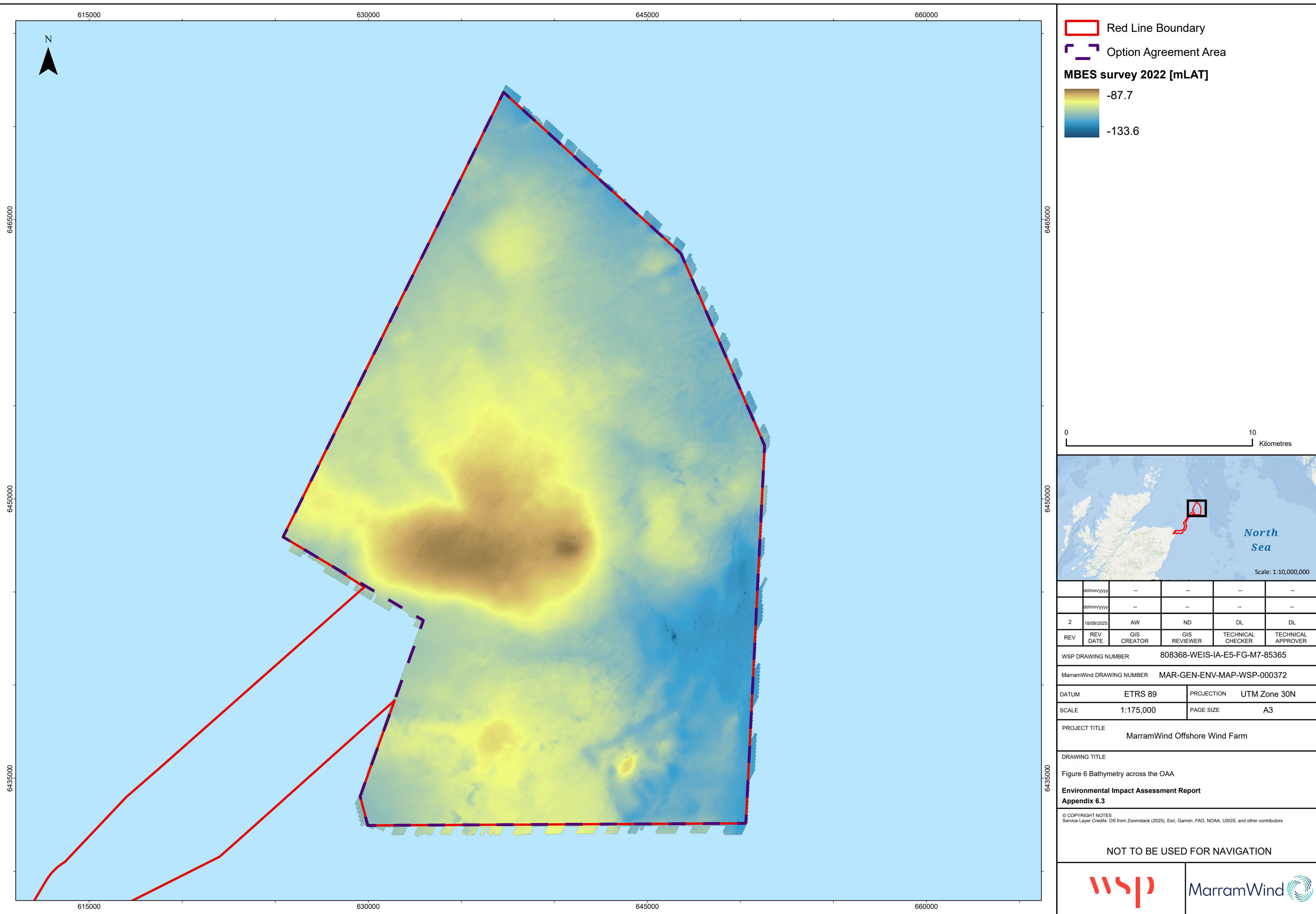
5.5.2.5 Ribbons or patches of sediment circa 0.1m to 0.3m height, interpreted to be 'sand ribbons' by Fugro (2023a), are also present on the bathymetric high (**Figure 7**). The majority of these overlie the sediment ridges. Some sandy patches are relatively localised and of variable shape and orientation; longer sand ribbons are up to 2.6km long and are mostly aligned with crest axis approximately south-west to north-east, nearly perpendicular to the more prominent seabed ridge crests. No smaller scale mobile bedforms were observed to be superimposed on the sand ribbons. Sand ribbon features are normally associated with low sediment abundance in higher current speed environments, and would be orientated parallel to the main flow axis – see Kenyon (1970a) which would appear inconsistent with the available current information (**Plate 3.2**). These appear more likely to be low relief (up to 0.25m) sand accumulations in the depressions between seabed ridges (more like sharp edged sand patches) caused or maintained by occasional larger storm events. This is discussed further in **Section 5.6**, in the context of sediment transport and seabed mobility.

5.5.2.6 A large number of depressions (circa 0.8m or more deep) were observed throughout the OAA. The vast majority are interpreted as relict pockmarks – with no indication of active fluid escape from the pockmarks (Fugro, 2023a). Analysis of the sub-seafloor geophysical data revealed the presence of numerous infilled pockmarks interpreted as relict pockmarks within the Witch Ground Formation in the south-east of the survey area. The correlation between seafloor depressions and relict pockmarks indicates that the majority of the depressions within the deepest sector of the OAA are likely to be an expression of the relict pockmarks.

5.5.2.7 Elongated pockmarks are present in the south-east of the survey area. This type of pockmark occurs on areas of seafloor influenced by bottom currents, where the depressions act as obstacles, inducing long erosional strips (Hovland *et al.*, 2002). The erosional strips are commonly defined as comet marks, with the distinctive patterns providing an indication of current intensities and predominant direction (Werner *et al.*, 1980). The alignment of the elongated pockmarks suggests a predominant bottom current in a south-east to north-west

direction within the deepest sector of the OAA. This is broadly consistent with the modelled tidal current data presented in **Plate 3.4**.

5.5.2.8 Relict ‘ploughmarks’ have also been mapped by Fugro (2023a). Based on sub-bottom profiler data, the relict ploughmarks are interpreted to be covered by the Holocene veneer and infilled with Witch Ground Formation sediments. These features are likely glacial in origin, potentially associated with scouring of the bed under the former British and Irish Ice Sheet (Clark *et al.*, 2022).



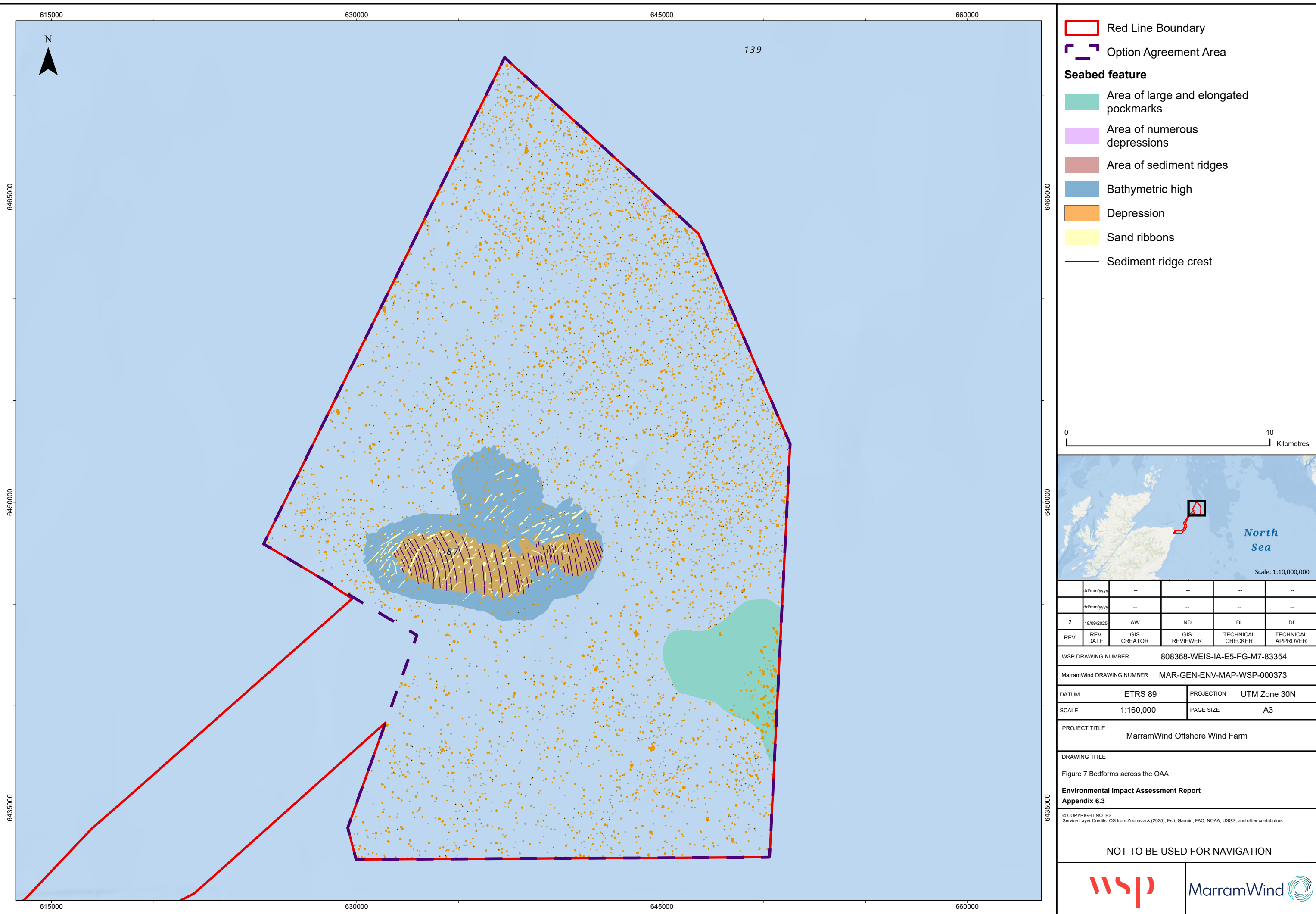
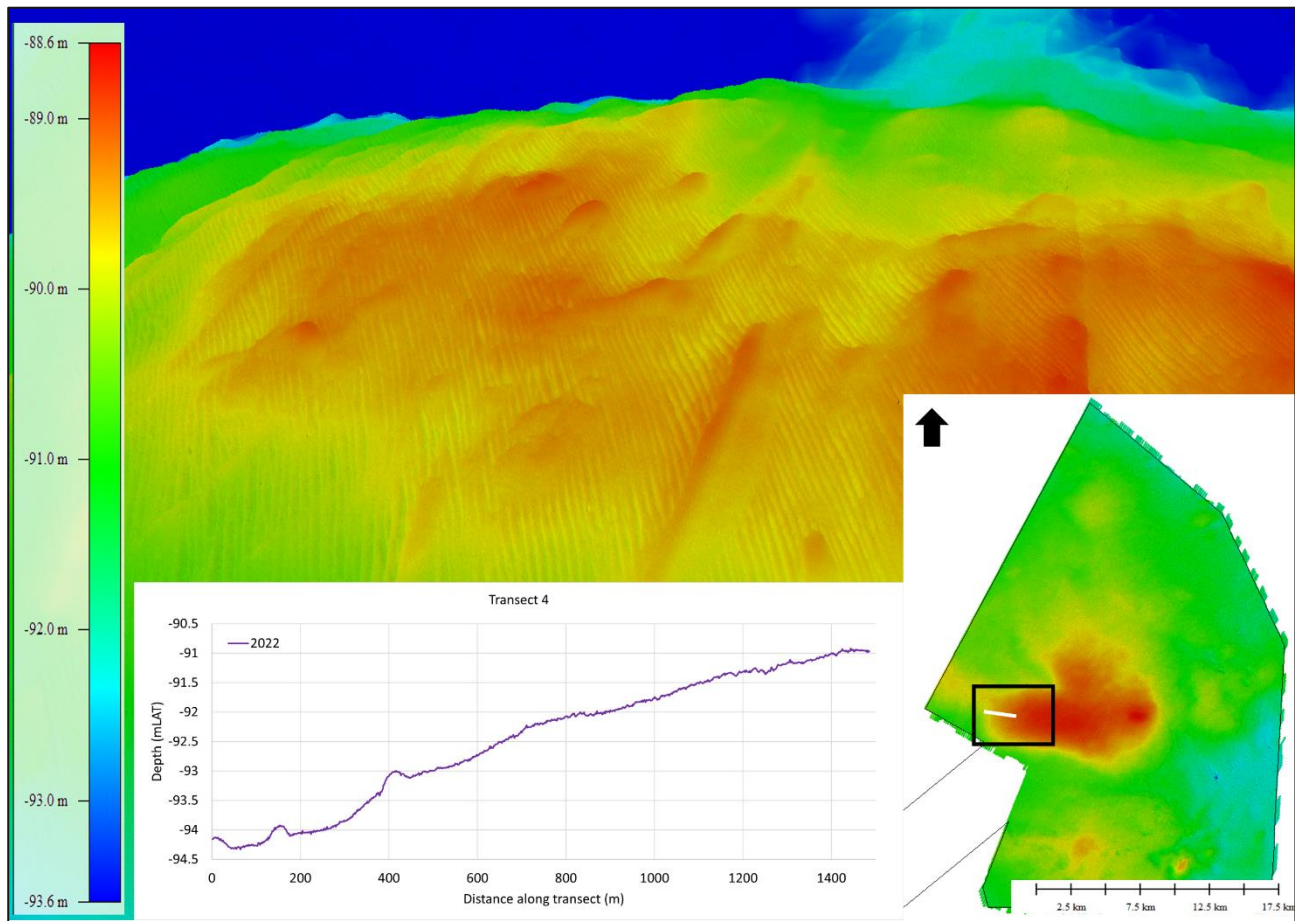
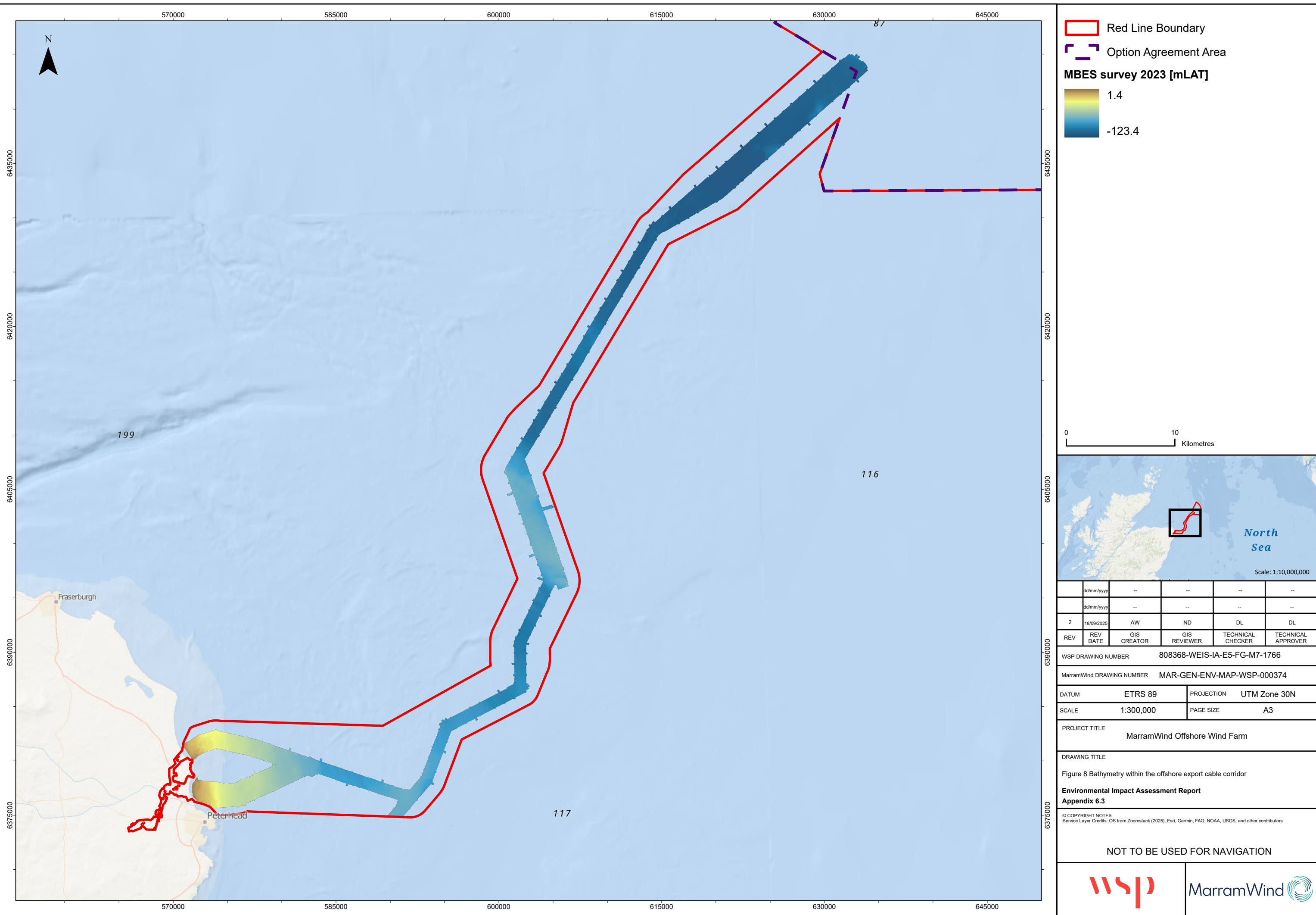


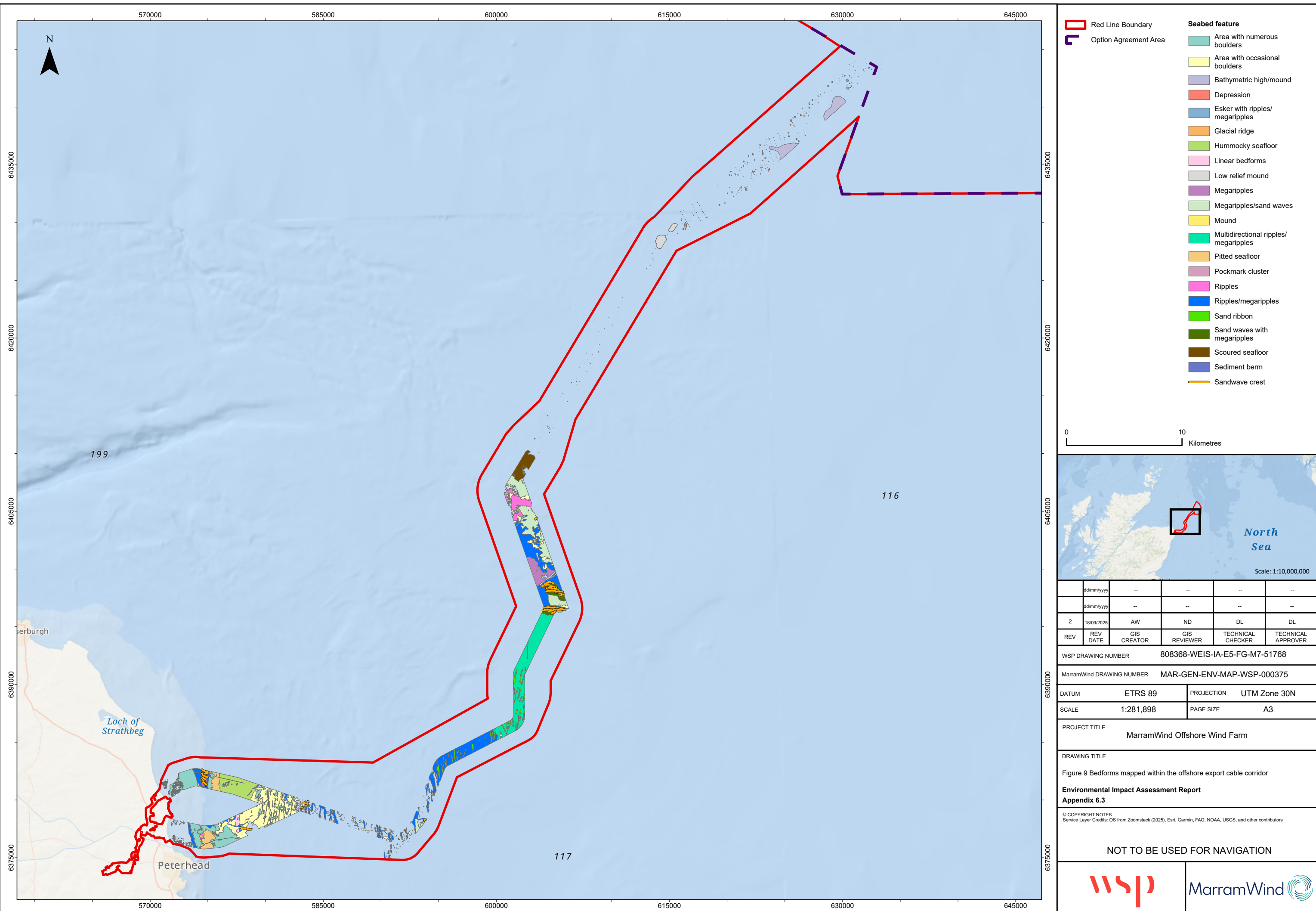
Plate 5.1 Bedform morphology within the OAA



5.5.3 Offshore export cable corridor

- 5.5.3.1 Seabed morphology within the offshore export cable corridor has previously been described by Fugro (2023b) and is summarised in **paragraph 5.5.3.2 et seq.** below and shown in **Figure 8**.
- 5.5.3.2 Maximum water depths reach more than -120m LAT along the offshore export cable corridor, with minimum water depths (of close to 0m LAT) found at the landfalls. Average seabed gradients are gentle (~1°), with a maximum gradient of ~76° observed in an area of outcropping bedrock close to the coast.
- 5.5.3.3 A range of active and relict bedforms have been identified (**Figure 9**).
- 5.5.3.4 Eskers, defined as sinuous ridges of glaciofluvial material deposited by a sub-glacial or englacial meltwater stream (Dove *et al.*, 2020), are observed within the surveyed area as positive relief features and are partially buried and post-dated by surficial ripples and megaripples.
- 5.5.3.5 Glacial moraines, although anticipated (Hall, 1990) were not observed in the Project geophysical survey. However numerous elongated low-relief glacial ridges draped by surficial Holocene sediments were mapped.
- 5.5.3.6 Pockmarks (with depressions of 0.8m or more) were identified in offshore areas of the route where the soft fine sediments of the Witch Ground Formation are present and underlie the Holocene veneer. There was no evidence of active fluid escape from the geophysical data.
- 5.5.3.7 Large-scale flow-transverse bedforms including ripples, megaripples and sand waves are observed from approximately 40km offshore to nearshore areas. In places, the height of the sandwave features exceeds 3m; the morphology of these features is considered further in **Section 5.5**, in relation to potential seabed mobility and net sediment transport. Ripple and Megaripples were also observed intermittently throughout the offshore export cable corridor.
- 5.5.3.8 A field of sand ribbons has been identified by Fugro (2023b) between approximately 20km to 30km offshore, ranging from 0.7m to 2.6m in height. The ribbons vary in length from 300m to 1.4km with a general north-north-east to south south-west orientation. They are typically perpendicular to ripple and mega-ripple crests (Kenyon, 1970a).
- 5.5.3.9 Two areas of pitted seafloor are observed within the approaches to the Scotstown and Lunderton landfalls, possibly caused by the presence of numerous boulders within the area. Close to the pitted seafloor, within the Scotstown approach the seafloor displays a hummocky appearance showing discontinuous and wavy sediment ridges varying in orientation. The hummocky seafloor may result from mobile sediments.





5.6 Sediment transport and seabed mobility

5.6.1 Overview

5.6.1.1 The determination of potential seafloor mobility or immobility and sediment transport pathways has been inferred both directly (from analysis and comparison of multiple historical bathymetric survey datasets) and indirectly, using regional scale sediment transport modelling. Findings from both sets of analysis are presented in this Section and combined to provide an overall conceptual understanding of sediment transport and seabed mobility within the study area.

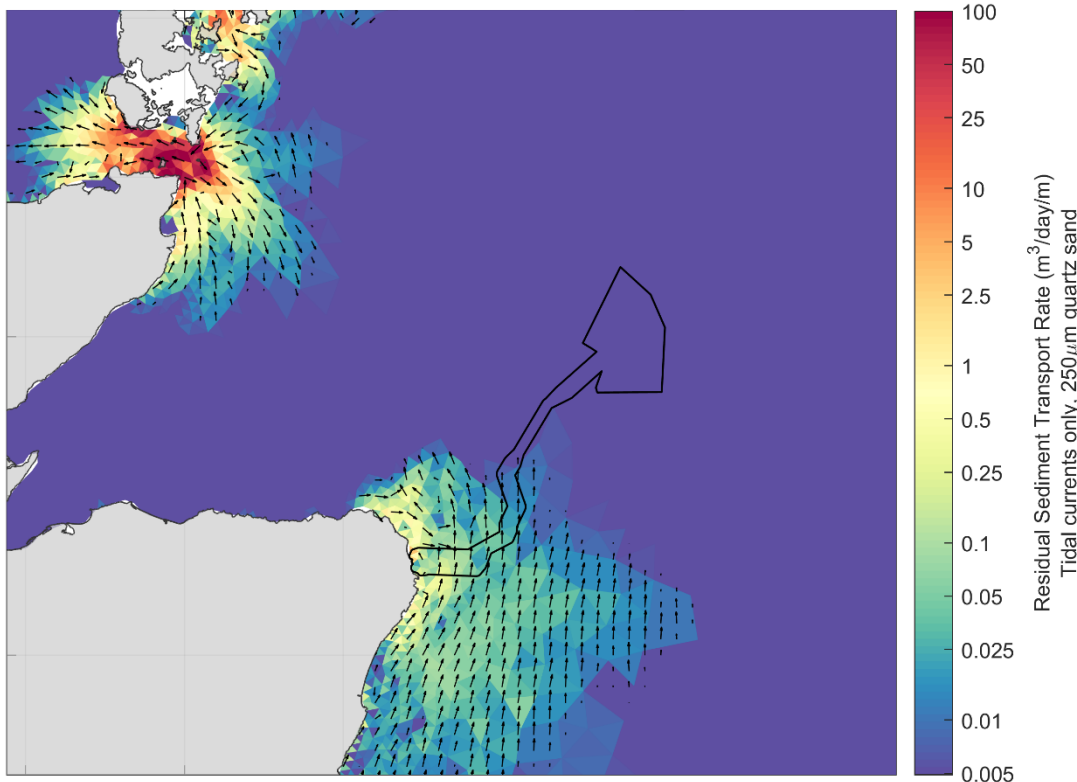
5.6.1.2 At the regional scale, bedload sediment transport is largely to the south in central / northern areas of the study area and to the north in southern parts of the study area. These region-scale patterns are driven by tidal asymmetry and result in the development of a bed load convergence zone off the coast of Peterhead, characterised by net long term sediment accretion. Wave driven transport dominates offshore, where tidal currents are weaker.

5.6.1.3 Sediment transport at the coast is described within the context of coastal cells and sub-cells in Ramsay and Brampton (2000a; 2000b). The study area is within sub-cell 2d (Cairnbulg Point to Girdle Ness) and sub-cell 3a (Portknockie to Cairnbulg Point), with a major cell divide at Cairnbulg Point. Within sub-cell 2d, net littoral drift is low, as northward wave-induced drift is generally cancelled-out by southward tidal currents. Within sub-cell 3a, there are many small pocket beaches that tend to be isolated from each other little accretion and little evidence of significant longshore drift (Barne *et al.*, 1996). Longshore sediment transport is dominated by wave action but tidal currents, particularly at high tide, may also transport sediment.

5.6.2 Sediment transport in the Option Agreement Area and offshore export cable corridor

5.6.2.1 Patterns and rates of potential sediment transport in the study area have been investigated using regional scale sediment transport modelling, as presented in the UK Renewables Atlas (ABPmer, 2025b). The underlying HD model is the SEASTATES Northwest European Shelf Hindcast model (ABPmer, 2017), run in a tide-only mode for a ~15 day period (one Spring-neap cycle) in November 2025. The Sand Transport (ST) module is enabled as part of the same model run to simulate the resulting temporally and spatially varying rate of potential transport for representative 250 micrometres (μm) (0.25mm) diameter sand. The resulting timeseries of instantaneous sediment transport rate and direction has been analysed to create a map of residual (long term net) potential sediment transport rate and direction (**Plate 5.2**). Units have been converted to the estimated volumetric rate of transport (m^3), per day, per metre width of seabed perpendicular to the direction of net transport.

Plate 5.2 Baseline residual sediment transport rate and direction, for 250µm quartz sand, predicted over a representative Spring-neap tidal period (ABPmer, 2025b)



5.6.2.2 Potential sediment transport is the rate that would occur, given the presence of an unlimited supply of the sediment type being assessed. In practice, some areas of the seabed will have limited or no mobile sediment remaining to transport (due to long term net transport away from that area) and so the actual rate for naturally present sediment will be lower than the maximum potential value in practice.

5.6.2.3 The instantaneous rate of potential sediment transport is generally proportional to the depth average current speed excess above a threshold value for initial motion (~0.3m/s-0.4m/s), squared. The net rate of potential sediment transport is also sensitive to any repetitive asymmetry or difference in the peak magnitude or duration of current speed on consecutive flood and ebb tides. These factors can result in disproportionately higher transport rates in areas of higher current speed and / or tidal asymmetry.

5.6.2.4 Key findings are summarised below:

- Potential net sediment transport rates are very low or negligible within the OAA and in offshore sections of the offshore export cable corridor, due to naturally low tidal current speeds that are insufficient to cause motion or transport of sand.
- Potential net sediment transport rates become higher with increasing proximity to the coast, due to generally higher current speeds accelerated around the Fraserburgh headland and peninsula.
- Potential net sediment transport direction around the Fraserburgh headland and peninsula is generally to the north, with some counter circulatory southerly transport closer to the coastline to the north of the landfall, directed out of the Moray Firth. The convergence of the sediment transport pathways around the landfall might explain the

relatively thicker accumulation of Holocene (sandy) material at the landfall, observed in the Project geophysical survey (**Figure 4**).

- Waves are not accounted for in the sediment transport model results shown above. However, occasional additional seabed sediment disturbance might also be expected due larger storm waves in relatively shallower water depths (<~50m water depth, for instance, close to the coastline). Wave action does not tend to cause measurable sediment transport in a particular direction but can temporarily enhance the rate of tidally induced transport, in the direction of the tidal current at the time of the storm. Wave action can also cause wave aligned seabed ripple features (up to a few tens of centimetres in height and up to a few metres length).

5.6.3 Seabed mobility in the Option Agreement Area and offshore export cable corridor

5.6.3.1 Observations of historical changes in seabed level can be used to help identify areas where the seabed may potentially be mobile over the lifetime of the Project. Historic bathymetric data is available from the UKHO, with 4m to 8m resolution data available across much of the offshore export cable corridor: this historic bathymetry data can be compared directly with the high resolution (0.5m) multibeam collected for the Project in 2022 (Fugro, 2023a; 2023b) (**Figure 2**). It is noted that the higher (4m) resolution UKHO data is only available in some locations where sandwaves have been mapped by Fugro (2023b) and no historic bathymetry data is available for the OAA.

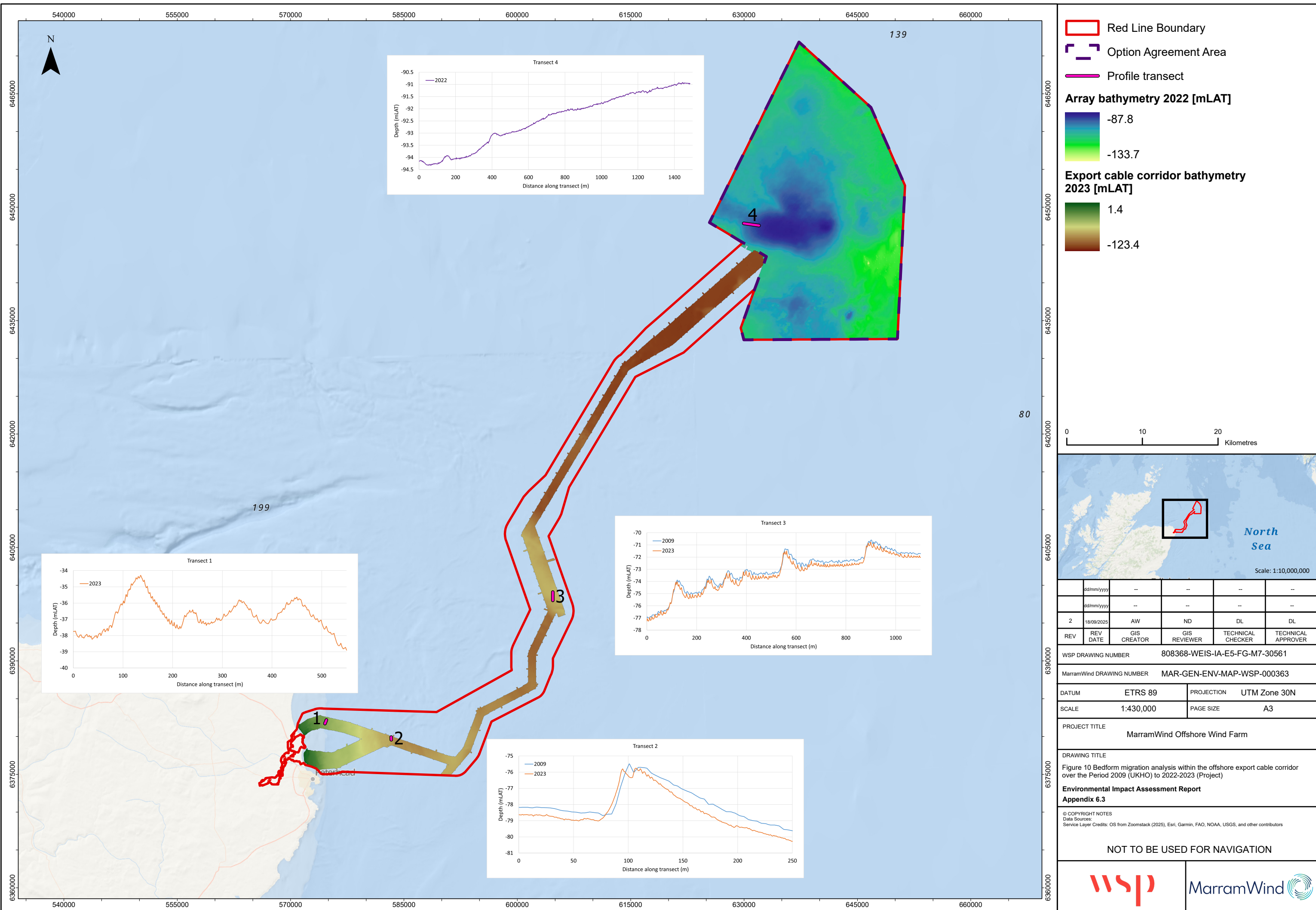
5.6.3.2 Additional sources of historic bathymetry were also sought – including that available through the BGS Strategic Environmental Assessment (SEA) portal (BGS, 2025) – but no other data was available from the OAA or offshore export cable corridor.

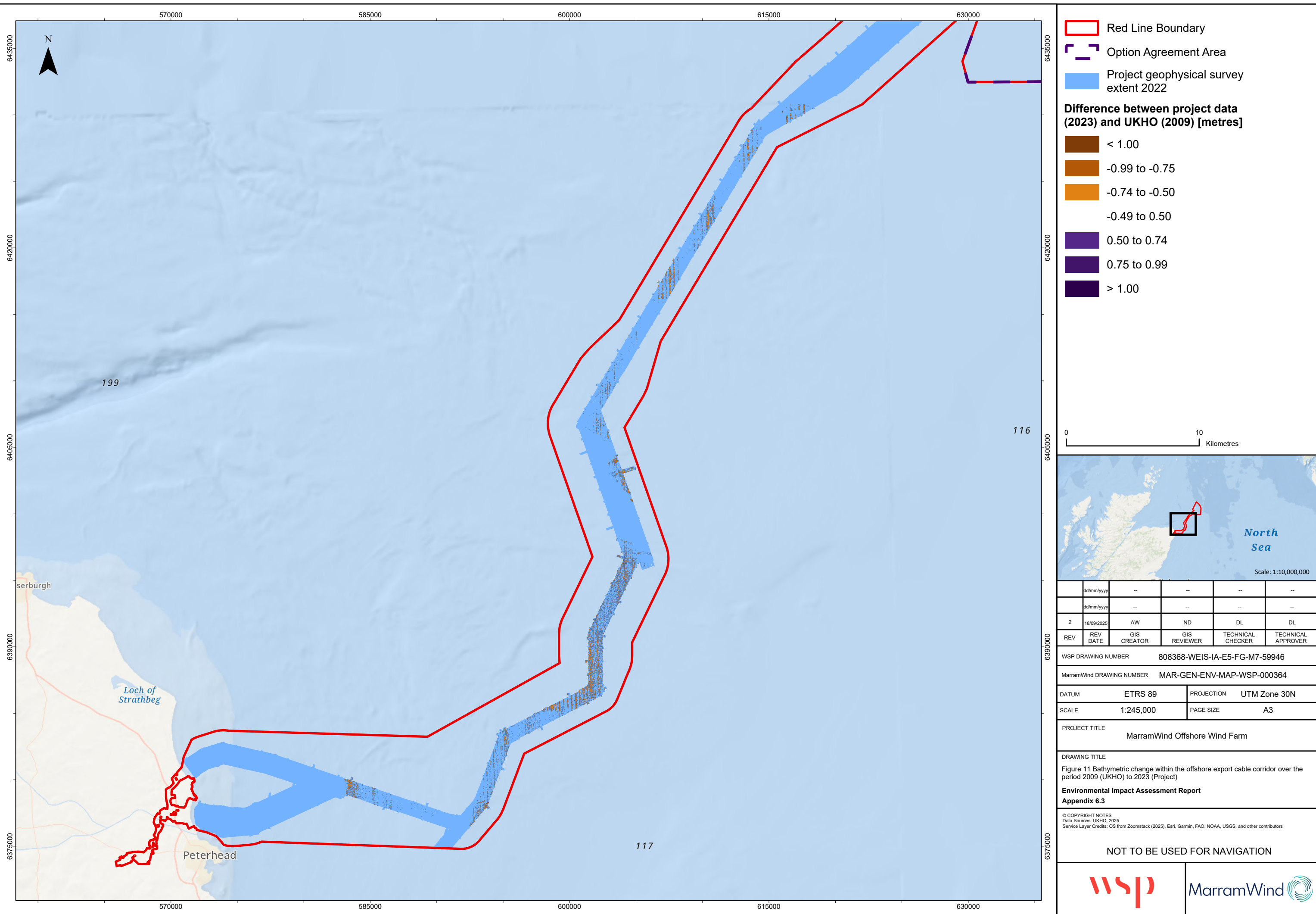
5.6.3.3 Because of the relative coarseness of the UKHO (4m to 8m resolution) data, it is not expected that this will resolve smaller bedforms such as ripples and small megaripples which are known to be present along the route (**Figure 9**). As such, it does not necessarily follow that all areas identified as showing no change between the 2009 and 2022 surveys are immobile.

5.6.3.4 Allowing for vertical uncertainty in the two measured data sets, and the relatively coarse resolution of the UKHO (2009) data, there is limited or no meaningful evidence of widespread seabed level change (erosion or accretion) within the offshore export cable corridor or OAA (**Figure 10** and **Figure 11**).

5.6.3.5 Larger sandwave features located approximately halfway along the offshore export cable corridor did not appear to migrate measurably during the 13-year interval between surveys (**Figure 10**). Some limited reshaping of an isolated barchan dune type feature in the nearshore area was measurable, but the overall position of the feature remained largely unchanged.

5.6.3.6 Where present, smaller ripple and megaripple features (not resolved by the UKHO data) are likely to migrate and evolve over shorter timescales of weeks to months, depending on the strength of tidal conditions. As they migrate, the local seabed level will appear to vary about the mean seabed level over time, by half the crest to trough height (for instance, approximately $\pm 0.15\text{m}$ to 0.3m).





5.6.4 Conceptual understanding of seabed change

5.6.4.1 Conceptual understanding of the of the coastal and offshore system in which the Project is located is summarised in **Figure 12** and set out below. This draws upon a combination of (i) the sediment transport modelling; (ii) the direct evidence of bathymetric change since 2009; and (iii) consideration of established relationships between current speed and bedform development (for example, Belderson *et al.*, 1982) to identify areas of more (or less) seabed mobility and the direction of sediment transport / bedform migration.

5.6.4.2 Included on **Figure 12** are a series of 'Behaviour Zones' within the OAA and offshore export cable corridor. The purpose of these zones is to identify sub-areas that exhibit key behavioural similarities with respect to seabed mobility. The meaning of (the full possible range of) mapped categories are summarised in **Table 5.3**.

5.6.4.3 Close to the landfall (within 5km of the coast), within the offshore export cable corridor, the seabed is characterised as a sandy veneer over bedrock. The thickness of the sediment veneer (described in **Section 5.6.3**) is relatively more variable in the nearshore area, being locally thicker (up to several metres) in some areas, and thin or absent in other areas where bedrock is outcropping. In the shallowest nearshore parts of the route (water depth <5m to 10m LAT), wave induced ripples (height ~0.1m to 0.2m) are evident and are likely to be occasionally mobile during larger storm events. The cross-shore exchange of sediment between the beach and shallow sub-tidal areas by wave action may also result in episodic or seasonal variation of the beach and seabed level in the order of up to a few metres (this is not directly visible in the available data, but is a reasonable assumption based on normal beach processes).

5.6.4.4 In the adjacent slightly deeper water nearshore, tidal currents are sufficient to cause more frequent mobility of the sandy veneer where it is present. Smaller current induced ripple bedforms (height typically 0.3m, but up to 0.6m) are evident in areas of intermediate sediment veneer thickness. Larger sand wave type bedforms (height up to 2.5m) with ripples superimposed are present in a narrow area of greater sediment thickness within a few hundred metres of the beach (transect 1 in **Figure 10**). An isolated barchan dune feature (height 3.8m) is also visible in the nearshore area (transect 2 in **Figure 10**).

5.6.4.5 Ripple bedforms (height 0.3m) are extensively present within the nearshore half of the offshore export cable corridor, up to ~40km from the coast. This corresponds to the area of accelerated tidal current speed around the Fraserburgh Headland and associated net sediment transport (shown in **Plate 5.2**). Localised areas of larger sandwaves (example in transect 3 in **Figure 10**) are present towards the offshore edge of this area, where a greater volume of sand has accumulated at the end of the sediment transport pathway. The transect comparison in **Figure 10** indicates that the overall shape and crest positions of these features did not change meaningfully in the 13 years between the surveys.

5.6.4.6 Beyond this area, in the offshore half of the offshore export cable corridor and in all of the OAA, tidal current speed is normally insufficient, and the water depth is too large for waves to cause sediment mobility on a regular basis. Mainly sandy sediment is still present in a thin veneer but there is an absence of current induced bedforms that are interpreted as mobile. The seabed level in this area is unlikely to be naturally variable except possibly during very large storm events. Even then, vertical change is expected to be less than approximately 0.25m.

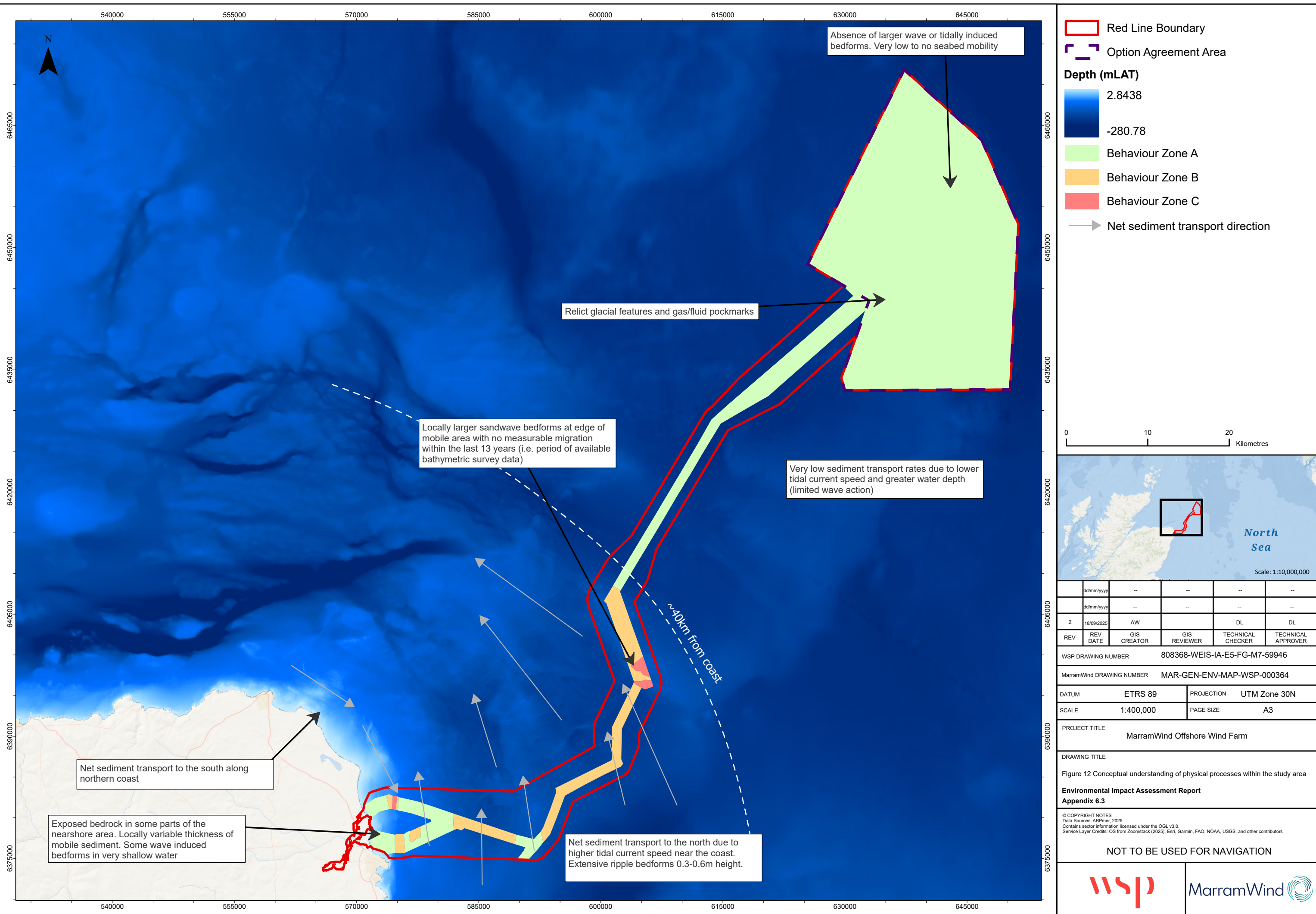
5.6.4.7 It is noted here that Fugro (2023a) has identified 'sand ribbons' within the OAA, which have a height of circa 0.1m to 0.3m (**Figure 7**). Sand ribbons are bedform features found in areas characterised by high (>c.1m/s) current speeds and form longitudinally to the main axis of flow (Belderson *et al.*, 1982). Given the OAA is characterised by relatively low current speeds (**Section 3.3**) with the main axis of flow broadly north to south, it is considered unlikely that these bedforms are sand ribbons. Instead, these features could potentially be

sharp edge sand patches which are local accumulations of sand found in areas characterised by weak tidal currents and formed by the action of waves occasionally stirring the bed during very large storms (Kenyon, 1970b).

5.6.4.8 Localised gas or fluid release related pockmarks have also been mapped by Fugro (2023a). No evidence of active gas / fluid release was found during the survey so these features are presumed to be relict. Elongated pockmarks – such as those mapped in the south-east of the OAA – typically occurs on areas of seafloor influenced by strong bottom currents (Hovland *et al.*, 2002). Whilst present day tidal currents are unlikely to be of sufficient strength to have caused this elongation, it is possible that surge currents during very large storms – which may reach approximately 0.6m/s during a 1 in 50 year storm (Health and Safety Executive, 2002) – may be responsible. Alternatively, elongation of the features may have occurred sometime in the past – perhaps during the early Holocene – when tidal currents may have been stronger in this region as a consequence of the very different geographic configuration of the North Sea (for example, Uehara *et al.*, 2006).

Table 5.3 Behaviour zones and associated characteristics identified in the OAA and along the offshore export cable corridor

Behaviour zone	Description	Further information
A	Little to no expected variability >0.25m.	Limited or no active present-day sediment transport - features present likely to be relict.
B	Variability of order <1m realistically possible.	Active development and migration of superficial ripples to smaller mega-ripple bedforms.
C	Variability of order 1m to 3m realistically possible.	Gradual development and migration of bedforms up to larger mega-ripples and smaller sand waves.



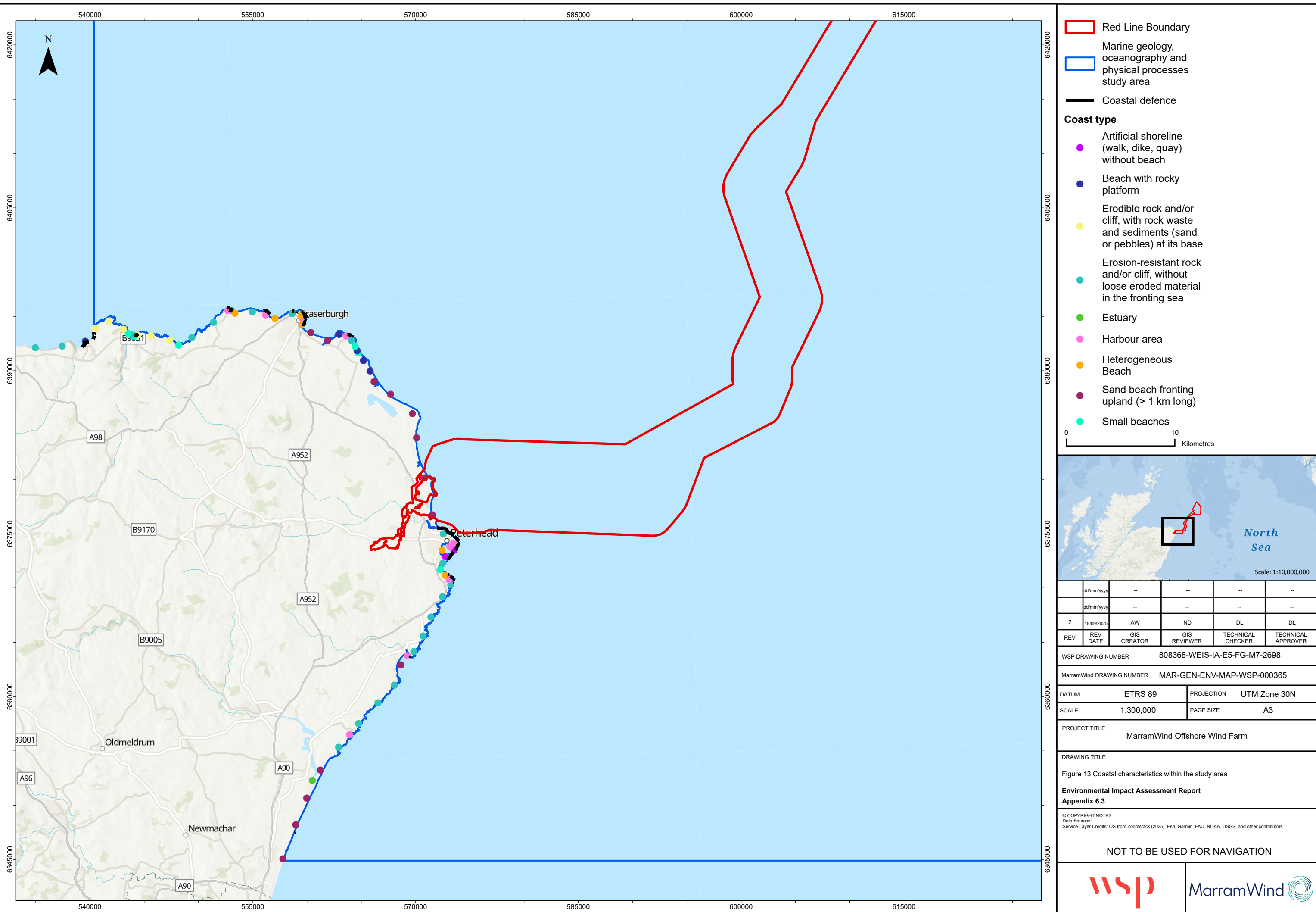
6. Coastal Geomorphology and Characteristics

6.1.1.1 This Section describes the coastal characteristics within the study area, with particular focus on the landfall. Consideration is also given to the potential for future change over the lifetime of the Project.

6.2 Regional overview

6.2.1.1 The coastline in the study area extends from Troup Head (in the north-west) to the River Ythan (in the south-east). Rocky / clifffed coastlines which are resilient to marine erosion dominate much of the study area. However, extensive sandy beaches with accompanying dune systems are present between Cairnbulg Point and Peterhead and are located within the Loch of Strathbeg SSSI (**Figure 13**).

6.2.1.2 No formal Shoreline Management Plan has been announced by Aberdeenshire Council for coastlines within the study area although present Scottish Planning Policy guidance is that new development requiring new defences against coastal erosion or coastal flooding will not be supported except where there is a clear justification for a departure. Most of the coastline within the study area is undefended, reflecting (at least in part) its resilience to erosion. However localised artificial defences are in place, especially around the larger coastal settlements of Peterhead and Fraserburgh.



6.3 Landfall

6.3.1.1 The options for cable landfall are as follows:

- Option 1: Lunderton - all export cable cables would make landfall at Lunderton based on the following scenarios:
 - ▶ all export cable circuits make landfall at Lunderton North (Option 1a); or
 - ▶ all export cable circuits would make landfall at a combination of Lunderton North and Lunderton South (Option 1b); and
- Option 2: Scotstown and Lunderton - export cable circuits would make landfall at a combination of Lunderton (North and / or South) and Scotstown.

6.3.1.2 Both landfall zones include stretches of intertidal sand extending from dunes, through a dry upper shore zone, to mid and lower shore mobile sand. Hard substrate is also present. A more detailed characterisation of both landfalls has been set out in APEM (2024) and is summarised below.

6.3.1.3 Lunderton is an exposed sandy beach, about 2km long extending north to south between two ill-defined rocky promontories. Most of the landfall area comprises a shallow sandy bay with gently sloping smooth or rippled clean sand on the mid to lower shore, about 300m wide. There is a clear demarcation of drier more steeply sloping sand on the upper shore with a weak strandline. Sand dunes flank the upper shore along the entire length of the beach. The northernmost rocky promontory is low and comprised medium boulders. The southernmost promontory, adjacent to Peterhead Golf Course, extends on to the upper shore almost to the dunes, with only a narrow strip of upper shore sand between the stones and dunes. It included some moderately high bedrock outcrops

6.3.1.4 Scotstown is an exposed sandy beach located in Rattray Bay, which extends about 5km north to south between Rattray Head and the rock / stony headland at Scotstown Head. The landfall itself is approximately 800m wide and is located just to the south of Annachie Burn and the St Fergus Gas Terminal. As at Lunderton, the beach is approximately 300m wide, flanked by dunes. At the southern end of the beach there is an indistinct headland with bedrock (Peterhead granite) outcropping on the mid shore. Boulders and cobbles of a range of sizes surround the rock on all sides. Sand and dunes extend behind the outcrop on the mid and upper shore.

6.3.1.5 The pattern of the build-up of salients (including at Rattray and Scotstown Heads) indicates a relatively stable regime, at present, in terms of net longshore drift. Rates of transport depend heavily on the wave conditions, though tidal currents acting in conjunction with waves are also likely to be capable of moving sediment. Cyclic seasonal effects of frontal dune undercutting and beach lowering under storm wave conditions and re-accretion due to swell wave and wind action are evident along this stretch of coastline (Ramsay and Brampton, 2000a).

6.3.1.6 The historic mapping evidence presented in Rennie *et al.* (2021) suggests that the position of MHWS both at Lunderton and Scotstown has either remained the same or slightly advanced in places over the past 50 years, by up to circa 40m. However, at least some of this change may be explained by survey inaccuracy. This pattern of stability is consistent with aerial imagery from the landfall for the period between 2008 and 2023, available from Google Earth (Google, no date) (**Plate 6.1** and **Plate 6.2**).

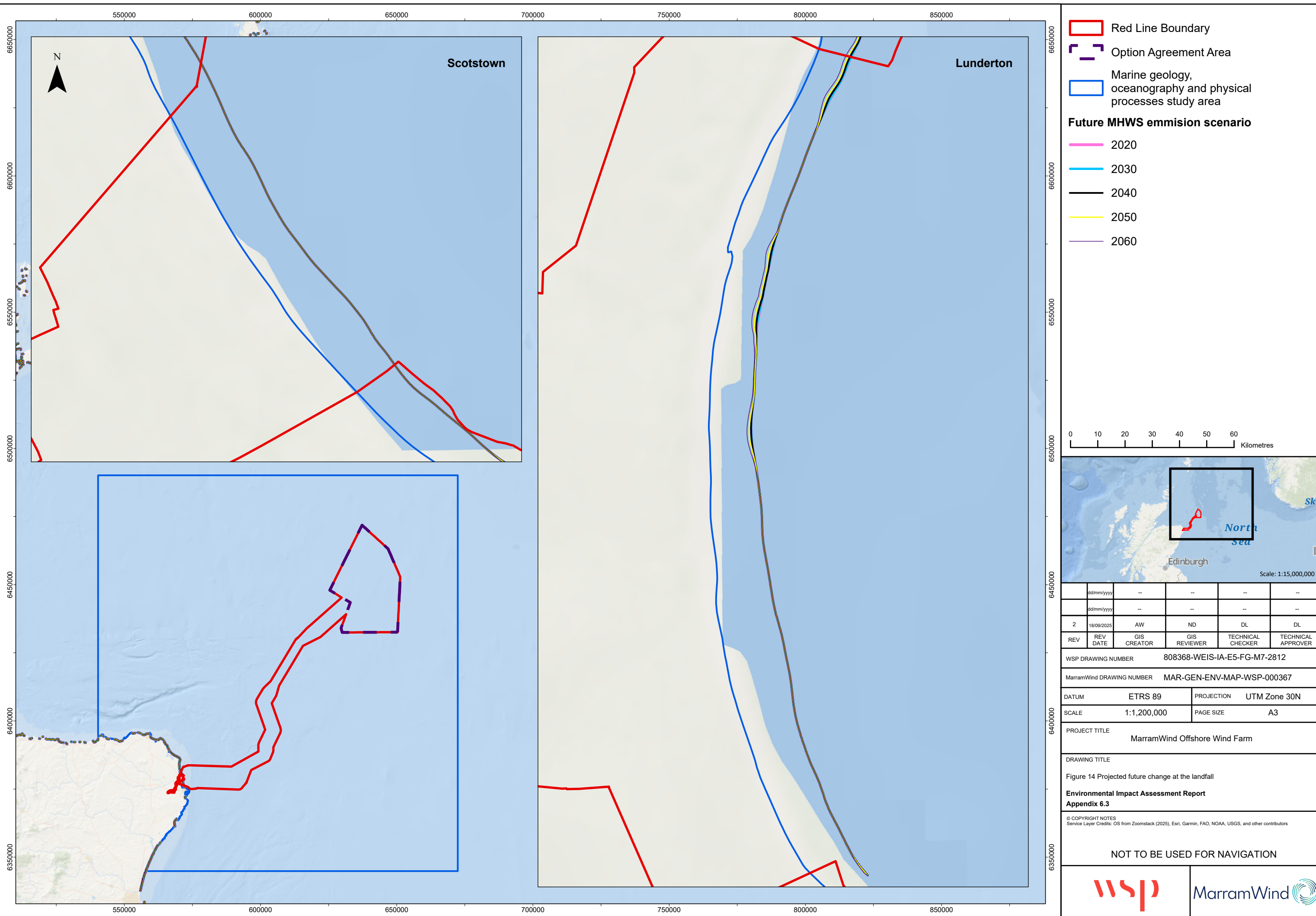
6.3.1.7 Negligible recession in the position of the MHWS contour is predicted by 2060 at Scotstown, even under a high sea level rise scenario. Up to c.15m of recession is predicted in places at Lunderton over the same time period although most areas are expected to see very little change (Rennie *et al.*, 2021) (**Figure 14**).

Plate 6.1 Aerial imagery of the landfall at Scotstown (Google, no date)



Plate 6.2 Aerial imagery of the landfall at Lunderton (North & South) (Google, no date)





7. Summary

7.1.1.1 This technical Appendix provides a high-level summary of the existing environment across the study area, with consideration given to bathymetry, water levels, currents, waves, stratification, seabed sediments and geomorphology. Key aspects are summarised below for the OAA, offshore export cable corridor and landfall zones.

7.2 Current baseline

7.2.1 Option Agreement Area

7.2.1.1 The OAA is located in a meso-tidal setting, with the mean Spring tidal range typically between approximately 1.7m to 1.9m. Mean Spring peak current speeds are weak and are typically less than approximately 0.4m/s. Flow direction is approximately northwards during the ebb tide and south south-east during the flood tide.

7.2.1.2 The OAA is exposed to longer wave fetches (distances of open water over which waves can develop) from the north to north-east. Smaller, but more frequently occurring, wave conditions generated by local winds predominately come from southerly directions. Significant wave heights of approximately 9.2m are predicted for a 1:1 year event, increasing to 13.8m for a 1:50 year event.

7.2.1.3 The OAA is located in an area described by van Leeuwen *et al.* (2015) as being “*seasonally stratified*”, defined as >120 days in the year where the water column is stratified and <90 in the year where the water column is fully mixed. During the Winter months (November to April), reduced solar heating and increased turbulent mixing from wind and waves result in very weakly stratified to mixed waters in the OAA, characterised by homogeneous temperature and density profiles, with PEA values around 30J/m³. With the onset of Spring and Summer, calmer weather and longer, warmer days enhance stratification, overcoming the mixing effects of tide and winds. From May to October, this leads to a vertical temperature gradient and an increase in PEA values. Over the 14-year analysis period (2010-2023), PEA typically reaches around 140J/m³ in mid-Summer, indicating a strongly stratified water column. However, there is variability in the strength of Summer stratification from year to year.

7.2.1.4 During Summer, elevated chlorophyll-a concentrations - likely associated with a tidal mixing front - are commonly observed west of the OAA. However, their exact positioning varies significantly between years.

7.2.1.5 The seabed within the OAA can be generally described as a widely distributed but thin veneer of relatively sandy sediment, laid down and reworked during the Holocene period (the last 11,700 years since the last major glacial period). The seafloor sediments mainly comprise a combination of sand and silt, varying from slightly silty fine to medium sand to fine to medium sandy silt. Silty fine to medium sand is the predominant seafloor sediment. The only patches of gravels present are located within some of the seafloor depressions, where there are accumulations of gravel (shell and lithic fragments) and occasional cobbles / boulders. The thickness of the surficial Holocene veneer within the OAA is typically thin (0.25m to 1m) and may be absent in some locations (exposed bedrock or other erosion resistant substrate). These surficial units are underlain by various sequences of Pleistocene age (the period between approximately 2.6 million years ago and 11,700 years ago).

7.2.1.6 Consideration of the project specific geophysical survey data shows that water depths within the OAA range between approximately -88m and -134m below LAT. The average gradient

within the OAA is very gentle ($<1^\circ$), with steep and very steep gradients mainly associated with the flanks of large depressions (relict pockmarks).

7.2.1.7 Across the OAA, tidal current speed is normally insufficient, and the water depth is too large for waves to cause sediment mobility on a regular basis. Mainly sandy sediment is still present in a thin veneer but there is an absence of current induced bedforms that are interpreted as mobile. The seabed level in this area is unlikely to be naturally variable except possibly during very large storm events. Even then, vertical change is expected to be less than approximately 0.25m.

7.2.2 Offshore export cable corridor

7.2.2.1 Tidal range increases with proximity to the coast along the offshore export cable corridor, increasing from around 1.9m at the offshore end to approximately 3.1m at the landfall zones (ABPmer *et al.*, 2008). Tidal current speeds also increase from offshore to nearshore, from around 0.4m/s where the offshore export cable meets the OAA to around 1m/s in the vicinity of the landfall zones. Residual flow fields are found to be relatively weak and variable along the offshore export cable corridor although the general trend is for residual flow in a southward and eastward direction.

7.2.2.2 Waves are generally from northerly or southerly directions although further inshore, towards the landfall, waves have a greater easterly component since they are progressively refracted as they approach the adjacent coastline.

7.2.2.3 Within the offshore export cable corridor, the seafloor sediments mainly comprise a combination of silt, sand, and gravel and are Holocene in age. Based on the results from the environmental grab samples, sand is the predominant main soil type with gradual changes in grain size across the route. Bedrock is observed outcropping at the seafloor in nearshore areas including at the landfall zones. The surficial Holocene sediments are generally between 0m to 1m thick. However, they reach a thickness of >5m in places.

7.2.2.4 Maximum water depths reach more than -120m LAT along the offshore export cable corridor, with minimum water depths (of close to 0m LAT) found at the landfalls. Average seabed gradients are gentle ($\sim 1^\circ$), with a maximum gradient of $\sim 76^\circ$ observed in an area of outcropping bedrock close to the coast. A range of relict bedforms have been identified including eskers, glacial moraines and pockmarks, the latter having formed from the escape of fluid or gas from the seabed.

7.2.2.5 Large-scale flow-transverse bedforms including ripples, megaripples and sand waves are observed from approximately 40km offshore to nearshore areas. Current speeds are sufficiently high for bedform migration to occur in these nearshore areas although clear and unambiguous evidence of this is not observed through comparison of the project geophysical survey data with older bathymetry data available from UKHO (UKHO, 2009). Beyond a distance of approximately 40km from the coast, in the offshore half of the offshore export cable corridor (and in all of the OAA), tidal current speeds are normally insufficient, and the water depth too large for waves to cause sediment mobility on a regular basis.

7.2.3 Landfall zones

7.2.3.1 The export cables may make landfall at Lunderton or at Scotstown and Lunderton.

7.2.3.2 Scotstown is an exposed sandy beach located in Rattray Bay, which extends about 5km north to south between Rattray Head and the rock / stony headland at Scotstown Head. The beach is approximately 300m wide, flanked by dunes. At the southern end of the beach there is an indistinct headland with bedrock (Peterhead granite) outcropping on the mid

shore. Boulders and cobbles of a range of sizes surround the rock on all sides. Sand and dunes extend behind the outcrop on the mid and upper shore.

7.2.3.3 Lunderton is an exposed sandy beach, about 2km long extending north to south between two ill-defined rocky promontories. Most of the landfall area comprises a shallow sandy bay with gently sloping smooth or rippled clean sand on the mid to lower shore, about 300m wide. Sand dunes flank the upper shore along the entire length of the beach. The northernmost rocky promontory is low and comprised medium boulders. The southernmost promontory, adjacent to Peterhead Golf Course, extends on to the upper shore almost to the dunes, with only a narrow strip of upper shore sand between the stones and dunes. It included some moderately high bedrock outcrops

7.2.3.4 The cross-shore exchange of sediment between the beach areas and shallow sub-tidal areas by wave action may also result in episodic or seasonal variation of the beach and seabed level in the order of up to a few metres (this is not directly visible in the available data, but is a reasonable assumption based on normal beach processes).

7.2.3.5 The available evidence indicates a relatively stable regime, at present, in terms of net longshore drift. This is supported by available historic mapping evidence. Cyclic seasonal effects of frontal dune undercutting and beach lowering under storm wave conditions and re-accretion due to swell wave and wind action are evident along this stretch of coastline.

7.3 Future baseline

7.3.1.1 The baseline is expected to evolve in response to natural variation (for example, lunar nodal cycle, North Atlantic Oscillation etc), wider changes in climate expected over the lifetime of the project, and anthropogenic management of the coast. These are discussed below.

7.3.1.2 By 2060, relative sea level may have risen by approximately 0.3m above baseline (1981-2000) levels (RCP 8.5) (Palmer *et al.*, 2018). A rise in sea level may allow larger waves, and therefore more wave energy, to reach the coast in certain conditions and consequently result in an increase in local rates or patterns of erosion and the equilibrium position of coastal features. Notwithstanding this, negligible recession in the position of the MHWS contour is predicted by 2060 at Scotstown, even under a high sea level rise scenario. Up to c.15m of recession is predicted in places at Lunderton over the same time period although most areas at Lunderton are expected to see very little change.

7.3.1.3 Some of the shoreline adjacent to the Project is defended. This includes parts of the coastline around Peterhead and Fraserburgh. The future evolution of the coastline in these areas will depend to some extent on any changes to the existing management strategies.

7.3.1.4 The UK Climate Impacts Programme dataset 'UKCP18' provides projections of changes to storm surge magnitude in the future as a result of climate change. These projections of change in extreme coastal water levels are dominated by the increase in mean sea level with only a minor (<10%) additional contribution due to atmospheric storminess changes over the 21st century (Palmer *et al.*, 2018).

7.3.1.5 The stratification dynamics in the North Sea are expected to undergo significant changes due to the changing climate. The timing of stratification is influenced by the interplay between solar heating and tidal mixing, with a smaller but notable contribution from wind-driven mixing. Global warming and changes to meteorological conditions is likely to alter the timing of Spring stratification, and subsequently the timing of the Spring phytoplankton bloom.

7.3.1.6 Model projections suggest that by 2100, the thermal stratification period in UK shelf seas will extend by approximately two weeks (Sharples *et al.*, 2025), with stratification occurring about one week earlier and breaking down 5-10 days later than present (Sharples *et al.*,

2022). Model projections also suggest that seas across the north-west European shelf, including the northern North Sea, will experience greater surface-to-bottom temperature differences as the seasonal heating cycle intensifies (Tinker *et al.*, 2016), resulting in stronger stratification. Alongside the strengthening stratification there will be small shifts in the position of tidal mixing fronts as thermal stratification pushes into shower waters and / or stronger tidal regions.

8. References

ABPmer, (2013). *SEASTATES Wave Hindcast Model: Calibration and Validation Report*. August 2013. [online] Available at: <https://www.seastates.net/downloads/> [Accessed: 11 August 2025]

ABPmer, (2017). *SEASTATES Northwest European Continental Shelf Tide and Surge Hindcast Database, Model validation report*. March 2017. [online] Available at: <https://www.seastates.net/downloads/> [Accessed: 11 August 2025].

ABPmer, (2025a). *SEASTATES data Explorer*. [online] Available at: www.seastates.net/explore-data/ [Accessed: 09 June 2025].

ABPmer, (2025b). *Modelled sediment transport layers covering the North Sea and the northwest European continental shelf*. [online] Available at: [https://www.renewables-atlas.info/](http://www.renewables-atlas.info/) [Accessed: 09 June 2025].

ABPmer, Met Office and POL, (2008). *Atlas of Renewable Energy Resources: Atlas Pages*. A Strategic Environmental Assessment Report, March 2008. Produced for BERR. Report and associated GIS layers. [online] Available at: <http://www.renewables-atlas.info/> [Accessed: 09 June 2025].

APEM, (2024). *MarramWind intertidal macrobiota survey 2023*. APEM Scientific Report P00012014-02 MarramWind Limited, 16/01/2024, v2.2 Final, 67 pp.

Barne, J.H., Robson, C.F., Kaznowska, S.S., Doody, J.P. and Davidson, N.C., eds., (1996). *Coasts and seas of the United Kingdom. Region 3 North-east Scotland: Cape Wrath to St. Cyrus*. Peterborough: Joint Nature Conservation Committee.

Baxter, J., Boyd, I., Cox, M., Donald, A., Malcolm, S., Miles, H., Miller, B. and Moddat, C., (2011). *Scotland's Marine Atlas: Information for the National Marine Plan*. Report by Scottish Government.

Belderson, RH., Johnson, M.A., and Kenyon, N.H., (1982). *Bedforms*. In: *Stride, AH (ed)*. Offshore tidal sands, processes and deposits. Chapman and Hall Ltd, London, UK pp 27-57.

British Geological Survey (BGS), (1984). *Peterhead 57N 02W sea bed sediments, 1:250,000 geological map*.

British Geological Survey (BGS), (2025). Strategic environmental assessment (SEA) data portal. [online] Available at: <https://webapps.bgs.ac.uk/data/sea/app/search> [Accessed 11 August 2025]

Brooks, A.J., Kenyon, N.H., Leslie, A., Long, D. and Gordon, J.E. (2011). *Characterising Scotland's marine environment to define search locations for new Marine Protected Areas. Part 2: The identification of key geodiversity areas in Scottish waters*. Scottish Natural Heritage Commissioned Report No.430.

Centre for Environment, Fisheries and Aquaculture Science (Cefas), (2016). *Suspended Sediment Climatologies around the UK. Report for the UK*. Department for Business, Energy & Industrial Strategy offshore energy Strategic Environmental Assessment programme

Chust, G., Allen, J. I., Bopp, L., Schrum, C., Holt, J., Tsiaras, K., Zavatarelli, M., Chifflet, M., Cannaby, H., Dadou, I., Daewel, U., Wakelin, S. L., Machu, E., Pushpadas, D., Butenschon, M., Artioli, Y., Petihakis, G., Smith, C., Garçon, V., Goubanova, K., Le Vu, B., Fach, B. A., Salihoglu, B., Clementi, E. and Irigoien, X., (2014). *Biomass changes and trophic amplification of plankton in a warmer climate*. Global Change Biology, 20(7), 2124-2139, doi: 10.1111/gcb.12562.

Clark, Chris D., Ely, Jeremy C., Hindmarsh, Richard C.A., Bradley, Sarah L., Ignecz, Adam; Fabel, Derek; Ó Cofaigh, Colm., Chiverrell, Richard C., Scourse, James D., Benetti, Sara., Bradwell, T., Evans, D.J.A., Roberts, D H., Burke, M., Callard, S Louise., Saher, Margot., Small, D., Smedley, R

K., Gasson, Edward G W., Gregoire, Lauren J., Gandy, N., Hughes, Anna L C., Ballantyne, Colin K., Bateman, Mark., Bigg, Grant R., Doole, J., Dove, D., Duller, G A T., Jenkins, Geraint T H., Livingstone, S L., McCarron, S., Moreton, Stephen., Pollard, David., Praeg, Daniel., Sejrup, Hans Petter., van Landeghem, K.J.J., Wilson, Paul A., (2022). *Growth and retreat of the last British–Irish Ice Sheet, 31 000 to 15 000 years ago: the BRITICE-CHRONO reconstruction*. *Boreas*, 51(4), 699–758. [online] Available at: <https://doi.org/10.1111/bor.12594> [Accessed: 11 August 2025].

Copernicus Marine Service, (2024a). *Atlantic- European Northwest Shelf- Ocean Physics Reanalysis*. [online] Available at: https://data.marine.copernicus.eu/product/NWSHELF_MULTIYEAR_PHY_004_009/description [Accessed: 06 May 2025].

Copernicus Marine Service, (2024b). *Atlantic- European Northwest Shelf- Ocean Biogeochemistry Reanalysis*. [online] Available at: https://data.marine.copernicus.eu/product/NWSHELF_MULTIYEAR_BGC_004_011/description?view=&option=&product_id= [Accessed: 06 May 2025].

Dorrell, R. M., Lloyd, C. J., Lincoln, B. J., Rippeth, T. P., Taylor, J. R., Caulfield, C. P., Sharples, J., Polton, J. A., Scannell, B. D., Greaves, D. M., Hall, R. A. and Simpson, J. H., (2022). *Anthropogenic Mixing in Seasonally Stratified Shelf Seas by Offshore Wind Farm Infrastructure*. *Front. Mar. Sci.* 9:830927.

Dove, D., Nanson, R., Bjarnadóttir, L.R., Guinan, J., Gafeira, J., Post, A., Dolan, M.F.J., Stewart, H., Arosio, R. and Scott, G., (2020). *A two-part seabed geomorphology classification scheme: (v.2) Part 1: Morphology Features Glossary*. [online] Available at: doi: 10.5281/ZENODO.4075248 [Accessed: 11 August 2025].

Environment Agency, (2019). *Coastal flood boundary conditions for the UK: update 2018*. Project SC060064.

Environment Agency, (2021). *What is coastal squeeze?* Project FRS17187.

Fugro, (2023a). *MarramWind Floating Offshore Windfarm: Geophysical and Environmental Offshore Windfarm Survey - Volume 1 of 11: Geophysical Results Report*. Report 220154-OWF-01 02.

Fugro, (2023b). *MarramWind Floating Offshore Windfarm: Geophysical, Environmental and Geotechnical Export Cable Corridor Survey - Volume 1 of 8: Geophysical Interpretation Report*. 230308-ECC-01 02.

Fugro, (2023c). *MarramWind Floating Offshore Windfarm: Metocean Survey Data*.

Garcia-Nieto, P. J., Garcia-Gonzalo, E., Fernandez, J. R. A. and Muiz, C. D., (2024). *Forecast of chlorophyll-a concentration as an indicator of phytoplankton biomass in El Val reservoir by utilizing various machine learning techniques: A case study in Ebro River basin, Spain*. *Journal of Hydrology*, 639.

Google, (no date). *Google Earth*. [online] Available at: <https://earth.google.com/static/multi-threaded/versions/10.86.0.2/index.html> [Accessed: 11 August 2025].

Gowen, R., Stewart, B., Mills, D., and Elliott, P., (1995). *Regional differences in stratification and its effect on phytoplankton production and biomass in the northwestern Irish Sea*. *J. Plankton Res.* 17, 753–769.

Hansom, J.D., Lees, G., McGlashan, J. and John S., (2004). *Shoreline Management Plans and Coastal Cells in Scotland*. *Coastal Management*, 32:3, 227-242.

Health and Safety Executive, (2002). *Environmental considerations. Offshore Technology Report 2001/010*. Health and Safety Executive.

Hill, A. E., Brown, J. Fernand, L. Holt, J., Horsburgh, K. J., Proctor, R., Raine R. and Turrell, W. R., (2008). *Thermohaline circulation of shallow tidal seas*. *Geophysical Research Letters*. 35(11).

Hill, V. and Cota, G., (2005). *Spatial patterns of primary production on the shelf, slope and basin of the Western Arctic in 2002*. *Deep Sea Res. II* 52, 3344–3354.

Holmes, R., Bulat, J., Henni, P., Holt, J., James, C., Kenyon, N., Leslie, A., Long, D., Musson, R., Pearson, S., Stewart, H., (2004). *DTI Strategic Environmental Assessment Area 5 (SEA5): Seabed and superficial geology and processes*. British Geological Survey Report CR/04/064N.

Holt, J., Hughes, S., Hopkins, J., Wakelin, S. L., Holliday, N. P., Dye, S., González-Pola, C., Hjøllo, S. S., Mork, K. A., Nolan, G., Proctor, R., Read, J., Shammon, T., Sherwin, T., Smyth, T., Tattersall, G., Ward, B., and Wiltshire, K. H., (2012). *Multi-decadal variability and trends in the temperature of the northwest European continental shelf: A model-data synthesis*, *Progress in Oceanography*. 106, 96-117, doi:10.1016/j.pocean.2012.08.001.

Hovland, M., Gardner, J.V., and Judd, A.G., (2002). *The significance of pockmarks to understanding fluid flow processes and geohazards*. *Geofluid*. 2, 127-136.

Judd, A.G., (2001). *Pockmarks in the UK Sector of the North Sea. Technical report (TR 002) produced for Strategic Environmental Assessment - SEA2*. Department of Trade and Industry, UK.

Kenyon NH., (1970b). The origin of some transverse sand patches in the Celtic sea. *Geological Magazine* 107: 389-394.

Kenyon, N.H., (1970a). *Sand Ribbons of European tidal sea*. *Marine Geology*. [online] Available at: [https://doi.org/10.1016/0025-3227\(70\)90078-2](https://doi.org/10.1016/0025-3227(70)90078-2) [Accessed: 12 August 2025].

MarramWind Limited, (2023). *MarramWind Offshore Wind Farm Environmental Impact Assessment – Scoping Report*. [online] Available at: <https://marramwind.co.uk/scoping-report> [Accessed: 12 August 2025].

Palmer, M., Howard, T., Tinker, J., Lowe J.A., Bricheno L., Calvert D., Edwards T., Gregory J., Harris G.R., Krijnen J., Pickering, M., Roberts, C., Wolf, J., (2018). *UKCP18 Marine Report*. [online] Available at: <https://www.metoffice.gov.uk/binaries/content/assets/metofficegovuk/pdf/research/ukcp/ukcp18-marine-report-updated.pdf> [Accessed: 12 August 2025].

Prichard, (2013). *The North Sea surge and east coast floods of 1953*. *Weather* – February 2013, Vol. 68, No. 2.

Ramsay D. L. and Brampton A. H., (2000a). *Coastal Cells in Scotland: Cell 2 – Fife Ness to Cairnbulg Point*. Scottish Natural Heritage Research, Survey and Monitoring Report No 144.

Ramsay D. L. and Brampton A. H., (2000b). *Coastal Cells in Scotland: Cell 3 – Cairnbulg Point to Duncansby Head*. Scottish Natural Heritage Research, Survey and Monitoring Report No 145.

Rennie, A. F., Hansom, J. D., Hurst, M. D., Muir, F. M. E., Naylor, L. A., Dunkley, R. A. and MacDonell C.J., (2021). *Dynamic Coast: The National Overview (2021)*. CRW2017_08. Scotland's Centre of Expertise for Waters (CREW). [online] Available at: <https://www.crew.ac.uk/dynamic-coast>. [Accessed: 04 July 2025].

Sharples, J., Holt, J., Wakelin, S., and Palmer, M. R., (2022). *Climate change impacts on stratification relevant to the UK and Ireland*. Marine Climate Change Impacts Partnership Science Review, 11pp.

Sharples, J., Holt, J., Wakelin, S., Palmer, M. R., Graham, J. A., (2025). *Climate change impacts on stratification relevant to the UK and Ireland*. Marine Climate Change Impacts Partnership Science Review, 13pp.

Sharples, J., Ross, O. N., Scott B. E., Greenstreet, S. P. R. and Fraser, H. (2006). *Inter-annual variability in the timing of stratification and the spring bloom in the North-western North Sea*. Continental Shelf Research, 26(6), 733–751. [online] Available at: doi:10.1016/j.csr.2006.01.011. [Accessed: 12 August 2025].

Simpson, J. H. and Bowers, D., (1981). *Models of stratification and frontal movement in shelf seas*. Deep Sea Research Part A. Oceanographic Research Papers. 28, 7, pp. 727-738.

Simpson, J. H. and Sharples, J. (2012). *Physical and Biological Oceanography of shelf Seas*. Cambridge University Press, CBO9781139034098

Tinker, J., Lowe, J., Pardaens, A., Holt, J., and Barciela, R., (2016). *Uncertainty in climate projections for the 21st century northwest European shelf seas*, *Progress in Oceanography*. 148 (Supplement C), 56-73. [online] Available at: <https://doi.org/10.1016/j.pocean.2016.09.003> [Accessed: 12 August 2025].

Uehara, K., Scourse, J. D., Horsburgh, K. J., Lambeck, K., Purcell, A. P., (2006). *Tidal evolution of the northwest European shelf seas from the Last Glacial Maximum to the present*. J. Geophys. Res., 111, C09025. [online] Available at: doi:10.1029/2006JC003531 [Accessed: 12 August 2025].

United Kingdom Hydrographic Office (UKHO), (2009). *Bathymetry survey data* [online] Available at: <https://seabed.admiralty.co.uk> [Accessed 12 August 2025]

United Kingdom Hydrographic Office (UKHO), (2025a). *Admiralty Tide Tables United Kingdom & Ireland*.

United Kingdom Hydrographic Office (UKHO), (2025b). *Vertical Offshore Reference Frames, United Kingdom Hydrographic Office*. [online] Available at: <https://datahub.admiralty.co.uk/portal/apps/sites/#/marine-data-portal/apps/2d71688069744cc6873768d39e0c2f2e/explore> [Accessed: 12 August 2025].

van Leeuwen, S., Tett, P., Mills, D., and van der Molen, J., (2015). *Stratified and non-stratified areas in the North Sea: Long-term variability and biological and policy implications*. Journal of Geophysical Research-Oceans, 120(7), 4670-4686.

Werner, F., Unsöld, G., Koopmann, B., and Stefanon, A., (1980). *Field observations and flume experiments on the nature of comet marks*. Sedimentary Geology. 26, 233-262. [online] Available at: [https://doi.org/10.1016/0037-0738\(80\)90013-5](https://doi.org/10.1016/0037-0738(80)90013-5) [Accessed: 12 August 2025].

Yamaguchi, R., Toshio, S., Richards, K. J. and Qiu, B., (2019). *Diagnosing the development of seasonal stratification using the potential energy anomaly in the North Pacific*. Climate Dynamics.

9. Glossary of Terms and Abbreviations

9.1 Abbreviations

Acronym	Definition
ABPmer	ABP Marine Environmental Research Ltd
BGS	British Geological Survey
CD	Chart Datum
Cefas	Centre for Environment, Fisheries and Aquaculture Science
EIA	Environmental Impact Assessment
EMDONet	European Marine Observation and Data Network
HD	Hydrodynamic
LAT	Lowest Astronomical Tide
MHWS	Mean High Water Spring
MPA	Marine Protected Area
OAA	Option Agreement Area
ODN	Ordnance Datum Newlyn
PEA	Potential Energy Anomaly
PP	Primary Production
RCP	Representative Concentration Pathway
SCO	Scottish Coastal Observatory
SEA	Strategic Environmental Assessment
SEPA	Scottish Environment Protection Agency
SPM	Suspended Particulate Matter
SSS	Side Scan Sonar
SSSI	Site Of Special Scientific Interest
ST	Sand Transport
Tp	Peak Wave Period
UKCP18	United Kingdom Climate Projections 2018
UKHO	United Kingdom Hydrographic Office

9.2 Glossary

Term	Definition
Highest Astronomical Tide	The highest tide level that can be predicted to occur under average meteorological conditions and any combination of astronomical conditions.
Holocene	The current geological epoch, which began approximately 11,700 years ago after the end of the last Ice Age.
Intertidal area	The area between MHWS and Mean Low Water Springs.
Lowest Astronomical Tide	The lowest tide level that can be predicted to occur under average meteorological conditions any combination of astronomical conditions.
Mean High Water Springs	The average tidal height throughout the year of two successive high waters during those periods of 24 hours when the range of the tide is at its greatest.
Mean Low Water Springs	The average tidal height throughout the year of two successive low waters during those periods of 24 hours when the range of the tide is at its greatest.
Mesozoic	A geological era that lasted from about 252 to 66 million years ago.
Morphology	Term used to describe channel form and its process of change in shape and direction over time
Pleistocene	A geological epoch that lasted from about 2.6 million to 11,700 years ago, preceding the Holocene.
Primary production	The process by which phytoplankton convert inorganic into organic material using sunlight through photosynthesis.
Pycnocline	A depth layer in a body of water where the water density changes rapidly with depth due to variations in temperature and/or salinity.
Quaternary Period	The most recent geological period, spanning from about 2.6 million years ago to the present.
Significant wave height	The average height of the highest one-third of waves observed over a given period.
Strom surge	A rise in sea level above the predicted astronomical tide, caused primarily by strong winds and low atmospheric pressure.
Tidal excursion ellipse	The approximate displacement path of water during a representative tidal cycle.

MarramWind 